OPTIMIZATION OF AN *IN VITRO* MODEL OF BIOFILM FORMATION ON VAGINAL EPITHELIAL CELLS TO TEST STRATEGIES FOR PROTECTION AGAINST BACTERIAL VAGINOSIS

OPTIMIZATION OF AN *IN VITRO* MODEL OF BIOFILM FORMATION ON VAGINAL EPITHELIAL CELLS TO TEST STRATEGIES FOR PROTECTION AGAINST BACTERIAL VAGINOSIS

By Amanda M. Bakke, B. Sc (HONS)

A Thesis Submitted to the School of Graduate Studies in Partial Fulfillment of the Requirements for the Degree of Master of Science

McMaster University
Hamilton, Ontario, Canada

DESCRIPTIVE NOTE

MASTER OF SCIENCE:
(2022) McMaster University
Department of Medical Sciences, Infection and Immunity
Hamilton, Ontario

TITLE: Optimization of an *in vitro* model of biofilm formation on vaginal epithelial cells to test strategies for protection against bacterial vaginosis

AUTHOR: Amanda M. Bakke, B.Sc.H (University of Guelph)

SUPERVISOR: Dr. Charu Kaushic

NUMBER OF PAGES: xiii, 139

ABSTRACT

Background: The composition of the vaginal microbiota (VMB) in the female genital tract (FGT) can impact the vaginal epithelium and protect against or increase risk of sexually transmitted viral infections. The VMB grows as a biofilm, a complex structure formed by bacteria for increased survival. When the VMB consists of a diverse bacterial community it correlates with pathogenic effects that lead to adverse health conditions and an increased risk of HIV infection. When the VMB contains *Lactobacillus* species, beneficial health effects and decreased susceptibility to infection are observed. The aim of this project is to optimize an *in vitro* model of biofilm formation for different bacteria associated with the VMB, identify the effects that biofilm has on vaginal epithelial cells and test biofilm treatment strategies. **We hypothesize that a *Lactobacillus* biofilm will enhance barrier function and decrease cytotoxicity of vaginal epithelial cells whereas dysbiotic biofilm will decrease barrier function and induce cytotoxicity. We also hypothesize that various conditions, such as presence of estradiol and eubiotic short-chain fatty acids, will stimulate *Lactobacillus* biofilm growth and suppress dysbiotic biofilm growth in a vaginal epithelial cell model**

Methods: For optimization of the biofilm model, VK2/E6E7 cells were grown in air-liquid interface (ALI) or liquid-liquid interface (LLI) cultures in presence or absence of *L. crispatus*, *L. iners*, *G. vaginalis* or *P. bivia* bacteria. Biofilm formation was assessed using FilmTracerTM SYPRO® Ruby biofilm matrix protein stain. Hormone effects were tested by adding estradiol (10^{-9} M) and progesterone (10^{-7} M) to culture media. Short-chain fatty acid (SCFA) effects were tested by adding lactic acid, acetic acid, succinic acid and butyric acid in varying concentrations to culture media. Enzyme effects were tested by adding sialidase to Vk2 cells before bacteria inoculation.

Results: A novel *in vitro* model of biofilm formation on vaginal epithelial cells was created. Vk2 cells in ALI and LLI cultures remained viable in anaerobic conditions and showed mucin-1 production in aerobic and anaerobic conditions. Matrix protein staining provided a means to accurately visualize and quantify biofilm formation in this model. *L. crispatus* and *L. iners* biofilm growth maintained vaginal epithelial barrier integrity without cytotoxicity. *G. vaginalis* and *P. bivia* biofilm growth significantly reduced barrier integrity ($p=0.0166$, $p=0.0115$) and increased cytotoxicity ($p=0.0024$, $p<0.0001$). Estradiol significantly increased the growth of *L. crispatus* biofilm in the co-culture system ($p<0.0001$). Progesterone significantly increased *G. vaginalis* biofilm growth in the Vk2 cell co-culture ($p=0.006$). *L. crispatus* biofilm formation in the estradiol condition, *G. vaginalis* biofilm formation in the progesterone condition and *P. bivia* biofilm growth in the normal media condition were significantly decreased in the presence of sialidase ($p<0.0001$, $p=0.0001$, $p=0.0380$).

Conclusion: A novel *in vitro* model of biofilm formation on a vaginal epithelial cell line that can be used to visualize and quantify biofilm growth was generated. This model was used to test various strategies for biofilm enhancement or dissociation. Estradiol enhanced beneficial *Lactobacillus* biofilm growth, while progesterone enhanced dysbiotic biofilm growth. Mucin-digesting enzyme sialidase was effective at dissociating all biofilms. This model can be used in the future to test different strategies of dysbiotic biofilm dissociation and enhancement of *Lactobacillus* biofilm in order to investigate treatments for Bacterial Vaginosis (BV) and reduce susceptibility to HIV transmission in women.

ACKNOWLEDGMENTS

I would like to give a special thank you to my supervisor Dr. Charu Kaushic for her continuous support and valuable expertise. I am forever grateful for the opportunity provided to me to join this laboratory. Beginning a Graduate Degree in the middle of a worldwide pandemic is not the ideal scenario, however Dr. Kaushic put her faith in my ability to adjust under the circumstances and thrive in her lab. I would not have been able to do so if it was not for her genuine care and concern for her students, her encouragement to do my best in all things, and her willingness to do anything in her power to help her students succeed. I thank her for helping refine my writing skills, advance my critical thinking skills and allow me to become a better researcher. To the other members of the Kaushic lab whom this degree would not have been possible without. To Dr. Aisha Nazli, without your guidance, assistance, and overall encouragement this project would not be what it is today. To Ingrid, Nuzhat and Christina, my emotional support system, my source of joy and levity when times were hard, and my dear friends, I would not be where I am today without you. To lab members past and present, Tushar, Andrew and Sidney, I will always cherish the sense of community this lab has given me.

I thank my committee members Dr. Lori Burrows and Dr. Jennifer Stearns for their unique insights and valuable advice. Without their generosity in allowing me to utilize multiple resources in their laboratories, including Dr. Burrows confocal microscope and Dr. Stearns anaerobic chamber, this project would not be complete.

Finally, I would like to thank my family and friends who have been a tremendous support system my whole academic career. To my mother, you are my best friend, my rock, and my biggest supporter, I don't know what I would do without you. To Paula and Tyler, your love, support and encouragement has always kept me going. To the rest of my family, distance doesn't feel so hard when the support and love I receive from you all is ever present. To my incredible group of friends, I will never be able to fully express the meaning of your friendship. Ruta and Kaku, your love and support is constant, deep and life-long and means the world to me. Malaya, you have been by my side for over 10 years, and I wouldn't have it any other way. Dominika, meeting you through this degree has been one of greatest things to come from it, I will cherish our friendship the rest of my life. There are countless more thanks to give, one page could never be enough to describe the endless gratitude I have for the amazing people in my life.

DECLARATION OF ACADEMIC ACHIEVEMENTS

All experiments were conceived and designed by Amanda Bakke and Dr. Charu Kaushic. *Lactobacillus crispatus* SJ-3C-US (PTA10138) from ATCC was provided by Dr. Nuch Tanphaichitr (University of Ottawa). Dr. Lori Burrows provided bacterial strain *P. aeruginosa* (ATCC BAA-47). Amanda Bakke performed all experiments. Dr. Aisha Nazli contributed to PNA FISH experimentation and visualization. Amanda Bakke wrote this dissertation with contributions from Dr. Charu Kaushic.

Table of Contents

LIST OF FIGURES AND TABLES

LIST OF ABBREVIATIONS

AAV: Adeno-Associated Virus

ALI: Air-Liquid Interface

ATCC: American Type Culture Collection

AMP: Antimicrobial Peptides

BV: Bacterial Vaginosis

BCA: Bicinchoninic acid

BAP: Biofilm Associated Protein

CVs: Cervicotypes

CVM: Cervicovaginal Mucus

CFU: Colony Forming Units

COCs: Combined Oral Contraceptives

CSTs: Community State Types

c-di-GMP: Bis-(3′-5′)-Cyclic Dimeric Guanosine Monophosphate

DMPA: Depot Medroxyprogesterone Acetate

eDNA: Extracellular DNA

EPS: Extracellular Polymeric Substances

FGT: Female Genital Tract

HSV-2: Herpes Simplex Virus 2

HPV: Human Papilloma Virus

HIV: Human Immunodeficiency Virus

H_2O_2: Hydrogen Peroxide

IFR3: Interferon Regulatory Factor 3

IFNβ: Interferon Beta

IL-1RA: Interleukin-1 Receptor Antagonist

IL-1α: Interleukin 1 Alpha

IL-6: Interleukin 6

IL-8: Interleukin 8

KSFM: Keratinocyte Serum Free Media

LDH: Lactate Dehydrogenase

LLI: Liquid-Liquid Interface

MPA: Medroxyprogesterone Acetate

MMP-9: Metalloproteinase-9

MIC: Minimum Inhibitory Concentration

NK: Natural Killer

NET: Norethisterone

NHP: Non-Human Primate

NFκB: Nuclear Factor Kapa-B

OD: Optical Density

SCFA: Short Chain Fatty Acids

SIV: Simian Immunodeficiency Virus

TLR2: Toll-like Receptor 2

TLR4: Toll-like Receptor 4

TER: Transepithelial Resistance

TNF-α: Tumor Necrosis Factor Alpha

VMB: Vaginal Microbiota

CHAPTER 1: INTRODUCTION

1.1 HIV-1 Infection in women

The Human Immunodeficiency Virus (HIV) epidemic continues to persist globally. In 2021 there were approximately 40 million people living with HIV worldwide, and 54% of all cases were identified in women and girls.[1] With the COVID-19 global pandemic causing disruptions to HIV treatments and prevention strategies, infections are on the rise again, with approximately 1.5 million new infections in 2021.[1] Therefore, combating this epidemic remains a global priority. In Sub-Saharan Africa, which has the highest prevalence of HIV worldwide, women and girls accounted for 63% of new HIV infections in 2021.[1] Sexual mucosal transmission is the primary route of infection for this virus.[2] HIV transmission through the female genital tract (FGT) is 5 times more likely compared to the male genital tract and 40% of annual HIV transmission occurs in the FGT, leading to the increased burden of infection seen in women.[3-5] These alarming statistics highlight the importance of understanding the underlying causes of increased susceptibility of women to this infection and the role of the FGT in HIV transmission.

HIV is a retrovirus belonging to the *Lentiviridae* genus.[2] This genus of virus is defined by long incubation periods and slow progression of disease.[2] Studies with non-human primates (NHP) have shown that persistent systemic infection with simian immunodeficiency virus (SIV) is dependent on local tissue events that happen within 4 weeks of viral inoculation, highlighting the importance of early stage infection.[2] NHP models show that SIV can cross the mucosal epithelial barrier with a small number of viral particles within hours post-exposure.[2,4,5] HIV viral particles cross the epithelium through mechanisms such as endocytosis or penetration through gaps between epithelial cells to reach their targets.[5] HIV primary target cells are $CD4^+$ T cells

comprising 90% of productively infected cells within the founder population.[2,4,6] The founder population is defined as cells having detectable viral RNA within 3-4 days post infection.[2] Infection occurs by interactions between cell surface CD4 and the gp120 viral envelope protein, as well as CXCR4 or CCR5 chemokine co-receptors, resulting in virus and cell membrane fusion.[6] The founder population of infected CD4+ T cells undergoes local expansion 1 week post infection, allowing dissemination of infected cells to the draining lymph nodes, and results in the establishment of a self-propagating systemic infection in the secondary lymphoid tissues.[2] Therefore, systemic infection in women, through heterosexual intercourse, requires viral particles within HIV-containing semen to cross the epithelium in the FGT. The mucosal epithelial barrier within the FGT is variable in physiology, based on the specific site, and offers different levels of protection against infection.

1.2 The Female Genital Tract

The FGT comprises an upper and lower tract each with distinct morphology and physiology.[3] The upper tract consists of the endocervix, uterus, fallopian tubes and ovaries.[3] Its epithelium is characterized by a single layer of columnar epithelial cells above a continuous basement membrane.[3,4] Tight junctions within the columnar epithelium block the passage of large molecules or pathogens to the immunologically active basal layer.[4,7] The transformation zone, between the endocervix and the ectocervix is defined by the transition from columnar epithelial cells to the stratified squamous epithelium of the lower tact.[3] This area of the FGT is the most immunologically active, where immune cells such as lymphocytes and HIV target CD4+ T cells reside in high quantities.[3,4] The presence of immune cells can be increased during heightened periods of inflammation, making this site more vulnerable to HIV-1 infection.[4] The upper FGT is immunologically active, with the cells comprising this epithelium expressing a wide range of

Toll-like receptors (TLRs).[4,8] The expression of various TLRs and consequent ability to activate cytokine and chemokine production enables the upper tract epithelial cells to respond to pathogens.[8] Even though the upper tract columnar cells are joined by tight junctions, their single layered nature makes them easily accessible to pathogens compared to the multi-layered epithelium of the lower tract.[4] Also, HIV-mediated TLR activation can lead to the production of pro-inflammatory cytokines, such as tumor necrosis factor (TNF)-α by endometrial epithelial cells, leading to disruptions in the single layered mucosal barrier.[3,4,9,10] Neutralization of TNF-α production in cell co-cultures with HIV maintains transepithelial resistance (TER), a measure of barrier integrity, when compared to cultures in the absence of TNF-α neutralizing antibody.[10] This provided evidence that decreases in barrier integrity by TNF-α secretion during HIV-1 infection contributes to increased translocation of viral particles across the epithelium.

Reproductive sex hormones in the FGT fluctuate throughout the menstrual cycle which has varying impacts on immunity and susceptibility to infection.[3] The menstrual cycle has 2 phases, the follicular and the luteal phase.[11] The follicular phase, associated with preparation for ovulation and the development of ovarian follicles, has increasing estradiol levels throughout this phase.[11] A study from our laboratory looking at the effects of hormones on primary endometrial genital epithelial cells found that estradiol treatment strengthened the TER of the cell line and reduced the impairment of ZO-1 tight junction protein after HIV-1 infection, showing that estradiol presence can increase epithelial barrier strength.[12] Conversely, the luteal phase is characterized by increased progesterone, allowing for a more favourable environment for embryonic implantation.[13] To create the ideal conditions for implantation, the luteal phase causes a suppression of cytotoxic T-lymphocytes and natural killer cells, increased presence of CD4+ T cells, and a general increase in inflammation during what is called the “window of vulnerability”,

leading to increased HIV susceptibility.[13-16] This was confirmed in a study using NHP models and SIV infection at different stages in the menstrual cycle which found that 85% of successful infection happened during the progesterone-high luteal phase.[17]

The lower female genital tract has a distinct structure and physiology from the upper tract and transformation zone. Its immune functions and relationship with endogenous sex hormones varies from that of the other FGT compartments. This will be discussed in more detail as the lower tract is the focus of this project.

1.2.1 The Vaginal Epithelium

The lower FGT is comprised of the ectocervix and the vagina.[3] The vaginal epithelium is defined by its thick multilayer of stratified squamous epithelial cells.[3,4] The multilayered nature of this epithelium provides a greater barrier to infection compared to the single layered columnar epithelium of the upper tract.[4] Another mode of mechanical protection that the vaginal epithelium offers is the continuous sloughing of the superficial layers while the basal layers undergo differentiation and remain metabolically active.[3,4,9] The basal layer also contains tight junction molecules, adherens junctions and desmosomal adhesion proteins, which play a role in maintaining the integrity of the epithelium and enhancing barrier strength.[18] Vaginal epithelial cells of the lower FGT produce the hydrophobic glycoprotein mucin that forms a mucus layer important for many physiological functions.[3,7] There are a variety of mucin glycoproteins that are coded by the MUC gene family; they can be split into secreted and cell-surface associated mucins.[19] Mucin-1, the dominant mucin in the FGT, is a cell-surface associated mucin.[19,20] The mucus layer offers a protective barrier through its ability to trap pathogens, such as HIV viral particles, slowing HIV diffusion to the epithelium.[3,7,21] The mucus layer also contains immunoglobulins and antimicrobial peptides to help combat pathogen infection.[8]

The fluctuation of sex hormones in the FGT can impact the vaginal epithelium composition. The progesterone-high luteal phase in the menstrual cycle is characterized by a thickening of the mucus layer[3,16] However, studies have shown the presence of progesterone in the form of progestin-containing contraceptives can cause a thinning of the vaginal epithelium.[22,23] The follicular phase is associated with a thinning of the mucus layer[16], however a NHP study correlated the thickening of the vaginal stratified squamous epithelium with the presence of estrogen.[24] Another study found that the first 14 days of the menstrual cycle, the estradiol high phase, correspond to higher levels of Mucin-1, however the study also found this effect in women using Depot medroxyprogesterone acetate (DMPA), an anti-estrogenic hormonal contraceptive.[25] Therefore, hormone fluctuation impacts the mucus layer in different ways.

Despite the mechanisms of protection that the vaginal epithelium provides, the lower tract is the most likely target for viral infection. The vagina is the first area of contact during heterosexual intercourse for HIV-infected semen and is exposed to the most volume of semen.[4,7,21] Microtears in the vaginal epithelium during intercourse provide opportunity for viral particles to cross the epithelium and begin productive infection.[4,7,21] The large surface area of the vaginal epithelium also provides greater access for viral particle entry when breaches of the epithelium occur.[4,7,21] The presence of immune cells in the lower tract differs from the upper tract in number, location and fluctuation.[3,8,9,26] Langerhan cells and other dendritic cell subtypes, important in pathogen destruction, remain stable in the lower tract and are located within the squamous epithelium.[3,8,9,26] Natural Killer (NK) cells are present in the ectocervix to help combat viral infection.[3,8,9,26] The adaptive response in the vagina is important in reducing susceptibility to infection, with CD4+ and CD8+ T cells residing in the vaginal epithelium as well.[3,8,9,26]

However, increased presence of these HIV target T cells at the epithelium during prolonged inflammation or exposure to previous infection can increase risk of HIV infection.[3,27] Inflammation in the FGT is a risk factor for HIV acquisition and transmission and studying ways to combat chronic inflammation in this area may reduce susceptibility to infection.

The lower FGT has an added layer of protection to the mucosal barrier, depending on its composition, through the presence of the vaginal microbiota (VMB).[3] Bacteria colonization is also present in the upper FGT, however the quantity of bacteria in this area is much less than the lower genital tract.[3] A key area of focus for this project is the VMB and its influence on susceptibility to infection and will therefore be discussed in depth in the next sections

1.3 The Vaginal Microbiota

The VMB in the lower FGT is an important component of the vaginal epithelium and can play a key role in susceptibility to infection depending on its composition.[28] Studies have distinguished the various compositions the VMB can have using 16S rRNA gene sequencing and classification into different community state types (CSTs).[28] Early studies identified 5 CSTs designated I-V, with I, II, III and V dominated by different *Lactobacillus* species and IV being the most diverse group with high numbers of various anaerobic bacteria.[28] Recent and more in-depth studies of VMB sequencing have further classified microbiota composition into CSTs and cervicotypes (CVs) using molecular methods to characterize vaginal or cervical samples.[29] CSTs remain similar with CST-I, CST-II, CST-III and CST-V being dominated by *Lactobacillus crispatus, L. gasseri, L. iners* and *L. jensenii,* respectively.[29] CST-IV remains classified as dominance by a variety of facultative or obligate anaerobes, however sub-groups have been added to further specify the bacteria present, with CST-IVA showing *Gardnerella vaginalis* dominance and CST-IVC showing strict anaerobic bacteria dominance including *Prevotella*

spp.[29] CTs show similar trends to CSTs, with C1 and C2 dominated by *L. crispatus* and *L. iners* respectively and C3 and C4 dominated by *G. vaginalis* and a variety of strict anaerobes including *P. bivia* respectively.[29] Another important aspect when identifying VMB composition is variation among racial backgrounds. For example, *Lactobacillus* dominance significantly varies among healthy women of different racial backgrounds in the same geographic location (North America), with white women showing 90% dominance and Black and Hispanic women showing only 60% dominance.[28] This difference is even more pronounced in studies of healthy Black women in South Africa, with only 37% of women in this group found to have CVs with *Lactobacillus* dominance.[30]

The cervicovaginal bacteria in the lower female genital tract have been shown to influence baseline inflammation, epithelial barrier integrity, and immune function which has impacts on pregnancy, fertility and susceptibility to infection.[31,32] This is a key aspect of this project, therefore, different VMB dominance and the impact on these factors will be discussed in detail.

1.3.1 *Lactobacillus*-Dominant VMB and Protection against Infection

Lactobacillus spp. is a large genus of facultatively anaerobic, Gram-positive rod bacteria known for their ability to produce lactic acid.[33] *L. crispatus* bacteria dominates CST-I and is the most identified *Lactobacillus* species in the white and Asian women population.[34] This bacterium is associated with many positive health outcomes in the FGT due to a variety of mechanisms it uses to promote an optimal vaginal microenvironment and reduce susceptibility to infection.[28,35,36]

Lactic acid production is a defining trait of *L. crispatus* and plays an important role in maintaining the optimal acidic pH (3.5-4.2) within the lower FGT.[36,37] *L. crispatus* is also capable of producing hydrogen peroxide (H_2O_2) in the FGT to maintain a low oxygen

environment that prevents the colonization of pathogenic bacteria like *Neisseria gonorrhoeae*.[38,39] A study investigating lactic acid and H_2O_2 production by *Lactobacillus* species found that presence of these products has an antiviral effect against HSV-2.[40]

Another mechanism *Lactobacillus* species use to promote vaginal health and reduce risk of infection is strong adherence to the vaginal epithelium, with one study showing that *Lactobacillus* species adhere through surface proteins and carbohydrates, consequently interfering with the adherence of other urogenital pathogens allowing protection against infection.[41] A similar study looked at the ability of *L. crispatus* to adhere to vaginal epithelial cells and found that not only did it adhere more strongly than other *Lactobacillus* species, but displaced previously adhered pathogenic fungi such as *Candida albicans*.[42] Analysis of the *L. crispatus* genome has identified 103 adhesion proteins that play a role in colonization and interaction with host cells.[43] This included one protein, *Lactobacillus* epithelium adhesin (LEA), which is involved in blocking of *G. vaginalis* adhesion and could explain why *L. crispatus* can exclude or displace pathogenic *G. vaginalis* bacteria on epithelial cells.[43,44] Our laboratory used colonization of genital epithelial cell layers with probiotic *Lactobacillus* bacteria and found that cells were protected against HIV mediated reduction in TER and disruption of ZO-1 tight junction protein.[12] Previous research in our laboratory also looked specifically at the effect of *L. crispatus* on a vaginal epithelial cell line and found that these bacteria and cell co-cultures resulted in maintenance of cell viability and barrier integrity, determined through TER and lactate dehydrogenase (LDH) assays, and negated harmful effects of *G. vaginalis* and *P. bivia* bacteria.[45] Therefore, *Lactobacillus* adherence protects from colonization of pathogenic species and strengthens epithelial barrier function.

Lactobacillus bacteria can also have immune modulatory effects in the FGT to reduce inflammation and decrease risk of infection.[34,46,47] *L. crispatus* reduced the production of pro-inflammatory cytokines in vaginal epithelial cells when they were treated with TLR agonists that, in non-bacteria colonization models, significantly increased production of cytokines such as interleukin 6 (IL-6) and TNF-α.[36] Similarly, it was shown that *L. crispatus* adherence to a 3D model of vaginal epithelial cells does not result in overexpression of different inflammatory aspects like immune cell pattern recognition receptors and pro-inflammatory cytokines and could help reduce inflammation in the FGT.[46] Previous research in our laboratory found that co-cultures of vaginal epithelial cells with *L. crispatus* maintained or reduced the levels of pro-inflammatory cytokine production when compared to control cultures.[45] Therefore, a *Lactobacillus*-dominant VMB reduces susceptibility to infection through secretion of antimicrobial compounds, strong adherence to the epithelium resulting in strengthening of the epithelial barrier, and immune modulation to reduce inflammation in the FGT.

Not all *Lactobacillus* species have the same beneficial health outcomes, with *L. iners* bacteria showing variable impacts in the FGT. *L. iners* is the most commonly identified *Lactobacillus* species in the VMB, commonly found in the women with both *Lactobacillus*-dominant VMB and VMB with a large diversity of bacteria species.[34,48] *L. iners* has the smallest genome of all *Lactobacillus* species, and it is most closely related to *L. crispatus* and *L. gasseri* as they are found in the same clade.[48,49] *L. iners* contains some distinct features in its genome compared to other vaginal *Lactobacillus* species, such as specific genes for hydrolases and proteins for phosphate transport.[49] One feature of this bacteria that points to its possible virulence in the FGT is the presence of a cytolysin, an epithelial cell toxin, not found in other *Lactobacillus* species.[48,49] Some studies have speculated that the high prevalence of Bacterial

vaginosis (BV) associated with *L. iners* could be due to the absence of D-lactic acid and H_2O_2 production in this bacterium.[34,48,50,51] *L. iners* dominance in the VMB has often been associated with high instability and likely transition to dysbiosis.[30,52] Antibiotic treatment for BV in women induces *L. iners* dominance, which could be why BV reoccurrence after antibiotics is very common.[53] *L. iners* strongly adheres to the epithelium, not through conventional adhesion methods used by other *Lactobacillus* species, but through a fibronectin-binding protein that can bind human fibronectin in the glycoprotein extracellular matrix of vaginal epithelial cells stronger than any other *Lactobacillus* species.[51] This strong binding could contribute to its dominance after antibiotic treatment.[51] Previous research in our laboratory has shown the vaginal epithelial cell co-cultures with *L. iners* bacteria resulted in decreases in barrier function and cell viability and increases in inflammatory cytokine production equivalent to that of BV-associated bacteria.[45] Therefore, *L. iners* variable effects on the vaginal epithelium need to be studied further to determine if this bacterium is more closely related to its beneficial *Lactobacillus* genus or the pathogenic bacteria present in dysbiosis.

1.3.2 Dysbiotic VMB, Bacterial Vaginosis and Susceptibility to Infection

A VMB with CST IV classification is in a state of vaginal dysbiosis. When dysbiosis is used in the context of the VMB it is defined as a shift in the VMB from dominance of *Lactobacillus* species to dominance of a variety of facultative or strict anaerobic bacteria, and this definition of dysbiosis is used in this project.[28,29] CST IV can be further classified into sub-groups, one dominated by *Gardnerella vaginalis*.[29] *G. vaginalis* is a facultative anaerobic rod with close relatives in the *Bifidobacterium* family.[54,55] This bacterium is defined as Gram-variable due to its thin cell wall, which often stains Gram-positive.[54] A CST IV classification of the VMB, or more specifically the presence of *G. vaginalis,* is highly correlated with BV.[29,56] BV

is a common condition that effects 29% of women in the US and is associated with a variety of health issues including, problems with pregnancy, pre-term birth, and increased risk of STI's.[29,57] A VMB of CST IV classification results in a 4-fold increased risk of HIV infection compared to a *L. crispatus*-dominated VMB in South African women.[31] BV presents as inflammation of the vagina which includes pain, itching and discharge.[57] Although *G. vaginalis* is one of the most commonly identified bacteria in women with BV[58], this bacterium has also been identified in lower abundance in other CST classifications, as well as in women who do not present with BV symptoms.[57,59] Some studies have determined that *G. vaginalis* can be commensal or pathogenic, with the BV-associated pathogenic strains differing in their ability to produce enzymes that can degrade the vaginal mucus layer.[54,60,61] It has also been hypothesized that *G. vaginalis* in community with diverse groups of anaerobic bacteria leads to the clinical diagnosis of BV.[62] The driving factor for these multispecies communities to colonize the epithelium in a pathogenic way is biofilm formation, with *G. vaginalis* often cited as the anchoring bacteria that stimulates polymicrobial biofilm formation.[63-65] Biofilm formation by the VMB is an important concept in this project and will be discussed in detail in later sections.

The dysbiotic state associated with BV can facilitate weakening of the epithelial barrier, with one study showing human ectocervical cells exposed to combinations of BV-associated bacteria had increased paracellular permeability.[66] This permeability may be a mechanism of increased susceptibility to infection. Virulent, BV-associated strains of *G. vaginalis* and *P. bivia* can produce the enzyme sialidase, which cleaves the sialic acid residue of mucin glycoproteins found in the mucus layer, leading to its degradation.[61,67,68] *G. vaginalis* bacteria use sialic acid residues as an energy source for continued growth and colonization of the mucus membrane, allowing other harmful BV-associated bacteria access for colonization that leads to further loss

of the protective mucus layer in the epithelium.[61,69] The loss of this significant protective barrier in the FGT increases risk of HIV infection.[69,70] *G. vaginalis* bacteria also produce the cytotoxin vaginolysin.[71] Vaginolysin specifically binds to human CD59, leading to phosphorylation of epithelial p38-mitogen-activated protein kinase, which stimulates cell lysis and death.[71,72] *G. vaginalis* use of this toxin to facilitate epithelial cell death leads to strong bacterial adhesion and further degradation of the epithelium, increasing HIV access to the underlying target cell population.[57,72] Many studies have shown that the presence of *G. vaginalis* bacteria in the VMB can stimulate upregulation of pro-inflammatory cytokines and chemokines causing inflammation that damages the epithelium.[56,57] Co-cultures of vaginal epithelial cells with *G. vaginalis* bacteria-free supernatants have upregulation of various cytokines, including TNF-α.[73] *G. vaginalis* can also stimulate increased RANTES production in various vaginal epithelial cell lines, which is a chemokine implicated in recruitment of T cells to the epithelium.[74] The presence of *P. bivia* in the VMB is associated with elevated levels of the endotoxin lipopolysaccharide in the FGT, which can also modulate pro-inflammatory cytokine response.[75] Previous research in our laboratory looking at the effect of BV-associated bacteria on a epithelial cells found that *G. vaginalis* and *P. bivia* cultures on a vaginal epithelial cell line resulted in significantly decreased cell viability and barrier integrity, and increased production of various inflammatory cytokines when compared to control cultures.[45] Therefore, BV-associated bacteria can negatively affect vaginal epithelial barrier integrity through secretion of enzymes and cytotoxins that degrade the mucus layer and the epithelium, and stimulation of inflammatory cytokine and chemokine production which recruit HIV target cells and weakens the epithelial barrier. This can lead to increased susceptibility to HIV infection.

1.3.3 Female Sex Hormones and the VMB

Endogenous sex hormones in the lower FGT and hormonal contraceptive use can influence the composition of the VMB.[3] These effects have been detailed by studying composition of the VMB from puberty through to menopause.[3,76,77] When estrogen levels significantly decrease during menopause the VMB is much less likely to be dominated by *Lactobacillus* species.[3,13] The most notable proof of this effect comes from studies done in post-menopausal women given estrogen treatment, with results indicating a dramatic increase in the presence of *Lactobacillus* species in the VMB.[13,78] Another study looking at the effect of estrogen supplementation in post-menopausal women found that before estrogen treatment, a more dysbiotic VMB was common in study participants and women with a high percentage of *G. vaginalis* bacteria in their VMB were more likely to have atrophic vaginitis.[78]

Hormonal contraceptive effect on the VMB has also been examined. Combined oral contraceptives (COC) use combinations of progestin and estrogen for better menstrual cycle control and to minimize venous thrombosis and cardiovascular risk, with the estrogen component of this contraceptive remaining relatively stable.[79] DMPA is a progestin based injectable contraception that uses medroxyprogesterone acetate (MPA) as its synthetic progestogenic steroid to mimic progesterone action in the FGT and prevent pregnancy.[79] The area of research investigating hormonal contraception effect on different aspects of the FGT has become very active with the discovery that DMPA use is associated with a 40% increased risk of HIV infection when compared to women who use other hormonal contraceptives.[3,79,80] Analysis of changes in composition of VMB of women who had been using DMPA for 2 years showed a significant decrease in the presence of H_2O_2-positive *Lactobacillus* species.[81] A study done in our laboratory used 16S rRNA sequencing of the VMB of women on different contraceptives to

determine the effects on VMB composition and found that women using DMPA had significantly more diverse VMB and significantly lower presence of *Lactobacillus* dominance.[82] As stated previously, decrease in beneficial *Lactobacillus* species and shift towards dysbiosis has negative impacts on reproductive health and increases risk of infection, which contribute to why DMPA has a 40% increased risk of HIV infection. Other studies suggest that estradiol containing COCs may have beneficial effects on the VMB. A combined contraceptive vaginal ring has been correlated with an increase in *Lactobacillus* in the VMB over 1 year of usage.[83] Similarly, women using estradiol containing contraceptive vaginal ring show dominance of H_2O_2-positive *Lactobacillus* species.[84] Therefore, endogenous sex hormones and the use of hormonal contraceptives can have varying impacts on the composition of the VMB.

1.3.4 Vaginal Metabolites and the VMB

Another aspect of the vaginal microenvironment is the metabolome, the presence of microbe-produced and host-produced metabolites which can influence the development of clinical conditions in the FGT.[85] The metabolomic profile of a women's FGT is largely dependent on the species of bacteria present in the VMB and their respective metabolism.[86] States of dysbiosis in the VMB results in dramatic changes to the vaginal metabolome. One study that correlated metabolite and bacteria species presence found distinct metabolomic signatures in women with BV compared to BV-negative woman.[86] Also, women treated for BV whose VMB shifted to that of *L. crispatus* dominance also had high concentrations of metabolites that were negatively associated with BV, therefore confirming that specific bacteria have impacts on the metabolome.[86] *Lactobacillus* in the VMB produce lactic acid which helps maintain the acidic pH in the FGT and has implications in antimicrobial activity against pathogenic bacteria.[87] Therefore, the production of lactic acid has beneficial effects in the FGT.

Conversely, BV-associated bacteria are correlated with a shift away from lactic acid production towards the production of short-chain fatty acids (SCFA), fatty acids with less than six carbon atoms which lactic acid resembles but is not technically classified in this category.[87] However, for the remainder of this project when discussing eubiotic and dysbiotic SCFA conditions, lactic acid will be included with the SFCA. Therefore, production of SCFA by BV-associated bacteria, specifically compounds such as butyrate, acetate and succinate, leads to a dysbiotic microenvironment in the FGT and an increased risk of BV development.[87] One study proposed that the decreases in pro-inflammatory cytokine production seen in *Lactobacillus*-dominant VMB could be seen solely with the metabolites produced by these species, specifically lactic acid.[88] Direct exposure of cervicovaginal epithelial cells to lactic acid reduced some pro-inflammatory cytokine production, such as IL-6 and IL-8, and induced an anti-inflammatory state through Interleukin-1 Receptor Antagonist (IL-1RA) production.[88] Therefore, reduced susceptibility to HIV infection through the down-regulation of pro-inflammatory cytokines seen in *Lactobacillus*-dominant VMB could be due to the metabolites present in this microenvironment. Other studies have shown that prolonged exposure to SCFA like acetate, butyrate and succinate result in increased production of pro-inflammatory cytokines like TNF-α, which may contribute to the increased risk of BV development seen with these conditions.[89]

A systematic review and meta-analysis conducted by our laboratory (unpublished data) showed that there are specific classes of SCFA that are either up-regulated or down-regulated during states of dysbiosis.[90] This meta-analysis concluded that SCFA such as acetate, succinate and butyrate are up-regulated during periods of dysbiosis in the VMB, and lactate is down-regulated.[90] The meta-analysis also determined the concentrations in which these compounds are found in various states of eubiosis and dysbiosis.[90] These concentrations used in combination to

simulate eubiosis and dysbiosis in the FGT can be used to test the effects on vaginal epithelial cells, as well as bacteria growth on *in vitro* models of the vaginal epithelium.

1.4 Biofilms

Bacterial growth is mainly classified into two categories: planktonic bacteria, which are independent free-floating cells, or biofilms, which are aggerates of bacteria surrounded with self-produced matrices.[91,92] Biofilm research has become crucial in addressing many serious issues, such as food spoilage, infection of medical implants, and serious chronic infections.[93] Despite the negative impacts of biofilms, there are some beneficial uses of biofilm formation.[93] Many agricultural industries use biofilm-forming bacteria as biofertilizers to enhance crop growth and protect against pathogens.[93] More research on the beneficial effects of biofilm formation needs to be conducted to determine other areas of importance these structures could impact.

Many studies have focused on defining how biofilm grows, however most focus on biofilm formation in a laboratory setting which should be taken into consideration when discussing the proposed model of biofilm formation.[91,94] The most widely accepted model of biofilm formation includes 5 stages: reversable attachment, irreversible attachment, formation of microcolonies, maturation and dispersal.[93,94] The formation of biofilms is driven largely by the environment where biofilm is being formed, with initial attachment only occurring if environmental conditions are ideal.[94,95] Planktonic cell reversible attachment involves the cell appendages and other non-specific physical forces between cell and surface.[93,95] Irreversible attachment relies on motility elements like flagella as well as cell surface adhesion proteins to facilitate attachment to the surface.[93,95] An important part of irreversible attachment and initial biofilm formation is the production of bis-(3′-5′)-cyclic dimeric guanosine monophosphate (c-di-GMP).[94,95] Biofilm forming bacteria have different classes of proteins involved in the synthesis or degradation of c-

di-GMP which are controlled by environmental cues that determine the amount of c-di-GMP being produced.[94] This secondary messenger is involved in many critical cell functions including biofilm formation.[96] c-di-GMP can inhibit motility functions of bacteria as they prepare to attach and begin biofilm formation and will then stimulate biosynthesis of adhesions and extracellular polymeric substances (EPS) which aid in surface attachment and begin to form the main components of the biofilm matrix.[96] The biofilm matrix is the main structural component of biofilms, defined as a complex scaffold encasing the individual bacteria cells within the biofilm and creating many structural and chemical microenvironments to provide stability and protection.[92,97] The EPS that form the matrix depends on the bacteria forming the biofilm, but can include polysaccharides, proteins, DNA, and lipids.[92,93] One main component of the biofilm matrix is extracellular proteins involved in formation and stabilization of the biofilm structure.[92] Extracellular proteins connect bacteria and exopolysaccharides to maintain the architecture of the biofilm.[92] One important protein family found in many bacteria is the biofilm associated protein (Bap), involved in biofilm formation and the pathogenic effect some biofilms exert.[92] Extracellular DNA (eDNA) is another key component of the biofilm matrix which is actively secreted by bacteria within the matrix and plays a role in intracellular connection and resistance to antibiotics and antimicrobials.[92,93] Microcolony formation is the next step in the biofilm formation process, and starts with cell proliferation and continuing production of EPS which shapes the structure of the biofilm.[93,95] This process is also highly dependent on environmental cues, such as oxygen and temperature, that determine the shape the biofilm will take.[93,95] Biofilm maturation occurs as microcolony growth progresses and is accompanied by changes in gene expression that signal production of specific EPS for adhesion between cells.[93,95] Biofilm dispersal occurs when bacteria cells revert back to planktonic form in search of a different niche,

which happens in response to environmental cues.[93,95] Active dispersal occurs through the activation of genes involved in motility and EPS degradation and is controlled by decreasing c-di-GMP levels.[93,95]

Recently, an updated conceptual model of biofilm formation has been proposed that questions the importance of surface attachment of biofilms and instead places emphasis on bacteria aggregation.[91] The main premise of this model is that biofilm formation in a natural environment may not be a standardized process, as determined by *in vitro* studies in a laboratory setting, but rather dependent on general aggregation in its present environment. This is confirmed by chronic infections linked to biofilm aggregation rather than surface attachment, including cystic fibrosis and chronic dermal wounds, where bacterial aggregates grow in mucus and airway surface liquid. Therefore, the proposed updated model describes three major events in the biofilm life cycle: aggregation, growth and disaggregation. This model may be more all-encompassing, describing an open system where an influx of bacteria contributing to a continuously growing and changing biofilm is possible and can be used to depict biofilm formation regardless of the environment it is forming in. This theory of biofilm formation may be valuable for this project as the mucus layer of the vaginal epithelium is the proposed site of biofilm formation by the VMB. According to this model, biofilm growth in the presence of mucus relies on bacteria aggregation which can lead to surface attachment and is not restrictive to one or the other but rather a dynamic exchange between the two.[91]

1.4.1 *Lactobacillus*-dominant Biofilms in the VMB

The beneficial effects of *Lactobacillus* dominance in the FGT, such as strengthening of the epithelial barrier to prevent infection and blocking adhesion of urogenital pathogens, may be the result of biofilm formation of this bacteria on the vaginal.[98] Comparative genomics of 10

vaginal *L. crispatus* strains show various conserved genes involved in adhesion and EPS production, with some of the adhesions identified being mucus-binding proteins and fibronectin-binding proteins.[43] As indicated previously, adhesion to a surface and EPS production are key components of the initial attachment and biofilm matrix formation and the presence of these genes could be evidence of biofilm formation properties in this bacterium. A study tested the biofilm forming capabilities of 16 vaginal strains of *Lactobacillus* isolated from healthy women and found that all strains had some biofilm forming capability, but the strength of biofilm formation varied across strain and within strains.[99] One study isolated 2 strains of vaginal *Lactobacillus* species from healthy women and visualized biofilm formation on a slide culture with confocal laser scanning microscopy.[100] Biofilm formation by *Lactobacillus* species *in vitro* has not being studied in depth and should be researched more closely to determine if biofilm formation is one of the specific mechanisms of protection this bacteria uses to promote health in the FGT.

1.4.2 Dysbiotic Biofilms in the VMB

G. vaginalis biofilm formation is speculated to be a main mechanism of virulence this bacterium uses to adhere strongly to the vaginal epithelium resulting in adverse health effects like development of BV and increased risk of STI susceptibility.[72,101] Although it has been determined that BV is likely due to the presence of a polymicrobial community of biofilm forming bacteria, *G. vaginalis* is still cited as the anchoring bacteria that stimulates degradation of the mucus lining the vaginal epithelium and epithelial cell death through production of enzymes, cytotoxins and biofilm formation.[63,65] Confirmation of *G. vaginalis* biofilm formation came from an early study of vaginal biopsies from women with BV that found 90% of women had a dense bacteria biofilm attached to the vaginal epithelium and 60-95% of bacteria within the

biofilm was identified as *G. vaginalis*.[102] When looking more closely at the *G. vaginalis* genome to determine factors that contribute to its virulence, one study analysed three strains of *G. vaginalis* and found genes encoding glycosyltransferases that are important for the synthesis of EPS, which are necessary for biofilm formation.[54] Also, genes encoding the toxin vaginolysin, a *G. vaginalis* specific epithelial cell cytotoxin, was conserved in all three strains.[54] Vaginolysin has been the most commonly studied *G. vaginalis* virulence factor due to its highly conserved nature across the species and its implications in BV presence.[103] BV-isolated strains of *G. vaginalis* show higher expression of vaginolysin, confirming this cytotoxin's role in BV progression.[104] Another study compared the major transcriptomic features of planktonic *G. vaginalis* cultures to BV-associated *G. vaginalis* biofilms and found a large number of differentially expressed genes (~78%).[101] The upregulated genes included genes involved in hydrolase activity, genes encoding the LPXTG-motif cell anchor domain-containing protein involved in biofilm formation of Gram-positive bacteria, genes for glycosyltransferases, genes encoding vaginloysin, and genes encoding antimicrobial-specific resistance proteins belonging to efflux pump families.[101] The *G. vaginalis* genome contains the *bapL* gene, encoding the Bap-like (BapL) protein, which as indicated before is an important protein in biofilm formation and pathogenic infection.[62,105] Another mechanism which *G. vaginalis* uses to colonize the vaginal epithelium and form biofilm is the secretion of sialidase to degrade the mucus layer. There is a direct correlation in *G. vaginalis* strains with the presence of the sialidase A gene and biofilm formation.[61] Therefore, specific genomic factors contribute to *G. vaginalis'* ability to form biofilms.

Many studies have tried to classify the biofilm forming capabilities of other BV-associated anaerobic bacteria, and consistently find that *G. vaginalis* outgrows other bacteria

species. Investigation of biofilm formation and cytotoxicity of different BV-associated anaerobes found that *G. vaginalis* grows significantly thicker biofilm than other bacteria and has cytotoxic effects.[72] A study isolated 30 different strains of bacteria from BV-positive vaginal samples and tested their biofilm formation and cytotoxic abilities, with *G. vaginalis* outcompeting all 29 bacteria in each category.[106] *G. vaginalis* ability to displace *Lactobacillus* species from the epithelium is known, with one study showing a BV-associated strain of *G. vaginalis* interfere with *L. crispatus* adherence to a vaginal epithelial cell line.[44] BV strains of *G. vaginalis* have greater adhesion capability to epithelial cells and stronger displacement of already adherent *L. crispatus*.[104] Lastly, *G. vaginalis* has the greatest displacement of *L. crispatus* from cervical epithelial cells when compared to other BV-associated bacteria.[107] Therefore, *G. vaginalis* adherence capabilities exceeds that of other BV-associated anaerobes and in some cases can displace *Lactobacillus* species.

Despite the evidence for *G. vaginalis* dominance in BV-associated biofilm, many studies have confirmed that presence of other BV-associated anaerobes enhances *G. vaginalis* biofilm and leads to BV presence.[65] Determination of the presence of bacteria in vaginal samples from women with BV compared to healthy asymptomatic women found that the BV group had presence of many facultative or obligate anaerobes.[108] A study looked at the co-aggregation capability of other BV-associated anaerobes with *G. vaginalis* and found varying degrees of co-aggregation, with bacteria like *A. vaginae* and *P. bivia* having the most pronounced effect.[63] qPCR quantification and confocal microscopy of clinical samples quantified and visualized *G. vaginalis* and *A. vaginae* and found that for any samples that *A. vaginae* was present, so was *G. vaginalis*, and together the bacteria were present in higher concentrations when compared to

samples with individual bacteria.[109] Therefore, *G. vaginalis* presence may be necessary for certain BV-associated anaerobes to grow.

Many studies have indicated a symbiotic relationship between *G. vaginalis* and *P. bivia* specifically, which leads to strengthened multi-species biofilm found in BV conditions. *Prevotella* is a genus of gram-negative obligate anaerobes known for their colonization of human mucosal surfaces.[110] Studies investigating the role of *Prevotella* species in vaginal colonization found that vaginal strains of this bacteria have distinct genetic makeups compared to oral strains.[111] *P. bivia* has sialidase activity for the degradation of the vaginal mucus, similar to *G. vaginalis*, which may be why *Prevotella* is often identified as a prominent species in polymicrobial BV-associated biofilm.[68] *P. bivia* produces ammonia, used by *G. vaginalis* during growth. In return *G. vaginalis* produces amino acids, which enhance the growth of *P. bivia*.[112] This highlights the symbiotic relationship between these two bacteria. A study looking at changes in the VMB during induction of BV through daily vaginal swab collection found decreases in *L. crispatus* bacteria and subsequent increases in *P. bivia*, *G. vaginalis* and *A. vaginae*, indicating the role of these bacteria in BV progression.[113] Colonization of mouse vaginal epithelium using clinical isolated *G. vaginalis* and *P. bivia* found that both bacteria could colonize the epithelium alone and in co-culture, with *P. bivia* growth increasing in the co-culture model.[114] Our lab showed that co-cultures of *G. vaginalis* and *P. bivia* on vaginal epithelial cells enhanced the adverse effects on barrier integrity and cell cytotoxicity seen with individual bacteria cultures.[45] Therefore, these bacteria may act as co-conspirators in biofilm formation and BV development, which has adverse effects in the FGT.

1.4.3 Strategies for Biofilm Treatment and Limitations

Bacteria use biofilm formation as a protective mechanism that sustains their viability. For example, biofilms are more resistant to antibiotics and antimicrobial agents, with some studies showing biofilm resistance is 10,000 times that of planktonic cells.[92] Biofilm matrix components have proven antimicrobial properties, with charged polysaccharides and eDNA able to trap many types of antibiotics and block penetration into the biofilm.[92] eDNA is cited as the most important component of the matrix for resistance to antibiotics.[115] Antibiotic resistance genes on plasmids of bacteria and frequent horizontal gene transfer can also lead to high levels of antibiotic resistance within a biofilm.[92] Other studies have indicated that expression of multi-drug resistance genes in bacteria within the biofilm contribute.[115] Bacteria encapsulated within the biofilm have a slower metabolic rate and reduced cell division compared to planktonic cells, which results in protection against antibiotics that target actively dividing cells.[92] Efflux pumps are also upregulated in biofilm communities and allow the removal of intracellular toxins such as antibiotics.[92]

Due to increased antibiotic resistance, different strategies for dissociation of biofilm has been an active field of study in recent years.[116] Antimicrobial peptides (AMP) are cationic amphipathic molecules produced by many organisms, and are integral parts of the human innate immune system.[117] AMPs have known antimicrobial effects which disrupt the bacterial membrane, cause leakage of cellular content, and destabilize the biofilm matrix.[115,117] A benefit of AMPs is the reduction in antibiotic resistance seen with these molecules and their broad spectrum use against a variety of pathogens.[115] The discovery of thiopeptides is a more recent antimicrobial product which shows promise as a broadly acting antibiotic.[118] Thiopeptides are complex, thiazole containing peptide antibiotics that act as protein synthesis inhibitors.[118] There

are only two thiopeptides available for commercial use currently, but these antibiotic molecules are promising solutions to combat biofilm formation.[118] Using enzymes that degrade EPS in the biofilm matrix is another strategy of interest for biofilm treatment.[115] Common enzymes that have been studied include DNase to degrade eDNA in the matrix, proteinase K to degrade extracellular proteins, and lysozyme to degrade exopolysaccharides.[115] Lastly, studies into the use of small molecule natural antimicrobials, like Subtilosin, ε-Poly-L-Lysine, and Lauramide Arginine Ethyl Ester, to combat BV-associated biofilm have been done in plate models, and the use of these molecules in combination with antibiotics have been effective against *G. vaginalis* biofilm, but does not prevent *Lactobacillus* biofilm growth.[119,120] These strategies in combination with antibiotic therapies show promising results for biofilm treatment.

1.4.4 Strategies for BV-associated Biofilm Dissociation

G. vaginalis biofilm in the FGT has increased resistance to antibiotics, such as metronidazole, which is the most common treatment for BV.[101] Due to the antibiotic resistant nature of biofilm formed on the vaginal epithelium, BV reoccurrence rates are very high after this treatment.[121] One study tested clinical isolates of biofilm forming *G. vaginalis* compared to planktonic strains of *G. vaginalis* and found that the biofilm forming strains required significantly higher minimum inhibitory concentration (MIC) of metronidazole to dissociate biofilm than the planktonic strains.[122] Therefore, different strategies for the dissociation of BV-associated biofilm is needed to combat this condition in the FGT.

One target for biofilm treatment is the biofilm matrix.[123] The matrix is accessible to the surrounding environment making it a primary target for enzyme degradation.[123] Breakdown of the biofilm matrix by enzyme degradation to dissociate biofilm is a promising treatment option.[123] Human lysozyme is a ubiquitous secretory enzyme that hydrolyses beta-1,4-glycosidic

bonds in bacterial peptidoglycan.[124,125] Lysozyme alone or in combination with an antibiotic caused complete dissociation and prevention of *G. vaginalis* biofilm growth in a plate model.[124] Lysozyme for biofilm treatment demonstrates complete inhibition of *G. vaginalis* biofilm growth at all tested concentrations.[125] Another target in the biofilm matrix is eDNA, which can be degraded by the enzyme DNase.[126] DNase treatment was effective for *G. vaginalis* biofilm dissociation in a plate.[126] Studying the effectiveness of these and other enzyme treatments for biofilm dissociation in a vaginal epithelial cell model would be a novel area of research.

Hormones have a large influence on the vaginal microenvironment, and estrogen presence can shift the VMB towards *Lactobacillus* dominance.[78] Estrogen treatment decreases anaerobic Gram-negative bacteria and increases the prevalence of *Lactobacillus*.[78,127] A phase one clinical trial testing the safety, tolerability, and feasibility of a low dose, intravaginal estradiol ring alone or in combination with a *Lactobacillus*-based probiotics was recently completed by our group.[128] The trial found that this treatment was a safe and acceptable intervention and phase two will focus on the ability of this treatment to enhance vaginal health through VMB analysis.[128] The specific interactions between endogenous sex hormones and VMB biofilm have not been studied and may provide a novel mechanism for biofilm dispersal and BV treatment.

The use of *Lactobacillus* probiotics for BV treatment has been a developing area of research. A trial conducted in 64 women taking oral *Lactobacillus*-based probiotics found that two months of treatment increased *Lactobacillus* presence in the VMB without negative side effects.[129] *L. crispatus* has a variety of mechanisms it uses to combat *G. vaginalis* pathogenesis. Genetic analysis of *L. crispatus* bacteria found antagonistic molecular factors to *G. vaginalis*, including proteins inhibitory towards *G. vaginalis* adherence and pili formation, which could

prevent *G. vaginalis* pathogenicity and colonization.[43] *L. crispatus* colonization in low pH conditions of an *in vitro* porcine vaginal mucosa model completely inhibited growth of *G. vaginalis* on the mucosa.[130] *L. crispatus* pre-colonization of a cervical epithelial cell line inhibited growth and repressed vaginolysin expression of BV-positive *G. vaginalis* strains.[131] Therefore, *L. crispatus* should be investigated further as a potential probiotic treatment for biofilm dissociation and BV treatment.

1.5 Experimental Models of the Vaginal Epithelium

Various models of the female genital tract have been used to study the diseases and infections, including *ex vivo* and *in vitro* models. These systems have advantages and disadvantages, with one common disadvantage being the inability to capture complete and complex structural and physiological components of the FGT.[132] However, one common advantage is the ability to recapitulate and manipulate models that resemble this organ system and focus on specific mechanisms and pathways relevant to the research being conducted.[132] *In vivo* animals models are the ideal experimental models which most closely resemble the complex physiology and structure of humans and is an emerging field in the study of VMB interactions and relation to infection. However, these models are beyond the scope of this project.

Ex vivo primary cell cultures from the FGT tissue are closely related to *in vivo* conditions and are important cultures system in this area of study.[132] Studies in our laboratory have used *ex vivo* primary genital epithelial cell models to research ways in which HIV presence in the FGT impacts epithelial barrier function, showing that the inflammatory state caused by the presence of HIV can decrease barrier strength.[10] *Ex vivo* primary endometrial and endocervical cell cultures in our laboratory have also been used to investigate immune responses to HIV.[133,134] Exposure of primary cell cultures to HIV or the gp120 envelope glycoprotein found that cytokine production

and decrease in barrier function of these cells is mediated through the toll-like recptor-2 and -4 (TLR2/TLR4) pathway and nuclear factor (NF)-kB activation.[133] Our laboratory used primary endometrial cell cultures exposed to HIV virus or gp120 protein and found that this resulted in activation of interferon regulatory factor 3 (IFR3) through the TLR2 pathway and induced interferon (IFN)-β production which significantly increased epithelial barrier function.[134]

Other laboratories have studied various aspects of female reproductive health in *ex vivo* primary cell models as well. One studied isolated CD8+ T cells from endometrial tissue to determine the influence of endogenous sex hormones on CD8+ cell cytotoxicity and found that exposure to estradiol can suppress the cytotoxic activity of these cells.[135] Another study used isolated stromal fibroblasts from different *ex vivo* tissues recovered from hysterectomy patients, and when primary endometrial fibroblasts were exposed to estrogen, interferon-stimulated genes MxA and OAS2 were upregulated.[136] *Ex vivo* models of ectocervical cells have been used to test common microbicides for HIV prevention, like Tenofovir, showing safety and efficacy of this treatment for *in vivo* use.[137] A study testing a combination antiretroviral therapy (cART), lopinavir, for pregnant women used first-trimester placentae and/or decidua parietalis *ex vivo* samples found that this drug may cause inadequate placentation and lead to the reported negative birth outcomes associated with this treatment.[138] *Ex vivo* models have also been used in studies of the VMB. VEC-100 tissues derived from primary ectocervical cells showed the colonization capabilities of different VMB associated bacteria and found that colonization with BV-associated bacteria *P. bivia* induced higher interleukin-8 (IL-8) and NFkB activation.[139] The use of primary human vaginal/ectocervical cells grown on cell inserts to form a multilayer culture found that *G. vaginalis* exposure to apical and basolateral face of the model elicits different cytokine responses.[103] While studies with *ex vivo* models are expansive and important representatives of *in*

vivo conditions, genital tract tissues can be difficult to acquire and variations in due to different organs from which cells are derived and age of donor can influence results generated with these models.[140]

1.5.1 *In vitro* Models of Vaginal Epithelial Cells

Various vaginal epithelial cells lines have been used in a wide range of studies focusing on female reproductive health. One study investigated the inflammatory response of A431 cells that form a three-dimensional epithelial tissue resembling human vaginal mucosa to common infections like *C. albicans,* and found significant increases in gene expression for cytokines like IL-8 and TNF-α when exposed to line bacteria.[141] Another important area of study using vaginal epithelial cell lines is HIV research, including assessments of novel strategies for combating HIV infection. HEC-1A endometrial adenocarcinoma cell lines have been used to test a novel microbicide, UAMC01398, against HIV-1 infection and confirmed the safety and efficacy of this product.[142] A study constructed a novel a recombinant adeno-associated virus (AAV) vector that encodes human b12 anti-HIV gp120 BnAb and used AAV-BnAb gene transfer into different cervico-vaginal epithelial cell lines, like ectocervical cells (Ectl/E6E7), endocervical cells (Endl/E6E7), and vaginal cells (VK2/E6E7) as a strategy to combat translocation of HIV virus.[143]

A common cell line for studies relating to the vaginal epithelium is the Vk2/E6E7 cell line. This cell line was developed from normal vaginal cells, which were immortalized using a retroviral vector expressing human papilloma virus (HPV) type 16 E6 and E7 (LXSN-16/E6E7).[144] The viral oncogenes in this vector increase epithelial cell proliferation without complete transformation of the cell line.[145] This cell line has been used in the presence of MPA and norethisterone (NET), hormonal contraceptives, and progesterone to show that these

compounds regulate gene expression of inflammatory cytokines in these cells.[146] Vk2 cells show expression of hemoglobin-a/b in Vk2 cells in response to lipopolysaccharide.[147] One study used Vk2 cells to assess immune modulation in the presence of lactic acid, and showed increases in interleukin-1b (IL-1b) and IL-8 production.[148] Vk2 cells have been used to investigate interactions with pathogenic fungi like *C. albicans,* and showed that cells cultured in high glucose conditions had increased colonization of this pathogen.[149] Vk2 cells have also been used to study vaginal epithelium interactions with HIV infection and the mechanisms that may lead to infection. HIV gp120 binding to Vk2 cells shows subsequent dose dependant increase in matrix metalloproteinase-9 (MMP-9).[150] A study used Vk2 cells to show that HIV translocation uses intracellular trafficking to the endocytic recycling pathway.[151] Vk2 cells have also been used to study the safety and efficacy of different vaginal drug delivery systems, like the use of clinically approved antimicrobials, such as Gino-Canesten®, Sertopic® and Dermofix® among others.[152] Vaginal epithelial cell lines can be cultured in a monolayer system in tissue cultures plates.[132] The resulting *in vitro* vaginal epithelial cultures have been shown to generate an innate immune response when exposed to TLR agonists, including significant levels of cytokines such as IL-6 and IL-1b.[153] Another option for culturing vaginal epithelial cell lines involves culture insert systems, or transwells, which creates separate apical and basal chambers for the study of cell secretions and cell migration among other assays.[132] This type of culture system also allows for the formation of liquid-liquid interface (LLI) cultures or air-liquid interface cultures (ALI).

Our laboratory commonly uses the Vk2/E6E7 cell line in either LLI or ALI transwell system. Vk2 cells have significant differences in morphology and physiology when cultured in ALI verses LLI conditions.[145] In our lab, Lee, Y et al. (2016) showed clearly using H&E staining, that when cultured in ALI conditions Vk2 cells form a multilayer of stratified squamous

epithelium while LLI cultures result in a monolayer of simple squamous epithelium. The multilayered nature of ALI cultures better mimic *in vivo* conditions as the vaginal epithelium is composed of stratified squamous epithelial cells.[145] Both ALI and LLI cultures of Vk2 cells were also able to produce cytokeratin proteins, which are important proteins in the cytoskeleton complex of epithelial cells.[145] Some papers have suggested that culturing vaginal epithelial cells in an ALI system results in the production of mucus[132], but a recent review of various culture systems for modelling the vaginal epithelium outlined that a drawback of Vk2 cells in ALI culture is that mucus production has not been reported.[154] Another study of ALI cultures determined that secretory material is visible on ALI cultures after extended culture time (2-3 weeks).[155] The presence of a mucus layer in cell culture would add another structural component that closely resembles *in vivo* conditions and should therefore be studied more closely in this culture system.

1.5.2 *In vitro* Models of VMB Biofilm

Evidence that the VMB has an impact on FGT health has led to development of models investigating the interactions between vaginal epithelial cells and the bacteria in the VMB. Many studies focus on interactions of the VMB-associated bacteria separately, which is commonly done in plate models.[63,64,72,122,156,157] The use of plate models is valuable to study different aspects of colonization, biofilm formation and pathogenicity, as well as biofilm treatment. Plate models have been used to visualize planktonic bacteria growth, as well as growth of single and dual-species biofilm with different techniques like staining, specific probes and various microscopy techniques.[63,64,72,157] Although biofilm formation in plate models makes visualization and quantification easy, it is not an accurate representation of the *in vivo* physiology of biofilms and their interactions with epithelial cells. Therefore, developing *in vitro* cell models that sustain

biofilms are important for visualization and quantification of biofilm as well as determination of protective or cytotoxic effects and the mechanisms behind these interactions. Common cell models in VMB biofilm colonization assays include HeLa cell lines (ATCC CCL-2), ME-180 epithelial cell lines (ATCC HTB-33), End1/E6E7 (ATCC CRL-2615) and Ect1/E6E7 cell lines (ATCC CRL-2614).[71,72,106,139] Vk2/E6E7 (ATCC CRL-2616) cell lines have been used to model bacteria colonization as well, but this is not as common. Previous research in our laboratory used Vk2/E6E7 cells in co-culture with VMB associated bacteria to determine the varying effects these bacteria have on epithelial cells.[45] This research showed that bacteria of the VMB can influence different aspects of vaginal epithelial cells such as barrier integrity, cell cytotoxicity and inflammatory cytokine production. However, there was no visualization aspect of this project to model biofilm formation on cells or quantification methods utilized to accurately measure biofilm formation. The creation of a vaginal epithelial cell and VMB associated bacteria co-culture system for visualization and quantification would allow for the study of specific mechanistic interactions between epithelial cells and bacteria biofilms, as well as the ability to test various strategies for treatment of BV-associated biofilm.

CHAPTER 2: RATIONALE AND HYPOTHESIS

HIV remains a widespread epidemic which disproportionately affects women worldwide.[1] Understanding the role the FGT plays in HIV infection is important as 40% of HIV transmission occurs in this area.[3] One aspect of the FGT, the VMB, can impact HIV susceptibility depending on the species of bacteria present.[28] A *Lactobacillus*-dominant, eubiotic state in the VMB is correlated with beneficial health effects and decreased risk of HIV infection through strengthening of the vaginal epithelial barrier, reduction in inflammation in the FGT and killing of pathogens.[27,34,35] Dysbiosis in the VMB, classified by presence of a variety of anaerobic bacteria, positively correlates with the clinical condition Bacterial Vaginosis (BV).[28,55] This condition, as well as VMB dysbiosis, is correlated with adverse health effects in women and increased risk of HIV infection through degradation of the vaginal epithelial barrier, epithelial cell cytotoxicity and increased inflammation.[28,56] Many studies have tried to characterize the various interactions between the VMB and the vaginal epithelium that contribute to these beneficial or harmful effects in the FGT. Human clinical trials, *ex vivo* cell models, and *in vitro* cells models have all been used to better understand the contributions of the VMB to general FGT health. *In vitro* cell models are most common as they are easy to establish and maintain and can be manipulated in ways that allow analysis of specific interactions and pathways.[71,72,106,139] However, lacking in many *in vitro* studies is the visualization and quantification of biofilm formation on epithelial cells. It has been well established that the pathogenicity of a dysbiotic VMB which leads to the development of BV is highly correlated with biofilm formation of dysbiotic bacteria on the vaginal epithelium.[71,98] One highly prevalent dysbiotic bacteria, *G. vaginalis*, is the driving factor for biofilm development and pathogenicity in the VMB and is

highly correlated with presence of the adverse health effects mentioned. Biofilm formation is a highly conserved mechanism of pathogenicity and survival among bacteria and leads to increased resistance to antibiotic treatment.[89] Modeling biofilm formation of eubiotic and dysbiotic bacteria on vaginal epithelial cells with specific visualization strategies for identifying and quantifying biofilm is lacking in literature. Creation of such model would provide valuable insight into the specific mechanisms that *Lactobacillus*-dominant biofilm or BV-associated bacteria biofilm use for either protection or pathogenicity in the FGT. This type of model could also be used to test various strategies for combating the formation of dysbiotic vaginal biofilm which may have implications for BV treatment and reduction in the susceptibility to HIV infection. Strategies for the enhancement of eubiotic biofilm formation could also be tested in this model for combating infection in the FGT.

Within that context, this thesis set out to characterize and optimize an *in vitro* model of biofilm formation on vaginal epithelial cells, then use this model to investigate biofilm and Vk2 cell interactions and test novel biofilm treatment strategies. Based on previous research in our laboratory, **we hypothesize that a *Lactobacillus* biofilm will enhance barrier function and decrease cytotoxicity of vaginal epithelial cells whereas *P. bivia* and *G. vaginalis* biofilm will decrease barrier function and induce cytotoxicity**. Moreover, based on previous literature establishing treatments for VMB biofilm formation and previous research in our laboratory, **we also hypothesize that various conditions, such as presence of estradiol and eubiotic short-chain fatty acids, will stimulate *Lactobacillus* biofilm growth and suppress *P. bivia* and *G. vaginalis* biofilm growth in a vaginal epithelial cell mode**l. Specifically, previous research has shown that *Lactobacillus* bacteria, such as *L. crispatus*, enhance barrier function, decrease cell cytotoxicity and reduce inflammation in vaginal epithelial cells.[45] Therefore, biofilm formation

by this bacterium on a vaginal epithelial cell line should generate similar results. Also, studies have shown that various conditions in the FGT, including presence of the endogenous sex hormone estrogen and presence of eubiotic metabolites, like lactic acid, promote *Lactobacillus* growth.[78,86] Therefore, the use of these conditions for *Lactobacillus* biofilm enhancement is a promising strategy for vaginal epithelial cell health. Previous research has also shown that dysbiotic, BV-associated bacteria such a *G. vaginalis* and *P. bivia*, decrease barrier function and increase cell cytotoxicity and inflammation in vaginal epithelial cells.[45] Therefore, biofilm formation by this bacterium on a vaginal epithelial cell line should generate similar results. Also, studies have shown that various conditions in the FGT, including presence of the endogenous sex hormone estrogen and presence of eubiotic metabolites, like lactic acid, promote shifts to *Lactobacillus* dominance and eubiosis in the VMB.[78,86] Therefore, the use of these conditions for dissociation of BV-associated bacteria biofilm and enhancement of *Lactobacillus* biofilm is a promising strategy to combat infection and BV presence in the FGT and lead to increased vaginal epithelial cell health.

The hypothesis was tested through two specific aims:

Aim 1: Establish an *in vitro* biofilm growth model using select bacteria present in the VMB in a Vk2 cell line modelling vaginal epithelium.

Aim 2: Determine the effect of biofilm growth on vaginal epithelial cells and test different strategies for suppression of *P. bivia* and *G. vaginalis* biofilm growth and enhancement of *Lactobacillus* biofilm growth on cells.

CHAPTER 3: MATERIALS AND METHODS

3.1 Vk2 Cell Culture

The Vk2/E6E7 vaginal epithelial cell line (ATCC CRL-2616) was obtained from the ATCC (Manassas, VA, USA). This cell line was derived from normal human vaginal mucosal tissue and immortalized by transduction with E6/E7 gene. Vk2 cells were cultured in keratinocyte serum free media (KSFM; Thermofisher, Cat.17005042) until 80% confluency at 37°C in 5% CO_2. When bacteria were inoculated on cells, antibiotic free keratinocyte serum free media (AF-KSFM) was used. Cells were washed with phosphate buffered saline (PBS), and trypsinized using 1X trypsin- EDTA. Dulbecco's Modified Eagle Medium F-12 (DMEM/F-12; Thermofisher, Cat. 12634- 010) containing 10% fetal bovine serum (FBS) was added to the trypsinized cells to deactivate the trypsin. The cell suspension was centrifuged at 1500 rpm for 5 min, the supernatant was decanted, and the cell pellet was resuspended in KSFM. Cell counting was performed by trypan blue exclusion assay using a hemocytometer. 60,000 cells were seeded on the apical side of 0.4 μm transwells (VWR, Cat. 82050-022) in 24 well plates. Two hundred microliters of KSFM was added to the apical side of the transwell after cell seeding and mixed well to ensure even cell distribution, and 700 μL of KSFM was added to the basolateral side. To create liquid-liquid interface (LLI) cultures, media remained on the apical side of the well for the remainder of the incubation. To create air-liquid interface (ALI) cultures, one day after seeding the apical media was aspirated. Vk2 cultures were subsequently incubated at 37°C for 7-10 days depending on the experiment. Media was changed every alternate day.

3.2 Vk2 Cell Culture in Hormone Conditions:

For some experiments, Vk2 cells were grown in ALI or LLI cultures as described in ***3.1 Vk2 Cell Culture*** in media containing different hormones conditions. Hormones were used in following

concentrations: estrogen (E2) = 10^{-9} M and progesterone (P4) = 10^{-7} M. Vk2 cells were grown in aerobic conditions with hormones for 6 days. Anaerobic incubation in the GasPak EZ Anaerobe Container System (Becton Dickenson, Cat, 260001) at 37°C in 5% CO_2 was done after 6 days of aerobic growth when bacteria was co-cultured on cells. Control cultures were kept in hormone free media.

3.3 Vk2 Cell Culture in Short Chain Fatty Acid (SCFA) Conditions:

For some experiments, Vk2 cells were grown in LLI cultures as described in ***3.1 Vk2 Cell Culture*** in media containing different SCFA conditions. SCFA were used in following concentrations: Eubiotic SCFA = lactic acid (100mM), acetic acid (4mM), succinic acid (0.1mM), butyric acid (0.1mM), Dysbiotic SCFA = lactic acid (20mM), acetic acid (40mM), succinic acid (10mM), butyric acid (2mM). Anaerobic incubation for 24h in the GasPak EZ Anaerobe Container System (Becton Dickenson, Cat, 260001) at 37°C in 5% CO_2 was done after 6 days of aerobic growth when bacteria was co-cultured on cells. Control cultures were kept in SCFA free media.

3.4 Vk2 Cell Culture in Sialidase Conditions:

For some experiments, Vk2 cells were grown in LLI cultures in hormone conditions as described in ***3.2 Vk2 Cell Cultures in Hormone Conditions***. After 6 days of aerobic growth Vk2 cells were subjected to a 2-h incubation with 0.2 U/mg of the sialidase enzyme on the apical side of the cultures. The sialidase enzyme was removed before bacteria was inoculated on cells. Anaerobic incubation for 24h in the GasPak EZ Anaerobe Container System (Becton Dickenson, Cat, 260001) at 37°C in 5% CO_2 was done after 6 days of aerobic growth when bacteria was co-cultured on cells. Control cultures were not subjected to sialidase enzyme incubation.

3.5 Transepithelial Resistance (TER):

TER measurements to assess barrier integrity were taken using a voltohmmeter (World Precision Instruments). For ALI cultures, 200 µL of KSFM media was added to the apical well and incubated for 1 h at 37°C prior to TER measurement, then removed upon completion of TER measurements. TER assessment was presented as either raw TER values (Ohms/cm^2) for a specific day, or as % Pre-treatment TER: (TER of culture after treatment / TER of culture before treatment)*100%. The effect of anaerobic conditions on the Vk2 cells was determined by % pre-treatment TER: (TER of 48 h anaerobic culture / TER of 7 day aerobic culture)*100%. The effect of bacteria on the Vk2 cells was determined by % pre-treatment TER: (TER of bacteria and Vk2 cell co-cultures / TER of the Day 6 Vk2 cell culture before bacteria was added)*100.

3.6 Cell Viability via Lactate Dehydrogenase (LDH) Assay:

To evaluate cell viability, lactate dehydrogenase (LDH) assays were performed according to manufacturer's instructions using apical culture supernatants and maximum cell lysis supernatants as positive controls (Thermofisher, Cat. 88953). Maximum lysis controls were created by adding in 50 µL of lysis buffer provided in the kit to 9-day old ALI or LLI Vk2 cultures. To determine LDH activity, the value obtained at 680 nm (background) was subtracted from the values obtained at 490 nm (absorbance value) for each sample. Cell cytotoxicity was determined by comparing the LDH activity of each condition to the LDH activity of the maximum lysis control.

3.7 Mucin Production by Vk2 Cells:

Cell-associated mucin production by Vk2 cells from day 1 to day 10 of culture was evaluated by immunofluorescent technique. Vk2 cells were grown in duplicate for 10 days. LLI culture

supernatants were collected before fixing and stored at -20°C to analyze for secreted mucin. 200 µL of KSFM media was added to the apical side of the ALI wells, and after 2h of incubation, the apical supernatant was collected and stored at -20°C to analyze for secreted mucin by Human Carbohydrate Antigen 15-3 Mucin-1 ELISA Kit (Sigma Aldrich #RAB0375). ELISA Standards were made following assay kit instructions instructions. All samples and standards were added into a 96-well sterile flat bottom cell culture plate in 100 µL aliquots following the specified plate layout. The ELISA procedure was followed as per the kit instructions and absorbance was measured at 450nm on SpectraMax i3 spectrophotometer. Protein concentration (mU/mL) of samples was extrapolated from standard curve created using Standard absorbance values. Cells were fixed using 4% paraformaldehyde for 10min, washed with PBS 3 times, and stored protected from light at 4°C with 50 µL of PBS remaining in each well to prevent drying out of cells until staining was performed. Detection of mucin-1 on Vk2 cell surface was performed using 1:100 mouse anti-human MUC1 (CD227) antibody (BD PharmingenTM) in blocking solution (5% goat serum, 5% BSA, 0.1% Triton X-100 in PBS) for 1h at room temperature. Cells were washed 3 times with PBS, then incubated with 100 µL of goat anti-mouse Alexa Fluor 488 secondary antibody (Life Technologies; 1:1000 dilution in blocking solution) for 1 h at room temperature protected from light. After extensive washing, transwell membranes were excised from the polystyrene inserts and mounted on glass slides in mounting medium containing DAPI (Vector Labs, Burlingame, CA, USA). All samples were imaged on an inverted confocal laser-scanning microscope (Nikon Eclipse Ti2) using standard operating conditions (63× objective, optical laser thickness of 1µm, image dimension of 512 × 512, lasers: green 488 nm and red 594 nm laser lines). Mean Fluorescence Intensity (MFI) is a unit of measurement for fluorescence quantification used in all experiments where fluorescence is visualized and measured in this

project. MFI was quantified using mean gray area analysis in ImageJ from 2-3 randomly selected fields of view per well. Duplicate image quantification was averaged and reported (MFI).

3.8 Bacterial Stock Preparation:

Lactobacillus crispatus SJ-3C-US (PTA10138) from ATCC was provided by Dr. Nuch Tanphaichitr (University of Ottawa). *Prevotella bivia* (ATCC 29303), *Gardnerella vaginalis* (ATCC 14019) and *Lactobacillus iners* (ATCC 55195) were purchased from ATCC. *L. crispatus* was grown in ATCC medium 416 (*Lactobacillus* MRS broth/agar), *G. vaginalis* and *L. iners* were grown in ATCC medium 1685 (NYC III medium), and *P. bivia* was grown in ATCC medium 2107 (Modified Reinforced Clostridial (MRC) medium) at 37°C in anaerobic conditions using the GasPak EZ Anaerobe Container System (Becton Dickenson, Cat, 260001). Glycerol (20%) stocks were made for each bacterium and stored at -80°C for future use. The bacterial stock concentration was determined through serial dilutions plated onto MRS Agar (*L. crispatus*), tryptic soy agar supplemented with 5% sheep's blood *(L. iners* and *G. vaginalis*) or Columbia agar supplemented with 5% sheep's blood (*P. bivia*) to determine Colony Forming Units (CFU)/mL by the Miles and Misra technique.[158] *Pseudomonas aeruginosa* (ATCC BAA-47) was generously provided by Dr. Lori Burrows and was grown in ATCC medium 1634 (LB broth/agar).

3.9 Bacterial Growth Curve:

Bacteria was inoculated into the appropriate broth and grown for 24 h at 37°C in anaerobic conditions using the GasPak EZ Anaerobe Container System (Becton Dickenson, Cat, 260001). A 500 µL aliquot of grown culture was inoculated into 5 mL of fresh medium. The growth of

culture was tracked for 24 h, taking Optical Density at 600nm (OD_{600}) and CFU/mL measurements at 2 h time intervals.

3.10 Biofilm Growth in a Plate Model:

Bacteria stock was thawed, inoculated into broth and grown for 24 h at 37°C in anaerobic conditions using the GasPak EZ Anaerobe Container System. A 500 µL aliquot of grown culture was inoculated into 5 mL of fresh media. Cultures were grown at 37°C in anaerobic conditions using the GasPak EZ Anaerobe Container System until log phase was reached. *P. aeruginosa* (positive control) was grown for 24 h at 37°C in aerobic conditions with shaking at 250 rpm. Once cultures were grown, they were then serially diluted 1:10 in PBS and plated using two different methods. Twenty-four well sterile flat bottom cell culture plates were seeded with 500 µL of the first 5 culture dilutions, and 96-well sterile flat bottom cell culture plates were seeded with 200 µl of the first 5 culture dilutions in triplicate. Negative control wells contained broth medium only without bacteria. Plates were incubated at 37°C in anaerobic conditions using the GasPak EZ Anaerobe Container System. A separate plate was used for *P. aeruginosa* and was incubated at 37°C in aerobic conditions with shaking at 250 rpm. Different plates were used to test various incubation times (24 – 48 h). After the incubation period, excess broth was removed, and each well was washed twice with PBS. Plates were shaken vigorously with each wash to remove non-adherent bacteria. Remaining attached bacteria were fixed with 500 µL (24-well plate) or 200 µL (96-well plate) of 99% methanol per well for 15min. Methanol was removed, and once dry, plates were stained with 500 µL (24-well plate) or 200 µL (96-well plate) of 2% crystal violet stain per well for 15min. Excess stain was rinsed off with running tap water and plates were left to air dry. 24-well plates were imaged using an EVOS FL Life Technology Microscope. For 96-well plates, dye bound to adherent cells was re-solubilized with 160 µL of

33% (v/v) glacial acetic acid per well. The absorbance of each well was measured at 570 nm using a SpectraMax i3 spectrophotometer. The Abs_{570} of the biofilm was compared to the negative control (negative control = average Abs_{570} of negative control + (3XSD of negative control) to classify the biofilm forming capability into four categories (adapted from Stepanovic S, et al. 2000. *J Microbiol Methods* **40**):

Non-adherent: $Abs_{570} \leq$ negative control

Weak Biofilm adherence: $Abs_{570} \leq 2$ x negative control

Moderate Biofilm adherence: $Abs_{570} \leq 4$ x negative control

Strong Biofilm adherence: Abs_{570} > negative control X 4

3.11 Biofilm eDNA & Matrix Protein Staining in Plate Model:

Bacteria were grown in a 24-well plate model according to ***3.10 Biofilm Growth in a Plate Model***. After the incubation period, excess broth media was aspirated then each well was washed twice with 0.9% saline solution and vigorous shaking to remove non-adherent bacteria. Wells were stained with 500 µL of 1 µM SYTOX Green eDNA stain (Molecular Probes Invitrogen Detection Technologies), which binds to DNA in the sample, for 10 min or 500 µL of FilmTracerTM SYPRO® Ruby Biofilm Matrix stain (Molecular Probes Invitrogen Detection Technologies), which labels most classes of proteins, including phosphoproteins, fibrillar proteins, and other proteins in the biofilm matrix that are difficult to stain, for 30 min at room temperature. Images were taken on an EVOS FL Life Technology microscope. MFI was quantified using images from 2 randomly selected fields of view per well and mean gray area

analysis of each image on imageJ. Duplicate image quantification was averaged and reported as MFI.

3.12 Biofilm Growth in a Vk2 Cell Co-culture Model:

Bacteria stock was thawed, inoculated into broth and grown for 24 h at 37°C in anaerobic conditions using the GasPak EZ Anaerobe Container System. A 500 µL aliquot of grown culture was inoculated into 5 mL of fresh media in 15 mL polypropylene tubes containing 5 mL of appropriate broth and grown at 37°C in anaerobic conditions. Cultures were grown until cell density of 6,000,000 CFU/mL was reached as determined by specified culture inoculation time based on bacteria specific growth curve and confirmed with CFU/mL measurement. The grown bacteria culture tube was then centrifuged at 4000 rpm for 5 min. Excess media was decanted, and the pellet was resuspended in 10 mL PBS for a washing step. The culture was centrifuged again at 4000 rpm for 5 min. PBS was decanted, and the bacteria pellet was resuspended in AF-KSFM. An aliquot of 200 µL of bacteria cell suspension was added to the apical side of an already 6-day grown Vk2 cell ALI or LLI culture plate in AF-KSFM in duplicate. Negative control wells contained no bacteria in the apical media. The cultures were grown for a specified time period (24 - 48 h) at 37°C in anaerobic conditions.

3.13 Biofilm Matrix eDNA and Matrix Protein Staining in a Vk2 Cell Co-culture Model:

Biofilm of various bacteria were grown in an ALI or LLI Vk2 cell co-culture system according to ***3.12 Biofilm Growth in a Vk2 Cell Culture Model***. After the incubation period, the excess apical media was aspirated, and each well was washed twice with 0.9% saline solution. Plates were shaken vigorously with each wash to remove non-adherent bacteria. For matrix eDNA staining, apical wells were stained with 200 µL of a 1µM SYTOX Green eDNA stain for 10 min before fixing. For matrix protein stain, remaining attached bacteria were fixed with 200 µL of

4% PFA per well for 10 min. PFA was removed, and wells were washed twice with 0.9% saline than stained with 200 µL of FilmTracerTM SYPRO® Ruby Biofilm Matrix stain for 30 min. Transwell membranes were excised from the polystyrene inserts and mounted on glass slides in mounting medium containing DAPI. Images taken on Nikon eclipse Ti2 confocal laser scanning microscope. MFI was quantified using 2 different methods depending on the experiment. The first method used z-stack images from 2 randomly selected fields of view per well. Mean gray area analysis was conducted for each frame of the 20-step z-stack image on imageJ. Z-stack mean gray area was averaged, then duplicate image quantification was averaged and reported as MFI. The second method used 2-3 2D images from randomly selected fields of view per singular well. Mean grey area quantification on imageJ for each image was averaged and reported as MFI.

3.14 Biofilm Protein Quantification by BCA Assay in a Vk2 Cell Model:

Biofilms were grown in a LLI Vk2 cell co-culture system for 24 h. After the incubation period, the excess culture was removed, and each well was washed twice with 0.9% saline solution. A 50 µL aliquot of Pierce® RIPA protein lysis buffer (Thermo scientific, Cat. 89901) was added to wells and mixed thoroughly, then incubated for 30 min on ice. After incubation, well supernatants were mixed thoroughly again, collected and pooled for triplicate wells into properly labelled tubes. Samples were diluted 1:2 into RNase free water. BCA Assay Standards were made following Pierce™ Bicinchoninic acid (BCA) Protein Assay Kit (Thermo scientific, Cat. 23227) instructions. Working Reagent was made following the instructions for the same kit. All samples and standards were added into a 96-well sterile flat bottom cell culture plate in 10 µL aliquots following the specified plate layout. The working reagent was added to each well in 200 µL aliquots and the plate was covered with foil. The plate was mixed by shaking on plate shaker

for 30 s, then the plate was incubated at 37°C for 30 min. The plate was cooled to room temperature and absorbance was measured at 562nm on SpectraMax i3 spectrophotometer. Protein concentration of samples was extrapolated from standard curve created using Standard absorbance values.

3.15 Gram-positive Bacteria Antibody Staining in a Vk2 Cell Co-culture Model:

The detection of Gram-positive bacteria was tested on *L. crispatus*, *L. iners* and *G. vaginalis* bacteria using a mouse monoclonal anti-LTA (sc-58135) antibody (Santa Cruz Biotechnology Inc.). *L. crispatus*, *L. iners* and *G. vaginalis* were grown on Vk2 cells according to ***3.12 Biofilm Growth in a Vk2 Cell Culture Model***. After the incubation period, the excess apical media was aspirated, and each well was washed twice with 0.9% saline solution. Plates were shaken vigorously with each wash to remove non-adherent bacteria. Bacteria were fixed with 4% PFA for 10 min. PFA was removed, and plates washed twice with 0.9% saline. Anti-LTA antibody (0.5µg/mL) was added to each well and incubated for 1 h at room temperature. Cells were washed with 0.9% saline twice and goat anti-mouse Alexa Fluor 488 (Life Technologies) diluted 1:1000 in blocking solution (5% goat serum, 5% BSA, 0.1% Triton X-100 in PBS) was added, and wells were incubated for 1 h protected from light. Wells were washed twice with 0.9% saline. Transwell membranes were excised from the polystyrene inserts and mounted on glass slides in mounting medium containing DAPI. Images were taken on Nikon eclipse Ti2 confocal laser scanning microscope. MFI was quantified using the z-stack method as described in ***3.13 Biofilm Matrix eDNA and Matrix Protein Staining in a Vk2 Cell Co-culture Model*.**

3.16 Dual Bacteria and Biofilm Staining in Vk2 Cell Model:

Bacteria biofilm was grown in a LLI Vk2 cell co-culture system for 24h according to ***3.12 Biofilm Growth in a Vk2 Cell Culture Model***. After the incubation period, the excess culture was removed, and each well was washed twice with 0.9% saline solution. Plates were shaken vigorously with each wash to remove non-adherent bacteria. Wells were fixed with 4% PFA per well for 10 min. PFA was removed, and plates washed twice with 0.9% saline. Gram-positive antibody staining was conducted as per ***3.15 Gram-positive Bacteria Antibody Staining in Vk2 Cell Model.*** Next, wells stained with FilmTracerTM SYPRO® Ruby Biofilm Matrix stain for 30 min. Transwell membranes were excised from the polystyrene inserts and mounted on glass slides in mounting medium containing DAPI. Images taken on Nikon eclipse Ti2 confocal laser scanning microscope. MFI for each stain was quantified using the z-stack method as described in ***3.13 Biofilm Matrix eDNA and Matrix Protein Staining in a Vk2 Cell Co-culture Model.***

3.17 Peptide Nucleic Acid Fluorescence in-situ Hybridization (PNA FISH):

PNA FISH protocol was adapted from Machado *et al. BMC Microbiology* 2013, **13**:82. Peptide nucleic acid (PNA) probe Gard162 (Cy5-OO-CAGCATTACCACCCG) for identification of *G. vaginalis* was designed from sequence provided in the cited paper and ordered from PNA Bio Inc. The fluorescence in-situ hybridization (FISH) protocol was as follows: *G. vaginalis* biofilm was grown on Vk2 cells for 24h according to ***3.12 Biofilm Growth in a Vk2 Cell Culture Model***. After the incubation period, the cells were fixed with 4% PFA followed by 50% ethanol for 10 min each. After fixation, hybridization solution containing 10% (wt/vol) dextran sulphate, 10 mM NaCl, 30% (vol/vol) formamide, 0.1% (wt/vol) sodium pyrophosphate, 0.2% (wt/vol) polyvinylpyrrolidone, 0.2% (wt/vol) ficoll, 5 mM disodium EDTA, 0.1% (vol/vol) triton X-100, 50 mM Tris-HCl at pH 7.5 and 200 nM of the PNA probe was added to wells. Plate was

incubated for 90 min in moist 60°C water bath for hybridization. Next, wells were washed with pre-warmed washing solution (5 mM Tris-base, 15 mM NaCl, 0.1% (vol/vol) triton X-100 at pH 10) for 30 min in moist 60°C water bath. Wells were then air dried before transwell membranes were excised from the polystyrene inserts and mounted on glass slides in mounting medium containing DAPI. Images were captured on Nikon eclipse Ti2 confocal laser scanning microscope.

3.18 Biofilm Matrix Protein Staining in Hormone Containing Media in a Vk2 cell Model:

Vk2 cells cultures were grown in hormone containing media as described in ***3.2 Vk2 Cell Culture in Hormone Conditions.*** Bacteria were cultured on Vk2 cells as per ***3.12 Biofilm Growth in a Vk2 Cell Co-culture Model***, except for bacteria pellet re-suspension in hormone containing AF-KSFM. Bacteria biofilm was grown in a LLI Vk2 cell co-culture system for 24 h. After the incubation period, the excess culture was removed, and each well was washed twice with 0.9% saline solution. Plates were shaken vigorously with each wash to remove non-adherent bacteria. Wells were fixed with 4% PFA per well for 10 min. PFA was removed, and plates washed twice with 0.9% saline. Wells were stained with FilmTracerTM SYPRO® Ruby Biofilm Matrix stain for 30 min. Transwell membranes were excised from the polystyrene inserts and mounted on glass slides in mounting medium containing DAPI. Images taken on Nikon eclipse Ti2 confocal laser scanning microscope. MFI was quantified using the 2D image method as outlined in ***3.13 Biofilm Matrix eDNA and Matrix Protein Staining in a Vk2 Cell Co-culture Model.***

3.19 Biofilm Matrix Protein Staining in SCFA Containing Media in a Vk2 cell Model:

Vk2 cells cultures were grown in short-chain fatty acid (SCFA) containing media as described in ***3.3 Vk2 Cell Culture in SCFA conditions.*** Bacteria were cultured on Vk2 cells as per ***3.12***

Biofilm Growth in a Vk2 Cell Co-culture Model, except for bacteria pellet re-suspension in SCFA containing AF-KSFM. Bacteria biofilm was grown in a LLI Vk2 cell co-culture system for 24 h. After the incubation period, the excess culture was removed, and each well was washed twice with 0.9% saline solution. Plates were shaken vigorously with each wash to remove non-adherent bacteria. Wells were fixed with 4% PFA per well for 10 min. PFA was removed, and plates washed twice with 0.9% saline. Wells were stained with FilmTracerTM SYPRO® Ruby Biofilm Matrix stain for 30 min. Transwell membranes were excised from the polystyrene inserts and mounted on glass slides in mounting medium containing DAPI. Images taken on Nikon eclipse Ti2 confocal laser scanning microscope. MFI was quantified using the 2D image method as outlined in ***3.13 Biofilm Matrix eDNA and Matrix Protein Staining in a Vk2 Cell Co-culture Model.***

3.20 Biofilm Matrix Protein Staining in a Mucin Deficient Vk2 cell Model:

Bacteria biofilm was grown in a LLI Vk2 cell co-culture system for 24 h as per ***3.12 Biofilm Growth in a Vk2 Cell Co-culture Model***. Two hours prior to bacteria inoculation on cells, 0.2 U/mg of sialidase enzyme (Roche, Cat. # 11 080 725 001) was inoculated onto treatment group of cells for mucin degradation as described in ***3.4 Vk2 Cell Culture in Sialidase Conditions***. Sialidase enzyme was removed, and bacteria was inoculated on cells by normal protocol. After the incubation period, the excess culture was removed, and each well was washed twice with 0.9% saline solution. Plates were shaken vigorously with each wash to remove non-adherent bacteria. Wells were fixed with 4% PFA per well for 10 min. PFA was removed, and plates washed twice with 0.9% saline. Detection of mucin-1 production on Vk2 cell surface was performed for all wells using mouse anti-human MUC1 (CD227) antibody (BD PharmingenTM); 1:100 dilution in blocking solution: 5% goat serum, 5% BSA, 0.1% Triton X-

100 in PBS. Next, wells were stained with FilmTracerTM SYPRO® Ruby Biofilm Matrix stain for 30 min. Transwell membranes were excised from the polystyrene inserts and mounted on glass slides in mounting medium containing DAPI. Images were taken on Nikon eclipse Ti2 confocal laser scanning microscope. MFI was quantified using the 2D image method as outlined in ***3.13 Biofilm Matrix eDNA and Matrix Protein Staining in a Vk2 Cell Co-culture Model.***

3.21 Bacteria qPCR Standard Curve Determination:

A qPCR standard curve was constructed for each bacteria of interest in this project to quantify the number of bacteria growing in the biofilm and Vk2 cell co-culture model. Various bacteria cultures of 1 mL quantity were grown to their exponential phase of growth as determined by ***3.10 Biofilm Growth in a Plate Model***. CFU/mL of each culture was determined using the standard method. Cultures were pelleted and re-suspended with 180 µL of Enzymatic Lysis Buffer (20mM Tris-Cl, 2mM sodium EDTA, 20 mg/mL Lysozyme from chicken egg white (Sigma-aldrich, CAS. 12650-880-3)) and incubated for 30 min at 37°C. DNA was extracted from each sample using the DNeasy® Blood & Tissue Kit (Qiagen, Cat. 69506) protocol. Next, 6-7 10-fold dilutions of stock extracted DNA for each bacterium was made depending on the starting culture CFU/mL. Real-time qPCR was performed using 5 µL of 1:10 diluted DNA samples, 7 µL of RNAse-free water, 12.5 µL of 2x RT2Real-Time SYBR® Green PCR master mix (Qiagen, Cat. 330523) and 0.25 µL of each forward and reverse bacteria-specific primers (Table 1) as received from the manufacturer (Integrated DNA Technologies) (100 µM), for each well. The Step OneTMReal-Time PCR system (Thermo Fisher Scientific, Canada) was used with settings as followed: Hot start 95°C; followed by 40 cycles at 95°C for 3 s, 49.5°C for 30 s, and 1 cycle at 72°C for 2 min. Hold at 4°C. Samples were run in triplicates. Standard curve was constructed by plotting Ct value against $Log_{CFU/mL}$ for each bacterium.

Table 1. Primer sequences for bacteria of interest in this project for qPCR quantification.

Bacteria	Forward Sequence	Reverse Sequence
L. crispatus	GATTTACTTCGGTAATGACGTTAGGA	AGCTGATCATGCGATCTGCTTTC
L. iners	TTGAAGATCGGAGTGCTTGC	TTATCCCGATCTCTTGGGCA
G. vaginalis	GGAAACGGGTGGTAATGCTGG	CGAAGCCTAGGTGGGCCATT
P. bivia	CTGCGCTTGGTCCTGGTGGTT	CTTCAGGCGACTCAATAGGACACAAA

3.22 Bacteria Quantification by qPCR in a Vk2 Cell Co-culture Model:

Bacteria biofilm was grown in a LLI Vk2 cell co-culture system for 24 h as per ***3.12 Biofilm Growth in a Vk2 Cell Co-culture Model***. After the incubation period, the excess culture was removed, and each well was washed twice with 0.9% saline solution. 180 µL of Enzymatic Lysis Buffer (20mM Tris-Cl, 2mM sodium EDTA, 20 mg/mL Lysozyme from chicken egg white (Sigma-aldrich, CAS. 12650-880-3)) was added to wells and mixed thoroughly, and incubated for 30 min at 37°C. After incubation, well supernatants were mixed thoroughly again, collected and pooled for triplicate wells into properly labelled tubes. DNA was extracted from each sample using the DNeasy® Blood & Tissue Kit (Qiagen, Cat. 69506) protocol. Real-time qPCR was performed using 5 µL of DNA samples, 7 µL of RNAse-free water, 12.5 µL of 2x RT2Real-Time SYBR® Green PCR master mix (Qiagen, Cat. 330523) and 0.25 µL of the forward and reverse bacteria-specific primers (Table 1) as received from the manufacturers (Integrated DNA Technologies) (100 µM), for each well. The Step OneTMReal-Time PCR system (Thermo Fisher Scientific, Canada) was used with settings as followed: Hot start 95°C; followed by 40 cycles at 95°C for 3 s, 49.5°C for 30 s, and 1 cycle at 72°C for 2 min. Hold at 4°C. Samples were run in triplicates. Bacteria quantification (CFU/mL) for each sample was determined through extrapolation from the qPCR standard curve of each bacteria previously created.

CHAPTER 4: RESULTS

4.1 Establish an *in vitro* biofilm growth model using select bacteria present in the VMB in a Vk2 cell line modeling vaginal epithelium

Previous studies have described *in vitro* models of bacteria colonization on epithelial cells lines.[72,106,139] However, visualization and quantification of biofilm formation on vaginal epithelial cells has not been established *in vitro*. Our lab has previously conducted experiments using co-cultures of vaginal bacteria and the Vk2 vaginal epithelial cell line to determine the varying effects on epithelium barrier integrity, cytotoxicity and cell viability of vaginal bacteria.[45] The missing aspect of this study was visualization of biofilm growth on Vk2 cells. In this aim, an *in vitro* model of vaginal bacteria biofilm growth on Vk2 cells was optimized. A novel way of visualizing and quantifying biofilm growth on an *in vitro* cell line was established. This aim was necessary to complete before testing different strategies for modifying biofilm growth, which was the focus of the second aim.

4.1.1 Characterize and optimize a Vk2 cell culture system for visualizing biofilm growth.

The optimal vaginal cell line and culture conditions that support vaginal bacteria biofilm growth were determined. The Kaushic lab commonly uses the Vk2/E6E7 (ATCC CRL-2616) cell line, an immortalized vaginal epithelial cell line, in either LLI or ALI cultures in a transwell model.[145] Vk2 cells have significant differences in morphology and physiology when cultured in ALI versus LLI conditions. The multilayered nature of ALI cultures better mimic *in vivo* conditions as the vaginal epithelium is composed of stratified squamous epithelial cells. However, it is not known if the multi-layered nature of ALI cultures may pose problems for biofilm growth *in vitro*. The monolayer provided by LLI cultures may be more ideal for this model. The different morphology of these culture systems may have differing impacts on

bacterial biofilm growth so ALI and LLI cultures were both tested during the optimization of the model. Vk2 cells were grown on cell cultures inserts under specific conditions as described in Materials and Methods (M&M 3.1) to generate LLI and ALI cultures.

In *in vivo* conditions vaginal epithelial cells are constantly exposed to an oxygen deficient environment.[159] The oxygen level in culture systems is not 21% as found in the air.[160] However, is it not known what the oxygen level in specific culture systems is and how it compares to *in vivo* organ systems. Regardless, an oxygen deficient environment is an important aspect of *in vivo* conditions to mimic in this project. Also, all bacteria being utilized in this project are either facultative anaerobes or strict anaerobes, meaning they need to be grown in oxygen deficient conditions.[33,75,161] Since the goal of Aim #1 was to create a co-culture model of bacteria and Vk2 cells, it was important to ensure that the viability of Vk2 cells was not compromised in anaerobic conditions. It was also important to ensure that different factors, such as cellular barrier integrity and cell viability, were not altered in anaerobic conditions, since these methods were used in Aim #2 to test biofilm growth effect on cells *in vitro*, and that any changes in barrier integrity and cell viability was in fact due to biofilm formation and not the lack of oxygen in culture conditions. There is currently no model to determine if vaginal epithelial cell cultures in ALI or LLI conditions are viable in a low oxygen environment.[154] Previous work in this lab optimized Vk2 cells grown in ALI cultures in low oxygen conditions by examining TER and trypan blue exclusion assay as indicators of cell viability. The current project confirmed that Vk2 cells in ALI and LLI cultures remained viable in oxygen deficient conditions using both TER measurements and lactate dehydrogenase (LDH) cytotoxicity assay (M&M 3.5 & 3.6). Vk2 cells were grown on two different plates in ALI and LLI cultures for 7 days in normal *in vitro* conditions and then either continued in normal incubation conditions or were transferred to

anaerobic chambers to grow in oxygen deficient conditions for 48 h. TER was not significantly reduced in any of the culture conditions when comparing the Day 7 TER measurement to the Day 9 TER measurement (Figure 1). LDH measurements in all culture conditions were significantly different from the positive control, indicating a lack of cell cytotoxicity and cell death (Figure 1). Therefore, anaerobic incubation conditions did not impact barrier integrity or cytotoxicity of Vk2 cells in ALI or LLI cultures.

Bacteria present in a eubiotic VMB, such as *L. crispatus*, have a mutualistic relationship with the vaginal epithelium, and strong adherence to the epithelium can positively influence the composition of the cervicovaginal mucus (CVM). A *G. vaginalis*-dominant VMB utilizes the CVM for attachment by degrading mucins through secretion of sialidase.[61] One study found that an *L. crispatus*-dominant VMB increased D-lactic acid in the CVM, which stimulated better trapping of HIV virus and a CVM colonized by a *G. vaginalis*-dominant VMB has reduced trapping of HIV virus.[162] The determination of mucin presence in this model of the vaginal epithelium with bacteria co-culture is important since dysbiotic bacteria use mucins as an energy source for colonization. The specific mechanisms that a *Lactobacillus*-dominant VMB use to enhance CVM trapping of pathogens and overall protection against infection could be analyzed in this model. Some papers have suggested that culturing vaginal epithelial cells in an ALI system results in the production of mucus[132], but a recent review of various culture systems for modelling the vaginal epithelium outlined that a drawback of Vk2 cells in ALI culture is that mucus production has not been reported.[154] Therefore, determination of mucin presence in both ALI and LLI cultures in a Vk2 cell line would be a novel aspect of this project.

Mucin was examined in the Vk2 cell line in both ALI and LLI culture systems by immunofluorescent staining using a specific mucin-1 antibody. Mucin-1 antibody staining for

ALI Vk2 cells in different hormone conditions over 10-day period (Figure 2A) and quantification by mucin-1 fluorescence on ImageJ (Figure 2B) was conducted (M&M 3.2&3.7). Culture supernatants were collected on different days to test for secreted mucin by using mucin-1 ELISA (Figure 2C) (M&M 3.7). Mucin production was present in all hormone conditions. An enhancement of cell surface expressed and secreted mucin production in cultures where estradiol was present was found when compared to cells cultured with progesterone containing media. There was an obvious peak in mucin production, both cell surface expressed and secreted, between Day 6 – Day 10 of culture. This experiment was repeated in ALI and LLI cultures in both aerobic and anaerobic conditions to determine if lack of oxygen influenced mucin production. As described in M&M 3.7, immunofluorescent staining for mucin-1 in varying cell culture conditions was performed between day 6 to day 9 of growth as mucin production peaked between 6-9 days of culturing cells in previous experiments (Figure 3A). Figure 3B shows that there was a significant decrease in mucin production in ALI cultures at day 8 and 9, or 72 and 96 h after switching cells from aerobic to anaerobic incubation compared to cells grown in aerobic conditions. LLI cultures tolerated anaerobic conditions better than ALI cultures and showed no significant differences in mucin production between aerobic and anaerobic incubation (Figure 3C). For ALI and LLI cultures in aerobic and anaerobic conditions (Figure 3D-E), aerobic conditions had no major differences in mucin production between these culture systems. However, mucin production in LLI cultures was more consistent in anaerobic conditions compared to ALI cultures. Whereas in ALI cultures we saw significant decrease in mucin production after 48 h incubation, in LLI cultures mucin production was maintained or slightly higher. This experiment was also repeated for both ALI and LLI Vk2 cell cultures in various hormone conditions (M&M 3.2&3.7) (Figure 4). ALI cultures grown in estradiol containing

media in both aerobic and anaerobic conditions showed significant increases in mucin-1 production on all days, except day 8 (Figure 4A-B). LLI cultures did not show as many differences in mucin-1 production between the hormone conditions, with cultures grown in estradiol containing media showing increases at Day 6 in aerobic conditions and day 7 in anaerobic conditions (Figure 4C-D).

In summary, Vk2 cells in ALI and LLI conditions produced mucin-1, which peaked between 6-10 days. Mucin production was not decreased in either culture system after 48 h of anaerobic incubation, therefore this time point was used in future experiments.

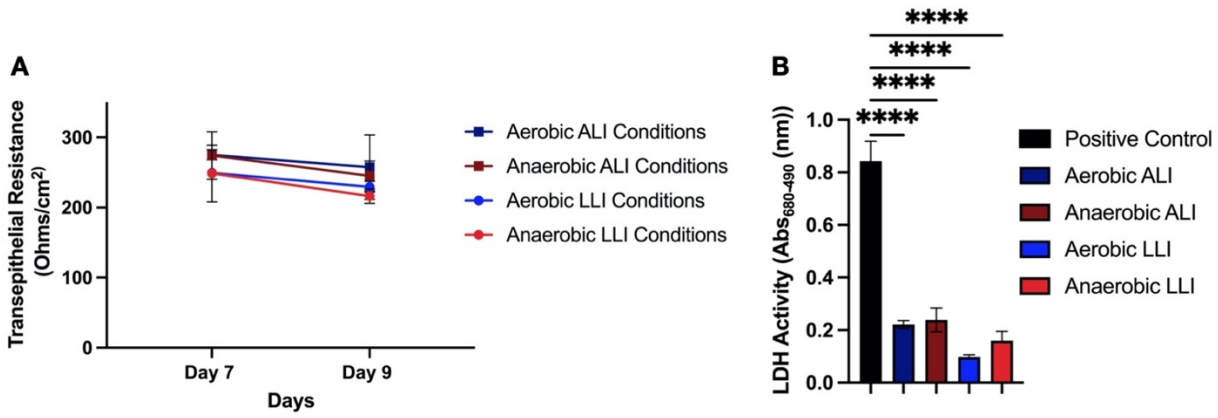

Figure 1. Anaerobic conditions do not affect either the barrier integrity nor the viability of Vk2 cells in ALI or LLI cultures. Vk2 cells were grown for 7 days in LLI conditions and ALI conditions, then incubated in aerobic or anaerobic conditions for 2 days. (A) TERs were measured on day 7 and day 9 for all conditions. B) LDH was measured in culture supernatants collected following anaerobic incubation to compare cell viability between aerobic and anaerobic conditions. Cell supernatants collected after complete lysis were used as a positive control. Representative of N=3 separate experiments with triplicate wells in each experiment. Data was analyzed with one-way ANOVA, with Bonferroni test to correct for multiple comparisons. ****$p<0.0001$.

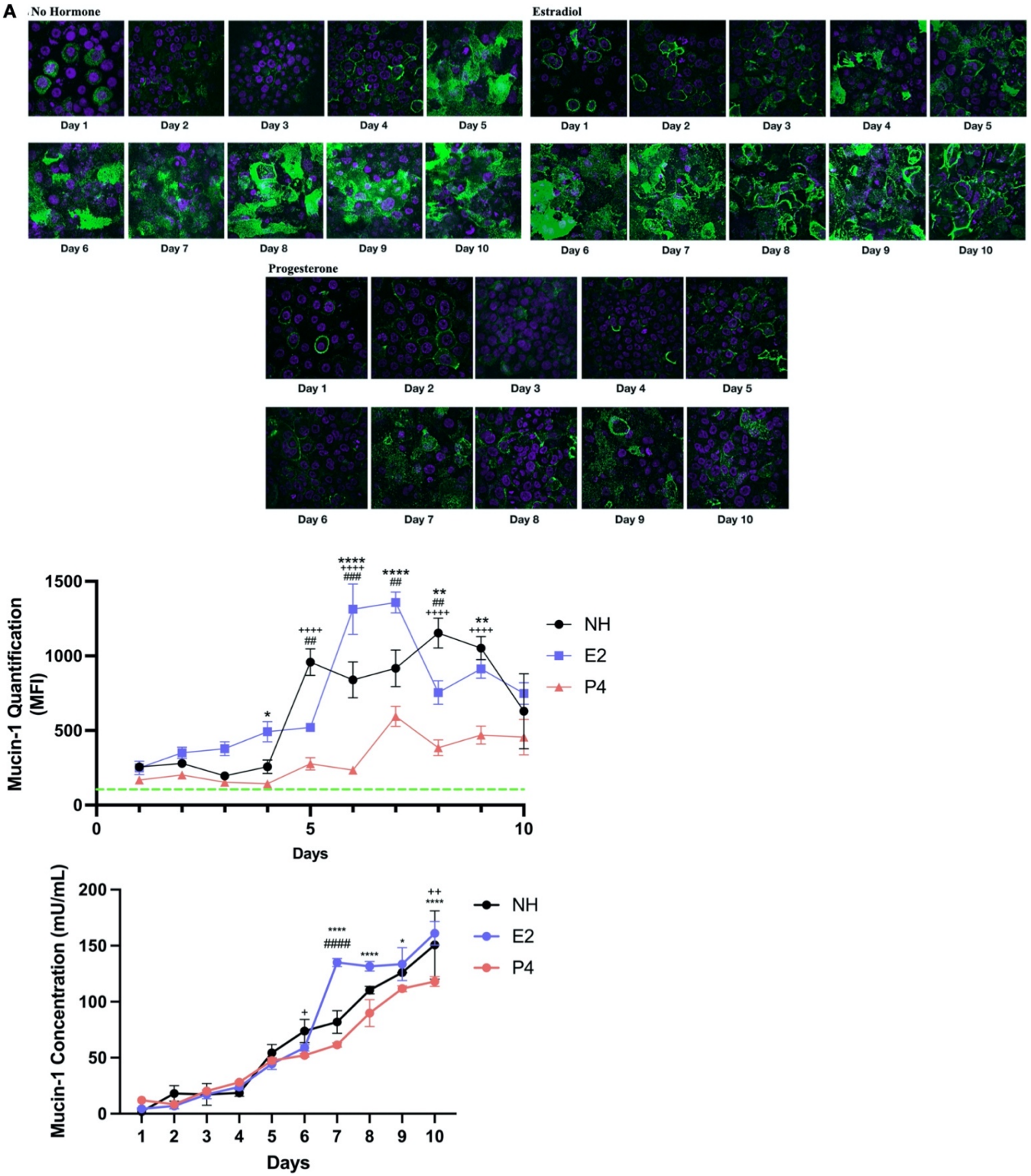

Figure 2. Mucin production in ALI Vk2 cell cultures is enhanced by estradiol treatment compared to progesterone treatment. Vk2 cells were grown in an ALI culture system for 10 days with various hormone treatments: no hormone (NH), estradiol (E2) and progesterone (P4). Each day, cell supernatant was collected and transwells were fixed and stored for mucin staining. A) Mouse anti-human MUC1 (CD227) antibody staining (green) of Vk2 cells (purple) over 10

days of NH ALI culture, E2 ALI culture, and P4 ALI culture B) Mean Fluorescence Intensity (MFI) quantification of images. Baseline Fluorescence, represented by dotted green line, defined as the minimum quantification for green fluorescence intensity on imageJ. C) Supernatants collected from above experiment were analyzed for secreted mucin by ELISA. The graph shows average secreted mucin concentration (mU/mL) in cell supernatants collected from Vk2 cells grown in different hormone conditions. Representative of N=3 separate experiments with duplicate wells for each condition. Data was analyzed with two-way ANOVA, with Bonferroni test to correct for multiple comparisons. ****p<0.0001, **p=0.0017, *p=0.421. Significance symbols: # is NH vs E2, + is NH vs P4, * is E2 vs P4.

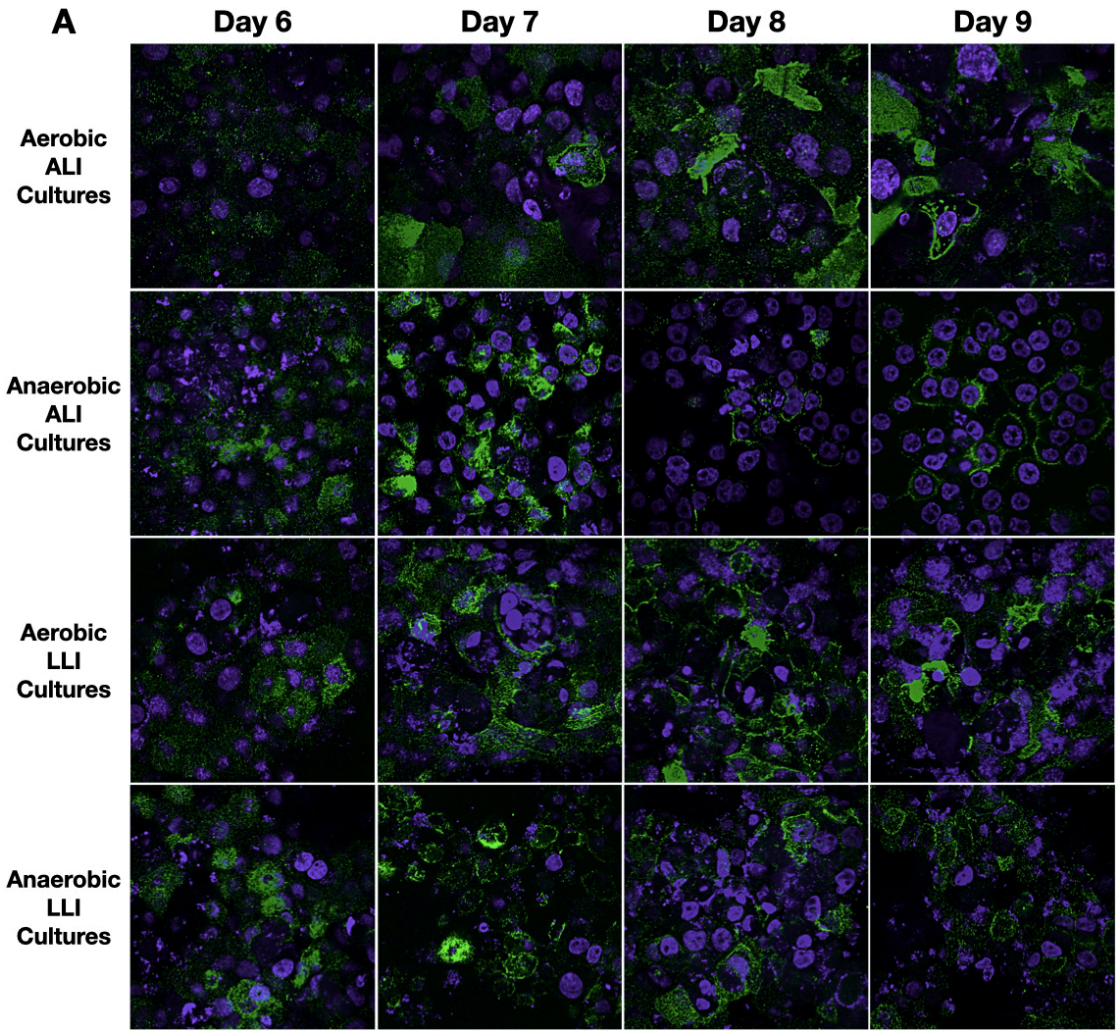

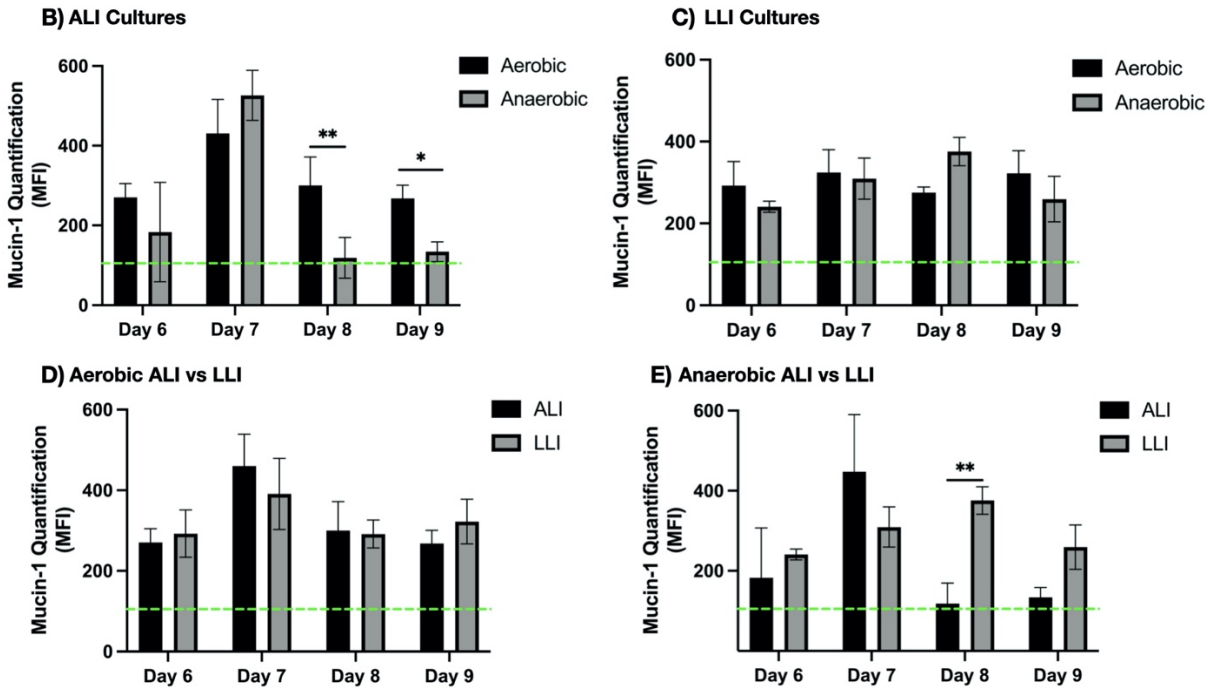

Figure 3. Mucin production in Vk2 cell cultures is consistent in ALI and LLI cultures and is not significantly affected by 24h or 48h anaerobic incubation. Vk2 cells were grown aerobically in an ALI or LLI culture system for 5 days. One replicate of each culture system was then incubated anaerobically from day 6 to day 9. Each day, transwell cultures of both aerobic and anaerobic plates were fixed and stored for mucin staining. A) mouse anti-human MUC1 (CD227) antibody staining (green) of 6 - 9-day Vk2 cell (purple) cultures. B) Mean Fluorescence Intensity (MFI) comparison of the aerobic and anaerobic ALI cultures. C) MFI comparison of the aerobic and anaerobic LLI cultures. D) MFI comparison between ALI and LLI cultures in aerobic conditions from day 6 – day 9. E) MFI comparison between ALI and LLI cultures in anaerobic conditions from day 6 – day 9. Baseline Fluorescence, represented by dotted green line, defined as the minimum quantification for green fluorescence intensity on imageJ. Representative of N=2 separate experiments with triplicate wells for each condition. Data was analyzed with two-way ANOVA, with Bonferroni test to correct for multiple comparisons. ****$p<0.0001$, ***$p=0.0005$, **$p=0.0019$, *$p=0.0216$.

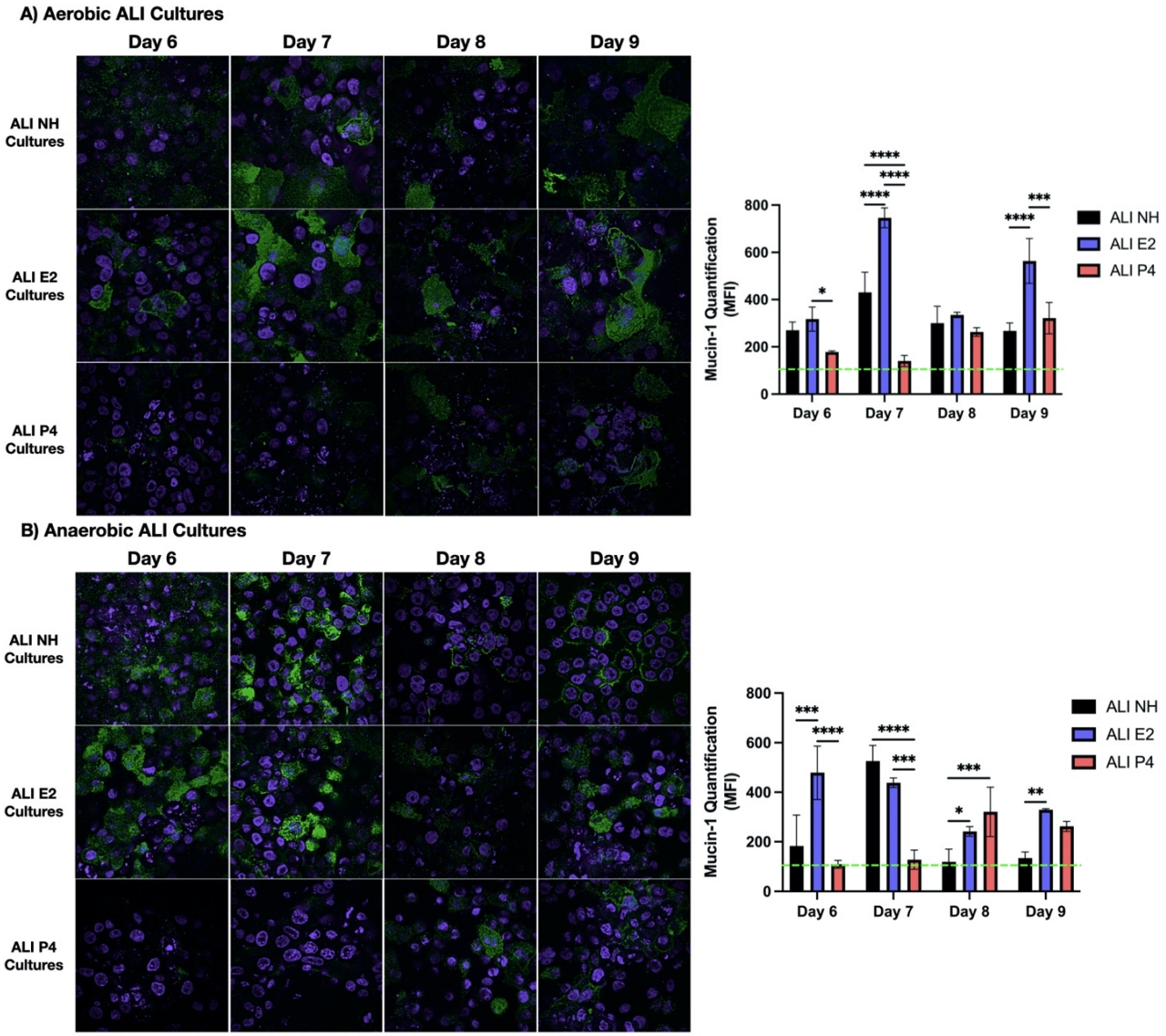
A) Aerobic ALI Cultures
Day 6
Day 7
Day 8
Day 9
ALI NH Cultures
ALI E2 Cultures
ALI P4 Cultures
Mucin-1 Quantification (MFI)
ALI NH
ALI E2
ALI P4
B) Anaerobic ALI Cultures

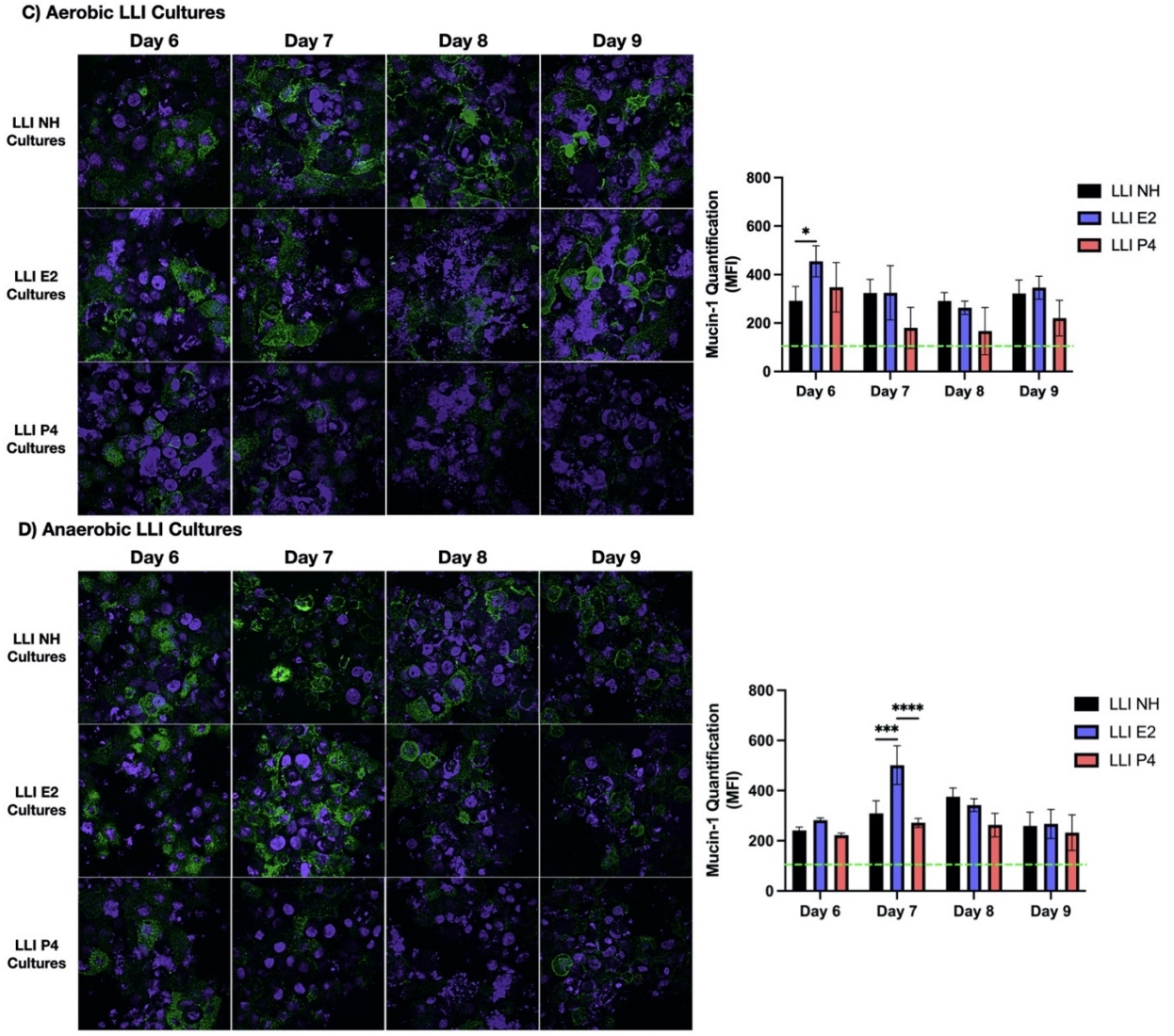

Figure 4. Mucin production in Vk2 cell cultures is significantly increased in the presence of E2. Vk2 cells were grown aerobically in an ALI or LLI culture system for 5 days with various hormone treatments: no hormone (NH), estradiol (E2) and progesterone (P4). One replicate of each culture system was then incubated anaerobically from day 6 to day 9. Each day, transwell cultures of both aerobic and anaerobic plates were fixed and stored for mucin staining. A) Mouse anti-human MUC1 (CD227) antibody staining (green) of 6 - 9-day aerobic ALI Vk2 cell (purple) cultures in various hormone conditions with Mean Fluorescence Intensity (MFI) quantification. B) Mouse anti-human MUC1 (CD227) antibody staining (green) of 6 - 9-day anaerobic ALI Vk2 cell (purple) cultures in various hormone conditions with MFI quantification. C) Mouse anti-human MUC1 (CD227) antibody staining (green) of 6 - 9-day aerobic LLI Vk2 cell (purple) cultures in various hormone conditions with MFI quantification. D) Mouse anti-human MUC1 (CD227) antibody staining (green) of 6 - 9-day anaerobic LLI Vk2 cell (purple) cultures in various hormone conditions with MFI quantification. Baseline Fluorescence, represented by dotted green line, defined as the minimum quantification for green fluorescence intensity on imageJ. Representative of N=2 separate experiments with triplicate wells for each condition. Data was analyzed with two-way ANOVA, with Bonferroni test to correct for multiple comparisons. ****$p<0.0001$, ***$p=0.0005$, **$p=0.0019$, *$p=0.0216$.

4.1.2 Establish vaginal bacteria specific growth characteristics through establishment of growth curves, biofilm morphology and growth patterns for each bacterium using a plate model of biofilm growth.

Previous research in the lab determined that optimal bacterial concentration for inoculation on Vk2 cells was at a multiplicity of infection (MOI) of 100 (6,000,000 CFU/mL per 60,000 Vk2 cells).[45] To ensure that this MOI was being used consistently, a growth curve was needed for each bacterium to ensure bacterial count was accurate. 48 h growth curves were determined through CFU/mL and OD_{600} measurements every 2 h (M&M 3.9). Growth curves for all 4 bacteria used in this project, *L. crispatus*, *L. iners*, *G. vaginalis* and *P. bivia*, were constructed (Figure 5). It was determined that *L. crispatus* and *G. vaginalis* both had exponential phases of growth between 2-6 h, whereas *L. iners* and *P. bivia* grew more slowly, with exponential phases between 24-32 h and 10-24 h, respectively. All bacteria grew above the desired 6,000,000 CFU/mL needed for Vk2 cell inoculation to achieve the ideal MOI of 100. Individual growth curves were used to determine the optimal time point and culture dilution needed to achieve this concentration for Vk2 cell inoculation for subsequent experiments.

Many methods to quantify, characterize and better understand biofilm growth and physiology have been established in literature.[163] One of the most well-established methods for quantifying biofilm growth in a plate model is the crystal violet assay.[164] This method has also been adapted and used for a variety of VMB associated bacteria. Therefore, it was used to quantify biofilm growth in plates (M&M 3.10). *P. aeruginosa* was used as a positive control as this bacterium forms biofilm readily in many environments. Through crystal violet staining and imaging on the EVOS FL Life Technology microscope, biofilm morphology of each bacterium of interest in this study was determined (Figure 6A). All bacteria were grown in their specified

growth medium in anaerobic conditions in a 24-well or 96-well sterile flat-bottom plate. *L. crispatus* had significant biofilm growth in a plate model compared to the negative control (Figure 6B). Although *L. crispatus* was the only bacteria which showed significant biofilm growth in a plate model through crystal violet quantification, these assays were still useful in visualizing early-stage biofilm morphology of the other bacteria. Given that most of the bacteria tested were not growing significant biofilm in a plate model, this model was not pursued further. These experiments were still valuable to determine if any bacteria of interest could form biofilm and visualize morphology of each bacterium. The presence of Vk2 cells provides important factors that would aid in the formation of biofilm. Mucin presence is one important component that would contribute to enhancement of biofilm growth.[25] In fact, mucin proved to be a very important component in biofilm growth through a similar assay conducted in a plate model in this project. Figure 7 shows that *G. vaginalis* grew a dramatically denser biofilm when mucin was present on the bottom of the cell culture plate as compared to no mucin coating or the no bacteria control. This indicated that plate models may be missing key components that would be present in Vk2 cells models, and therefore the crystal violet assay for quantification of biofilm may not give an accurate depiction for the ability of the bacteria used in this project to grow biofilm. However, these growth experiments were still useful in establishing methodology for biofilm growth assays and identifying morphology of bacterial biofilm growth.

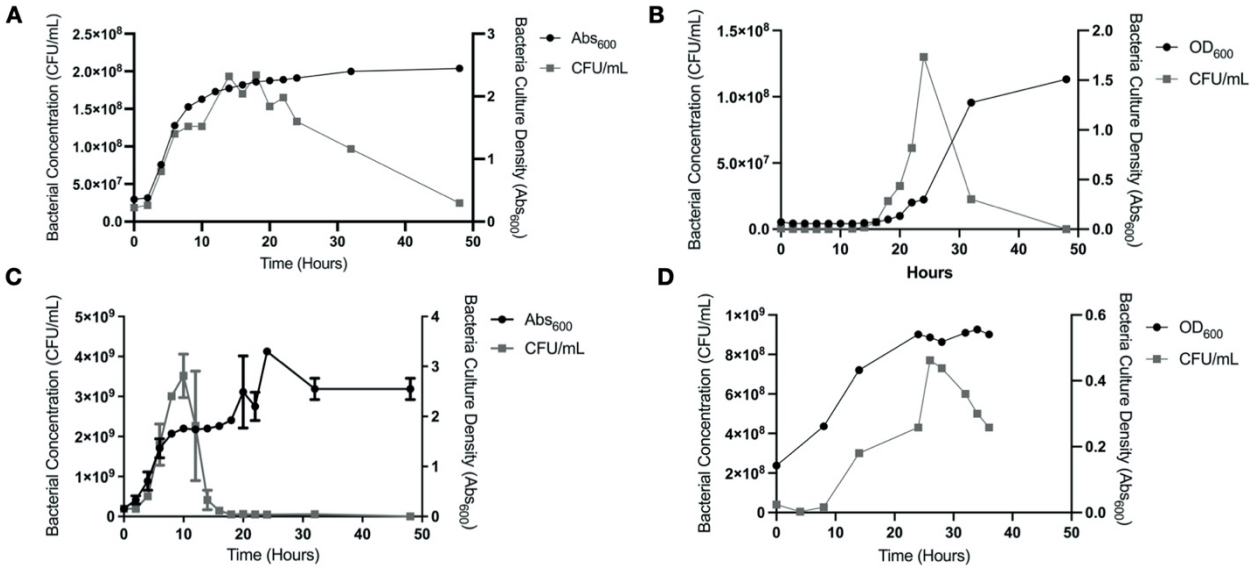

Figure 5. Growth curves of vaginal bacteria. *L. crispatus* (A), *L. iners* (B), *G. vaginalis* (C) and *P. bivia* (D) broth culture grown for 48 h in anaerobic conditions. Broth culture density (Abs_{600}) and live cell count (CFU/mL) by colony growth on plate was measured at 2-h time intervals. Representative of N=2 separate experiments for each bacterium.

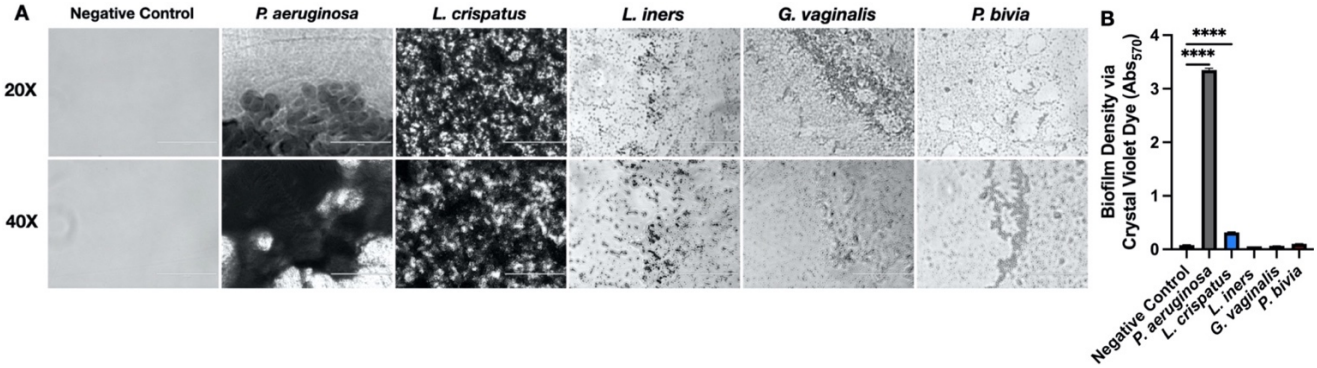

Figure 6. *L. crispatus* biofilm growth is significantly higher in density than other bacteria. A) Biofilm was visualized with crystal violet stain at 20X (top row, 200 µm) and 40X (bottom row, 100 µm) magnification. B) Bacteria biofilm grown in 96-well plates were stained with 0.1% crystal violet dye and Abs_{570} measured to determine the strength of biofilm by comparison of bacteria culture Abs_{570} to negative control (Negative control = average Abs of negative control + (3xSD of negative control)). Representative of N=3 separate experiments, with triplicate wells quantified by Abs_{570} in each experiment. Data was analyzed with one-way ANOVA, with Bonferroni test to correct for multiple comparisons. ****$p<0.0001$.

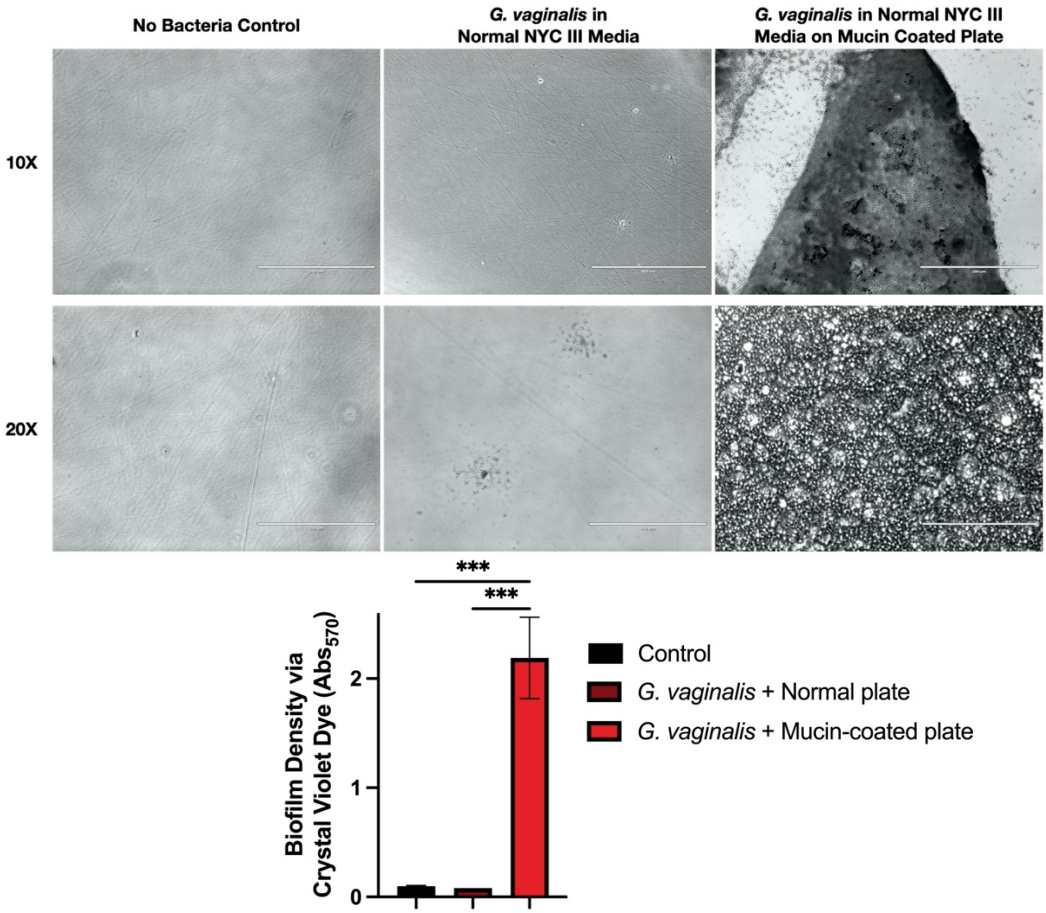

Figure 7. *G. vaginalis* biofilm growth is significant in a mucin-coated plate model compared to the normal plate conditions and no bacteria control. *G. vaginalis* was plated into 24-well plate with or without mucin-coated wells. Plates with bacteria were grown anaerobically at 37°C for 48 h. Images were captured on EVOS FL microscope (Life Technology). Biofilm was visualized with crystal violet stain at 10X (top row, 100 μm) and 20X (bottom row, 200 μm) magnification. B) Bacteria biofilm grown in 96-well plates were stained with 0.1% crystal violet dye and Abs_{570} measured to determine the strength of biofilm by comparison of bacteria culture Abs to negative control (Negative control = average Abs of negative control + (3xSD of negative control)). Representative of N=3 separate experiments, with triplicate wells quantified by Abs_{570} in each experiment. Data was analyzed with one-way ANOVA, with Bonferroni test to correct for multiple comparisons. ***p=0.0001.

4.1.3 Optimize various visualization strategies for biofilm growth in a plate model.

After establishment of optimal growth conditions for bacteria biofilm, the next objective was to test different visualization strategies for biofilm growth for each bacterium of interest. Staining for various components of the biofilm matrix was decided as the primary strategy for visualization of biofilm. The first option tested was SYTOX Green nucleic acid stain used for

staining of eDNA in biofilm matrix (M&M 3.11). Extracellular DNA is an important component of biofilm matrix.[92] It is a structural component involved in interconnecting bacteria within the biofilm and is important for surface attachment. Studies have used this staining method to visualize biofilm growth of a variety of bacteria.[97] Therefore, eDNA staining to assess biofilm growth in a plate model was tested first to see if comparable results could be generated with our bacteria of interest. Trends showed that *L. crispatus* had clear eDNA staining at 24 and 48 h compared to the negative control and *P. bivia* had clear eDNA staining at 48 h compared to the negative control (Figure 8). Therefore, this visualization method did work to stain eDNA in the biofilm of some bacteria and was validated for all bacteria in the Vk2 cell co-culture model moving forward.

The second visualization method tested was FilmTracerTM SYPRO® Ruby Biofilm Matrix staining (M&M 3.11). Matrix proteins make up a large component of the biofilm.[92] They are important in the structural aspects and architecture of the biofilm matrix.[92] Some studies have utilized this staining method to visualize biofilm growth.[165] Trends showed that *L. crispatus* had high protein matrix staining at 48 h compared to the negative control (Figure 9). This visualization method was used for further validation for all bacteria in the Vk2 cell co-culture model moving forward.

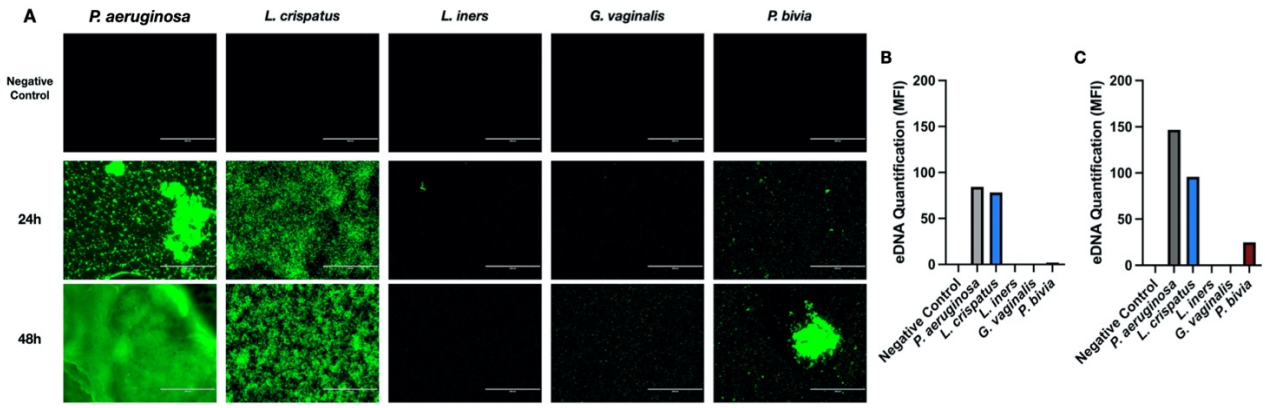

Figure 8. *L. crispatus* and *P. bivia* show eDNA staining in a plate model of bacterial growth. A) Bacteria grown anaerobically in 24 well plates for 24 and 48 h were stained with SYTOX green to visualize eDNA. Mean fluorescence Intensity (MFI) for 24 h (B) and 48 h (C) growth determined by mean gray area quantification of representative images from duplicate wells on imageJ. Representative of N=1 experiment.

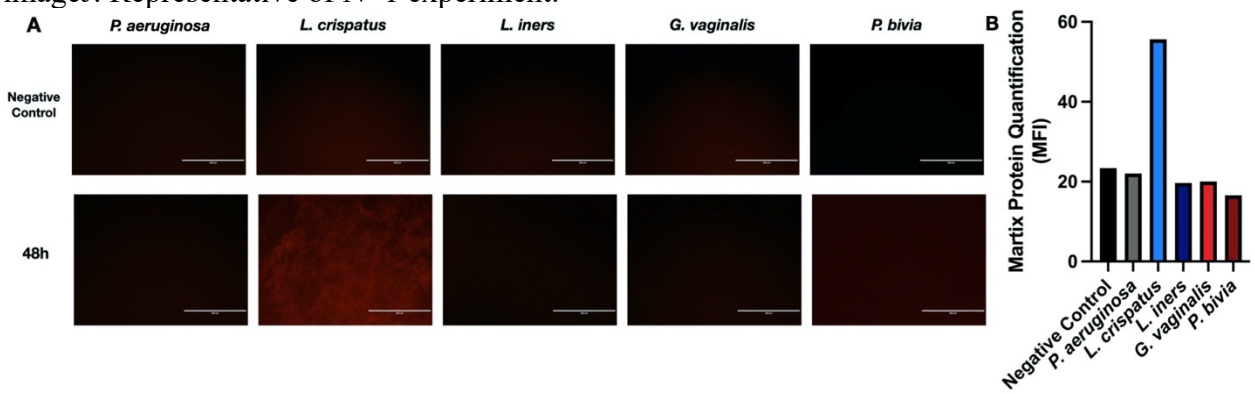

Figure 9. *L. crispatus* shows matrix protein staining in a plate model of bacterial growth. A) Bacteria grown anaerobically in 24 well plates for 48 h were stained with FilmTracerTM SYPRO® Ruby to visualize biofilm matrix proteins. B) Mean Fluorescence Intensity (MFI) for 48 h growth determined by mean gray area quantification of representative images from duplicate wells on imageJ. Representative of N=1 experiment.

4.1.4 Optimize visualization strategies to model bacterial biofilm growth on Vk2 cells.

After concluding that both eDNA staining and matrix protein staining could be used to visualize biofilm formation by the bacteria of interest in a plate model, these stains were then tested for visualization of the biofilm matrix of bacteria on Vk2 cell co-cultures. Preliminary staining of eDNA in the biofilm matrix was conducted with co-cultures of *L. crispatus* and *L. iners* bacteria on Vk2 ALI cultures at 24 and 48 h of bacteria growth and imaged on the EVOS FL Life Technology microscope. Triplicate co-culture wells were imaged, and fluorescence quantification for duplicate images from each well were averaged to determine MFI. Neither bacteria showed significant increase in eDNA stain quantitation compared to no bacteria control (Figure 10). Also, non-specific background staining of eDNA in Vk2 cells was present in the no bacteria condition. Moving forward from this experiment, it was determined that further testing of this stain would be done for all bacteria of interest in this project and visualization would be done with confocal microscopy to generate more detailed images with aspects like Vk2 cell

staining. These results were also repeated with all bacteria of interest in Vk2 cell co-cultures to determine if non-specific background staining was observed.

Preliminary testing of matrix protein biofilm stain on Vk2 cells was conducted with *L. crispatus* and *L. iners* bacteria on ALI and LLI cultures at 48 h of growth (M&M 3.12) and imaged on the EVOS FL Life Technology microscope (M&M 3.11). Triplicate co-culture wells were imaged, and fluorescence quantification for duplicate images from each well were averaged to determine MFI. *L. crispatus* had trends of increased matrix protein staining in both ALI and LLI conditions compared to the negative control (Figure 11). However, *L. iners* did not show increased staining compared to negative controls (Figure 11). In contrast to the eDNA staining, the no bacteria control for protein matrix staining had little to no background, indicating a reduction in non-specific staining of Vk2 cells. Like the eDNA staining experiment, it was determined that further testing of the matrix protein stain would be done for all bacteria of interest in this project and visualization would be done with confocal microscopy to generate more detailed images with aspects like Vk2 cell staining. These results were also repeated with all bacteria of interest in Vk2 cell co-cultures to determine if non-specific background staining was observed.

Further experiments were conducted to determine the pattern of staining for all bacteria of interest in this project in all combinations of cultures conditions. Confocal laser scanning microscopy was done for visualizing DAPI nuclear stain for Vk2 cells, as well as generating more accurate quantification of staining by capturing z-stacks (M&M 3.13). eDNA staining was tested first in all bacteria and Vk2 cell co-cultures (Figure 12-15). When Vk2 cells grown in ALI and LLI cultures were co-cultured with *L. crispatus* for 24-48 h, and stained for eDNA, no

significant staining was seen when compared to the no bacteria controls (Figure 12). It was also confirmed through visualization and high mean fluorescence intensity quantification of the no-bacteria controls that background staining occurred (Figure 12). When Vk2 cells grown in ALI and LLI cultures were co-cultured with *L. iners* for 24-48 hrs, and stained for eDNA, no significant staining was seen when compared to the no-bacteria controls (Figure 13). It was also confirmed through visualization and high mean fluorescence intensity quantification of the no bacteria controls that there was background staining that occurred (Figure 13). When Vk2 cells grown in ALI and LLI cultures were co-cultured with *G. vaginalis* for 24-48 hrs, and stained for eDNA, only the 24h ALI culture showed significant staining when compared to the no bacteria controls (Figure 14). It was also confirmed through visualization and high mean fluorescence intensity quantification of the no bacteria controls that there was background staining that occurred (Figure 14). When Vk2 cells grown in ALI and LLI cultures were co-cultured with *P. bivia* for 24-48 hrs, and stained for eDNA, no significant staining was seen when compared to the no bacteria controls (Figure 15). It was also confirmed through visualization and high mean fluorescence intensity quantification of the no bacteria controls that there was background staining that occurred (Figure 15). In conclusion it was confirmed that SYTOX Green nucleic acid eDNA stain is not the ideal biofilm staining method to use in this project.

Matrix protein staining was then tested for all bacteria and Vk2 cell co-cultures (M&M 3.13). When Vk2 cells grown in ALI and LLI cultures were co-cultured with *L. crispatus* for 24-48 hrs, and stained for matrix proteins, 24h ALI and LLI cultures and 48h ALI cultures showed significant staining when compared to the no bacteria controls (Figure 16). It was also confirmed through visualization and low mean fluorescence intensity quantification of the no bacteria controls that there was low background staining that occurred with this method (Figure 16).

When Vk2 cells grown in ALI and LLI cultures were co-cultured with *L. iners* for 24-48 hrs, and stained for matrix proteins, 24h ALI and LLI cultures and 48h LLI cultures showed significant staining when compared to the no bacteria controls (Figure 17). It was also confirmed through visualization and low mean fluorescence intensity quantification of the no bacteria controls that there was low background staining that occurred with this method (Figure 17). When Vk2 cells grown in ALI and LLI cultures were co-cultured with *G. vaginalis* for 24-48 hrs, and stained for matrix proteins, 24h ALI and LLI cultures and 48h LLI cultures showed significant staining when compared to the no bacteria controls (Figure 18). It was also confirmed through visualization and low mean fluorescence intensity quantification of the no bacteria controls that there was low background staining that occurred with this method (Figure 18). When Vk2 cells grown in ALI and LLI cultures were co-cultured with *P. bivia* for 24-48 hrs, and stained for matrix proteins, 24h LLI cultures and 48h ALI and LLI cultures showed significant staining when compared to the no bacteria controls (Figure 19). It was also confirmed through visualization and low mean fluorescence intensity quantification of the no bacteria controls that there was low background staining that occurred with this method (Figure 19). In conclusion, it was determined that the FilmTracerTM SYPRO® Ruby Biofilm Matrix Protein stain was an optimal stain for biofilm matrix visualization in this project and was used as the primary stain for visualization and quantification of biofilm growth on Vk2 cell co-cultures moving forward.

To validate the accuracy of matrix protein staining in identifying the quantity of proteins within the biofilm matrix for each bacterium, proteins were measured in the biofilm and Vk2 cell co-culture model. Proteins in the biofilm model were lysed and extracted from culture wells and quantified (μg/mL) by normal BCA Assay protocol and extrapolation of the standard curve (M&M 3.14). *L. crispatus* protein quantification with the BCA assay was significantly higher

compared to the no bacteria control (Figure 20). This is similar to results generated with the FilmTracerTM SYPRO® Ruby Biofilm Matrix Protein stain, where *L. crispatus* biofilm growth in Vk2 cell co-culture had significant staining compared to the other bacteria and Vk2 cell co-cultures and the no bacteria control. (Figure 20). This confirmed that the matrix protein staining was an accurate method for biofilm visualization and quantification in this model.

A key component of biofilms is the individual bacteria that form the biofilm matrix that become entrapped during biofilm formation and remain interconnected in the matrix by the various secreted proteins, eDNA and polysaccharides that establish the biofilm scaffold.[92] Visualization of individual bacteria within the biofilm matrix would add another component to the biofilm growth model. Therefore, a Gram-positive Bacteria Marker mouse monoclonal antibody raised against Gram-positive bacteria for the detection of lipoteichoic acid (LTA) was tested for *L. crispatus*, *L. iners* and *G. vaginalis* (M&M 3.15), to determine if this stain is viable option for the visualization of Gram-positive bacteria on a Vk2 cell model. *L. crispatus* and *L. iners* had very specific Gram-positive antibody staining compared to the no bacteria control in LLI cultures at 24 h (Figure 21). *G. vaginalis* did not have significant Gram-positive antibody staining in LLI cultures at 24 h (Figure 21A&C). Therefore, another method of visualization for *G. vaginalis* bacteria within the biofilm was needed. In conclusion, Gram-positive antibody staining is viable option for visualization of *L. crispatus* and *L. iners* individual bacteria cells in Vk2 cell co-culture. Next, dual staining of matrix protein stain and Gram-positive antibody stain was tested (M&M 3.16), to determine if these two visualization methods could be used in conjunction to create a more complete picture of biofilm formation on Vk2 cells. FilmTracerTM SYPRO® Ruby Biofilm Matrix Protein stain significantly decreased Gram-positive antibody staining for both *L. cirspatus* and *L. iners* when compared to single antibody staining (Figure

22). Therefore, it was concluded that dual staining is not a viable option for biofilm visualization and stains would be used separately moving forward.

G. vaginalis specific peptide nucleic acid (PNA) probe called Gard162 and fluorescence in-situ hybridization (FISH) procedure adapted from Machado, A. *et al* (2013) was tested to determine if it is a viable option for *G. vaginalis* individual bacteria cell visualization on the Vk2 cell co-culture model (M&M 3.17). The PNA FISH method specifically stained *G. vaginalis* bacteria on Vk2 cells, with no non-specific staining in the no bacteria control, as well as in control wells of *L. crispatus* and *L. iners* bacteria (Figure 23). Matrix protein staining was used in conjunction with the PNA FISH method to determine if these procedures could be done simultaneously to better visualize biofilm formation. Preliminary results showed that the *G. vaginalis* specific probe and matrix protein staining could be visualized in conjunction (Figure 23). However, images showed that denser areas of matrix protein staining had a dulling effect of the PNA FISH Probe. The experiment will be repeated to ensure these results remain consistent. The establishment of different visualization strategies for individual bacteria is valuable for future experiments where co-cultures of different bacteria species and Vk2 cells will be established to determine the effect of competition between different bacteria on biofilm growth.

Table 1 summarizes the optimal conditions which model biofilm formation on Vk2 cell co-cultures for each bacterium of interest in this project. FilmTracerTM SYPRO® Ruby Biofilm Matrix Protein stain is the ideal biofilm visualization stain for all bacteria in this project. Gram-positive antibody stain in single staining conditions is the ideal stain for detection of *L. crispatus* and *L. iners* bacteria on cells. Gard162 PNA probe and FISH protocol is the ideal method for visualization of *G. vaginalis* bacteria on cells. Matrix protein staining works well for *P. bivia*

biofilm visualization, and a second more specific method to stain individual bacteria needs to be developed in future. Lastly, all bacteria showed significant matrix protein staining in LLI cultures at 24-h and therefore this cell culture system was utilized in experiments testing biofilm enhancement or dissociation strategies in Aim #2.

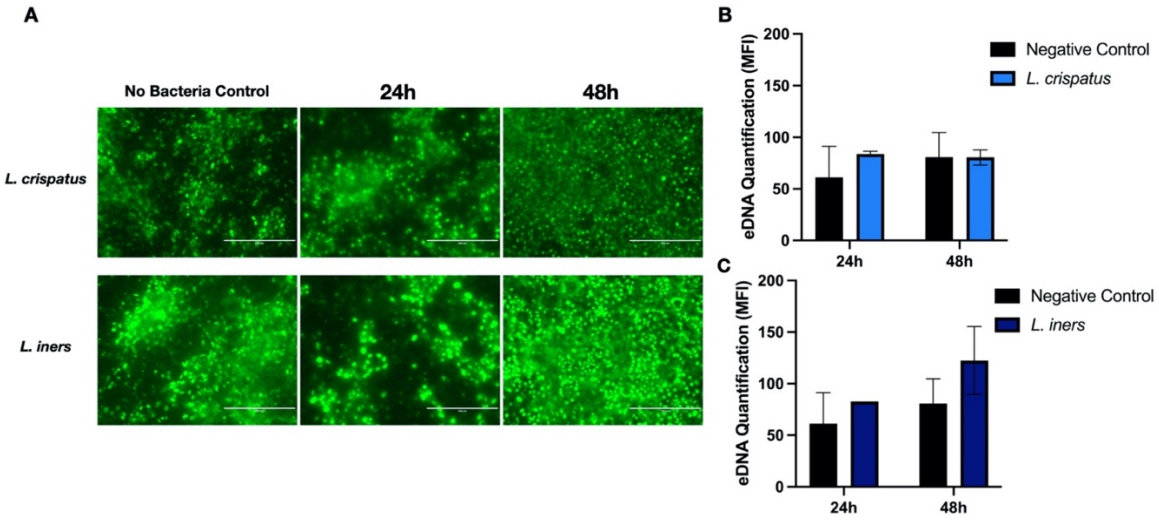

Figure 10. Vk2 cells containing *L. crispatus* and *L. iners* do not show increased eDNA staining compared to Vk2 cells grown without bacteria. A) Vk2 cells grown in ALI cultures for 6 days were inoculated with bacteria under anaerobic conditions for 24 and 48 hrs. Vk2 cultures containing bacteria were then stained with SYTOX green to visualize eDNA (green) on EVOS FL microscope (Life Technology). B) Mean Fluorescence Intensity (MFI) for 24 and 48 h *L. crispatus* and *L. iners* growth determined by mean grey area quantification of representative images from duplicate wells on imageJ. Representative of N=1 experiment.

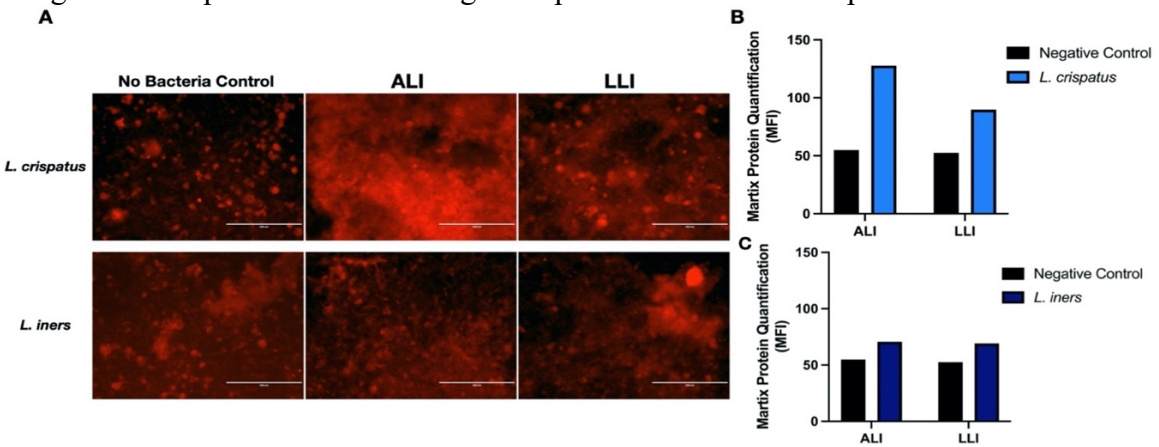

Figure 11. Vk2 cells containing *L. crispatus* and *L. iners* show trends of increased matrix protein staining compared to Vk2 cells grown without bacteria. A) Vk2 cells grown in ALI and LLI cultures for 6 days were inoculated with bacteria under anaerobic conditions for 48 hrs. Vk2 cultures containing bacteria were then stained with FilmTracerTM SYPRO® Ruby to visualize biofilm matrix proteins (red) on EVOS FL microscope (Life Technology). B) Mean

Fluorescence Intensity (MFI) for 48 h *L. crispatus* and *L. iners* growth determined by mean grey area quantification of duplicate representative images from singular well on imageJ. Representative of N=1 experiment.

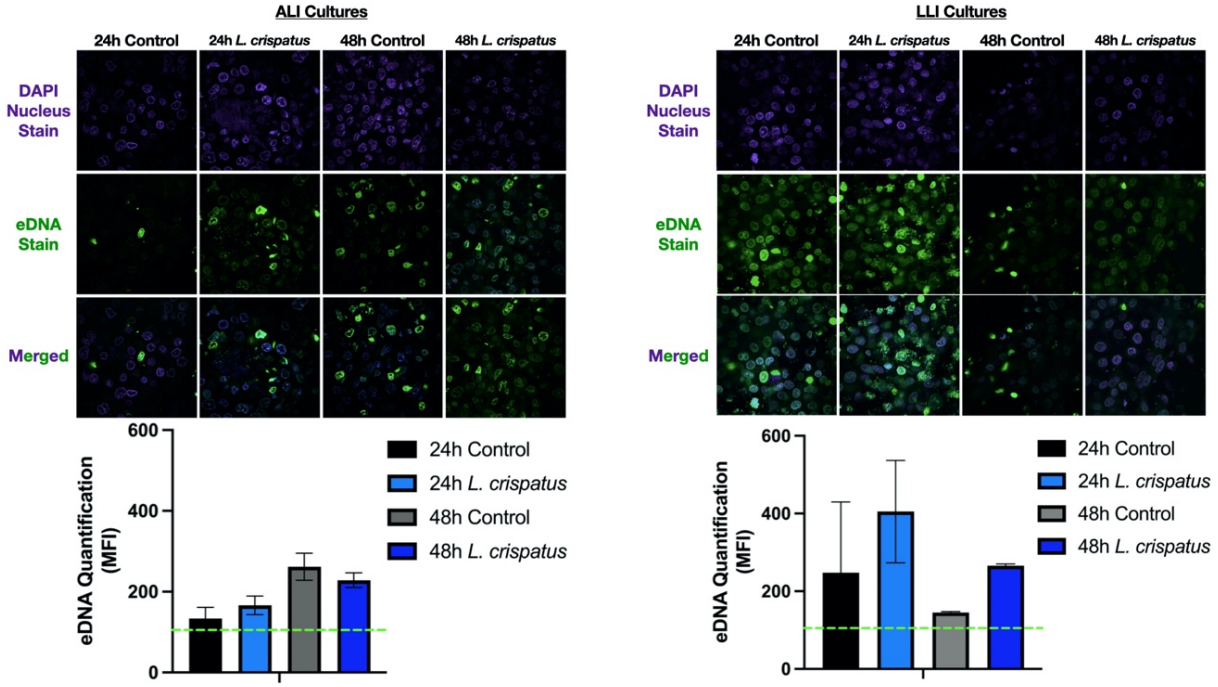

Figure 12. eDNA staining of *L. crispatus* biofilm on Vk2 cells shows nonspecific staining of Vk2 cells with no bacteria. *L. crispatus* at MOI of 100 were incubated anaerobically with ALI and LLI Vk2 cell cultures, grown under aerobic condition for 6 days, for 24 and 48 h. The cultures were then stained with SYTOX green to visualize eDNA (green) on Nikon eclipse Ti2 confocal laser scanning microscope. Mean Fluorescence Intensity (MFI) for 24 and 48 h *L. crispatus* eDNA production on both ALI and LLI cultures determined by mean gray area quantification of duplicate representative images from singular well on imageJ. Baseline Fluorescence, represented by dotted green line, defined as the minimum quantification for green fluorescence intensity on imageJ. Representative of N=3 separate experiments. Data was analyzed with one-way ANOVA, with Bonferroni test to correct for multiple comparisons.

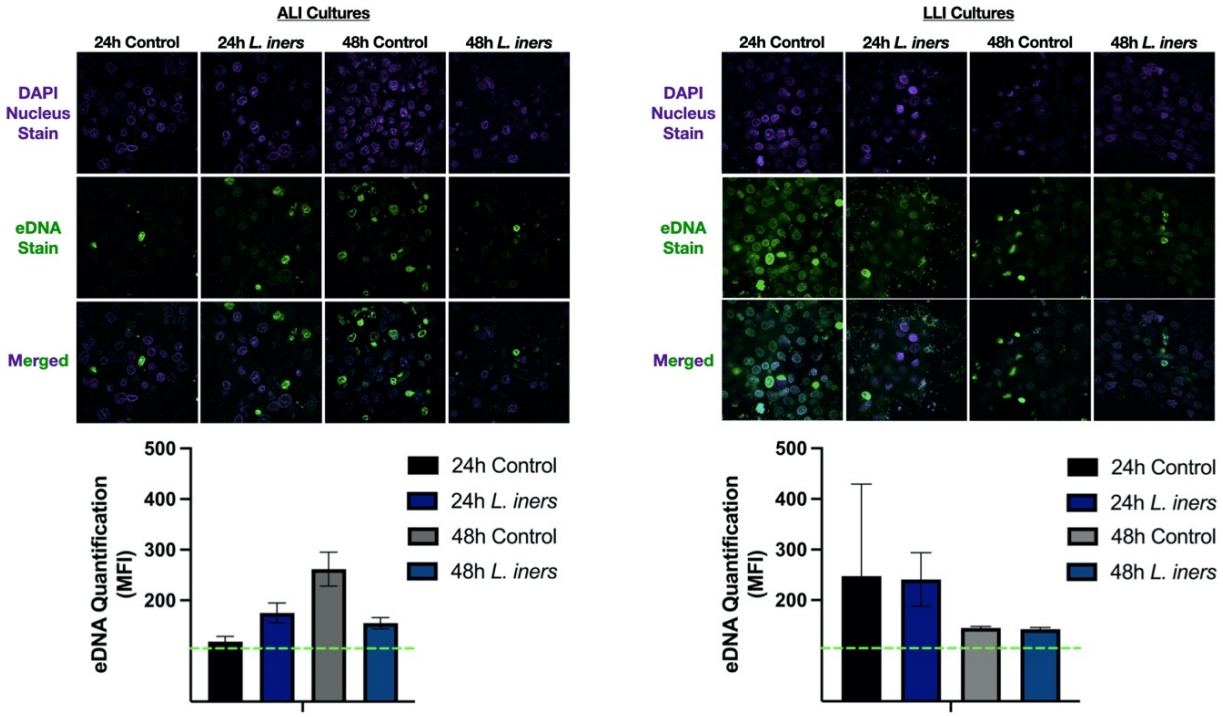

Figure 13. eDNA staining of *L. iners* biofilm on Vk2 cells shows nonspecific staining of Vk2 cells with no bacteria. *L. iners* at MOI of 100 were incubated anaerobically with ALI and LLI Vk2 cell cultures, grown under aerobic condition for 6 days, for 24 and 48 h. The cultures were then stained with SYTOX green to visualize eDNA (green) on Nikon eclipse Ti2 confocal laser scanning microscope. Mean Fluorescence Intensity (MFI) for 24 and 48 h *L. iners* eDNA production on both ALI and LLI cultures determined by mean gray area quantification of duplicate representative images from singular well on imageJ. Baseline Fluorescence, represented by dotted green line, defined as the minimum quantification for green fluorescence intensity on imageJ. Representative of N=3 separate experiments. Data was analyzed with one-way ANOVA, with Bonferroni test to correct for multiple comparisons.

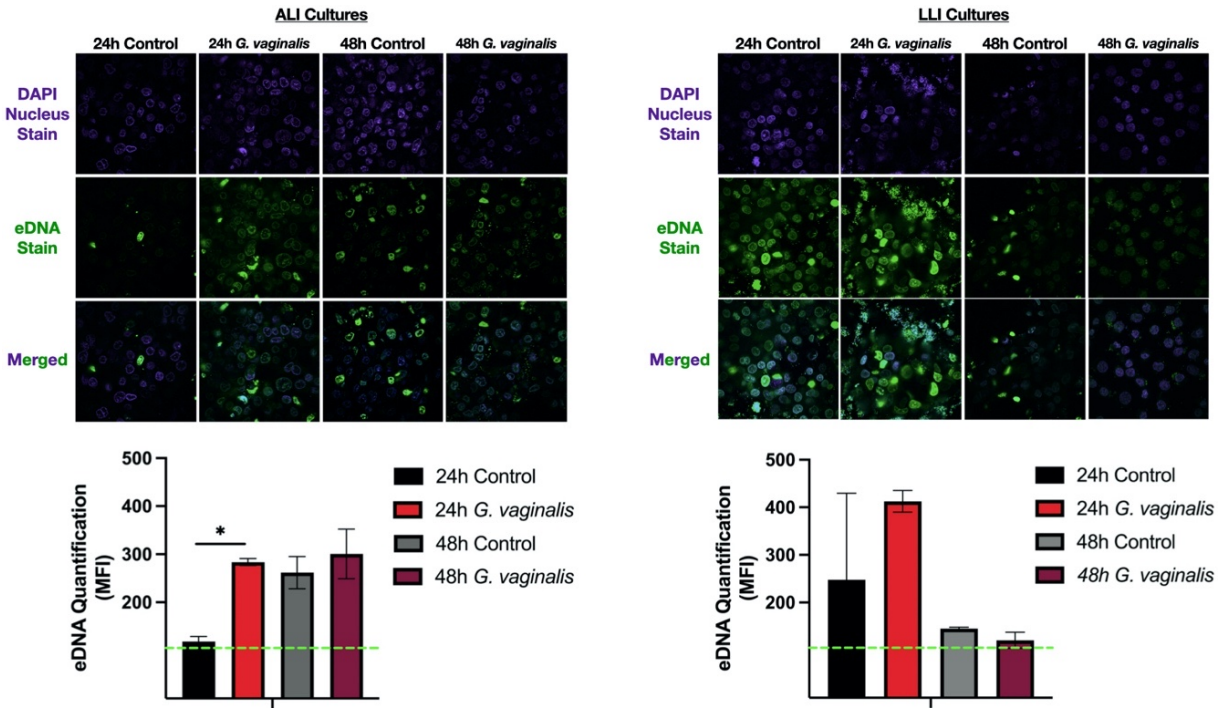

Figure 14. eDNA staining of *G. vaginalis* biofilm on Vk2 cells shows nonspecific staining of Vk2 cells with no bacteria. *G. vaginalis* at MOI of 100 were incubated anaerobically with ALI and LLI Vk2 cell cultures, grown under aerobic condition for 6 days, for 24 and 48 h. The cultures were then stained with SYTOX green to visualize eDNA (green) on Nikon eclipse Ti2 confocal laser scanning microscope. Mean Fluorescence Intensity (MFI) for 24 and 48 h *G. vaginalis* eDNA production on both ALI and LLI cultures determined by mean gray area quantification of duplicate representative images from singular well on imageJ. Baseline Fluorescence, represented by dotted green line, defined as the minimum quantification for green fluorescence intensity on imageJ. Representative of N=3 separate experiments. Data was analyzed with one-way ANOVA, with Bonferroni test to correct for multiple comparisons. *p=0.0184.

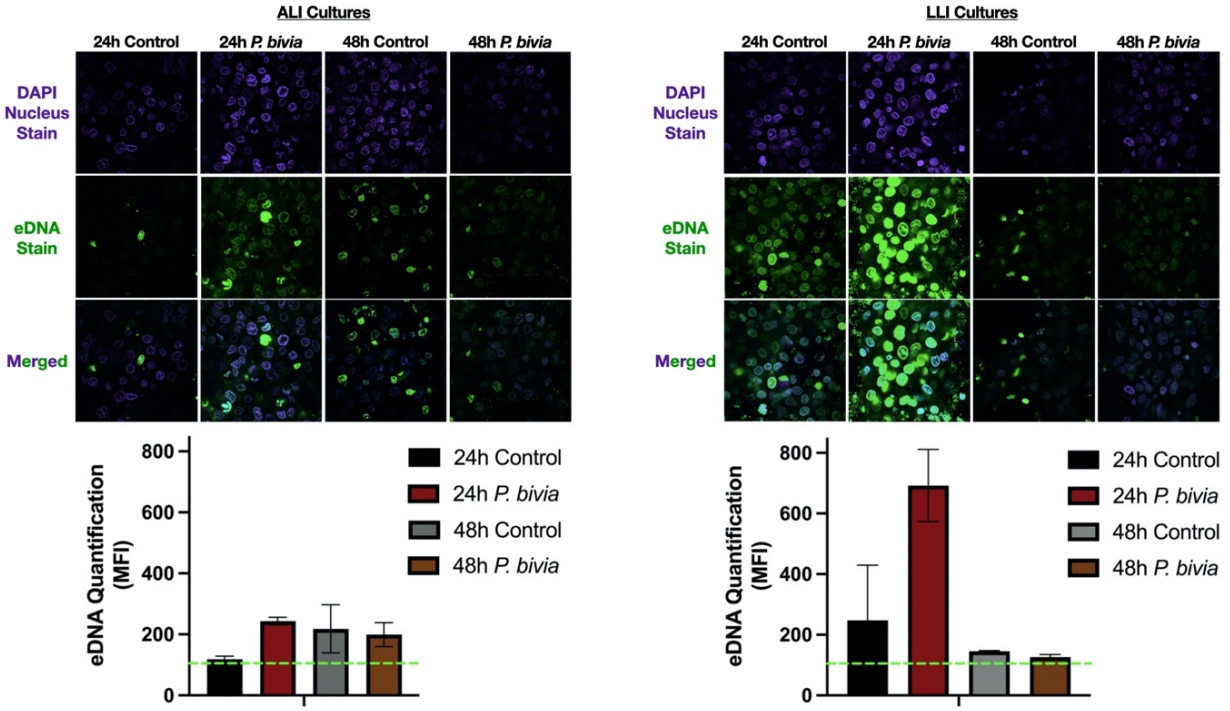

Figure 15. eDNA staining of *P. bivia* biofilm on Vk2 cells shows nonspecific staining of Vk2 cells with no bacteria. *P. bivia* at MOI of 100 were incubated anaerobically with ALI and LLI Vk2 cell cultures, grown under aerobic condition for 6 days, for 24 and 48 h. The cultures were then stained with SYTOX green to visualize eDNA (green) on Nikon eclipse Ti2 confocal laser scanning microscope. Mean Fluorescence Intensity (MFI) for 24 and 48 h *P. bivia* eDNA production on both ALI and LLI cultures determined by mean gray area quantification of duplicate representative images from singular well on imageJ. Baseline Fluorescence, represented by dotted green line, defined as the minimum quantification for green fluorescence intensity on imageJ. Representative of N=3 separate experiments. Data was analyzed with one-way ANOVA, with Bonferroni test to correct for multiple comparisons.

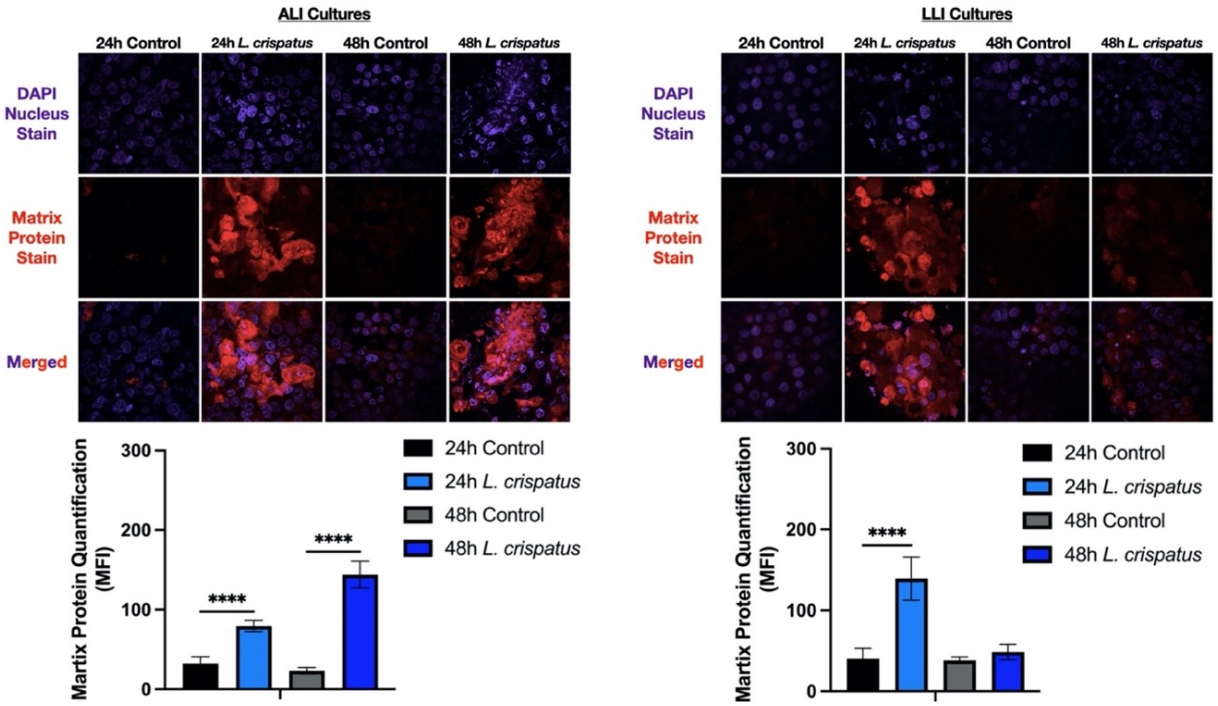

Figure 16. *L. crispatus* shows significant biofilm production in Vk2 cell co-cultures as compared to Vk2 cells with no bacteria when stained for biofilm matrix proteins. *L. crispatus* at MOI of 100 were incubated anaerobically with ALI and LLI Vk2 cell cultures, grown under aerobic condition for 6 days, for 24 and 48 h. The cultures were then stained with FilmTracerTM SYPRO® Ruby to visualize biofilm matrix proteins (red) on Nikon eclipse Ti2 confocal laser scanning microscope. Mean Fluorescence Intensity (MFI) for 24 and 48 h *L. crispatus* growth on both ALI and LLI cultures determined by mean gray area quantification of duplicate representative images from a singular well on imageJ. Representative of N=3 separate experiments. Data was analyzed with one-way ANOVA, with Bonferroni test to correct for multiple comparisons. ****$p<0.0001$.

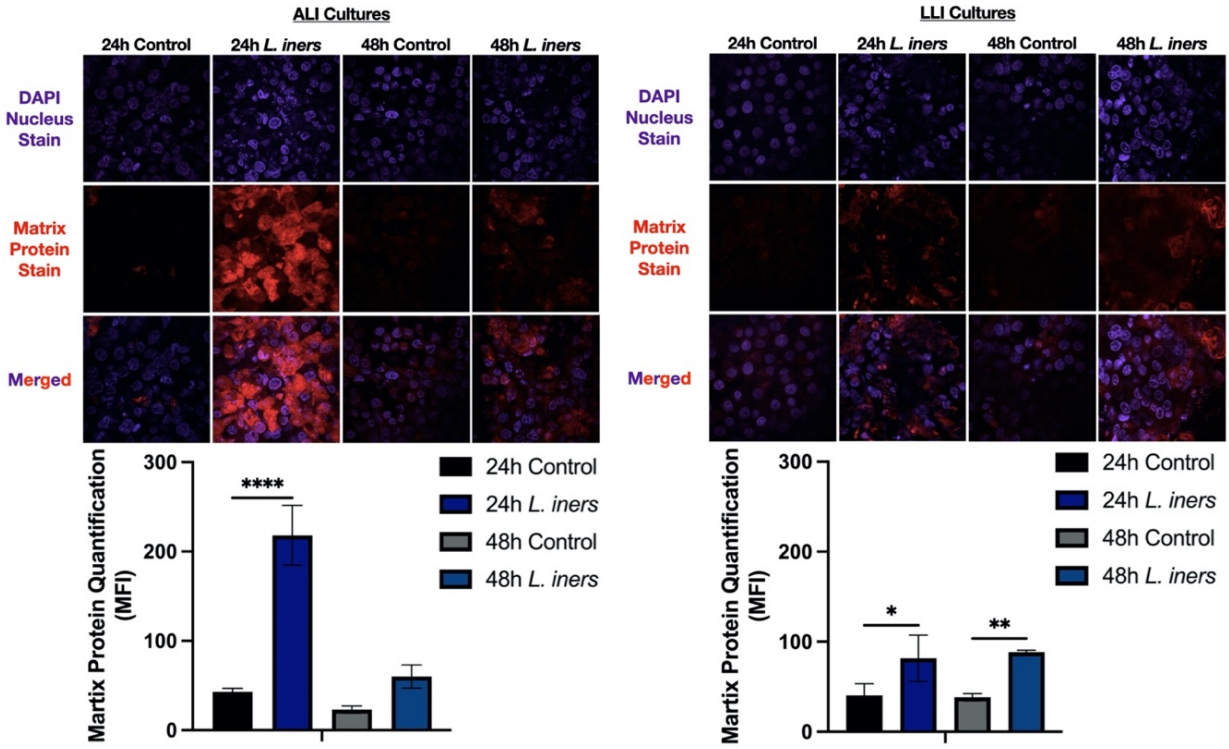

Figure 17. *L. iners* shows significant biofilm production in Vk2 cell co-cultures as compared to Vk2 cells with no bacteria when stained for biofilm matrix proteins. *L. iners* at MOI of 100 were incubated anaerobically with ALI and LLI Vk2 cell cultures, grown under aerobic condition for 6 days, for 24 and 48 h. The cultures were then stained with FilmTracerTM SYPRO® Ruby to visualize biofilm matrix proteins (red) on Nikon eclipse Ti2 confocal laser scanning microscope. Mean Fluorescence Intensity (MFI) for 24 and 48 h *L. iners* growth on both ALI and LLI cultures determined by mean gray area quantification of duplicate representative images from a singular well on imageJ. Representative of N=3 separate experiments. Data was analyzed with one-way ANOVA, with Bonferroni test to correct for multiple comparisons. ****$p<0.0001$, **$p=0.0032$, *$p=0.0157$.

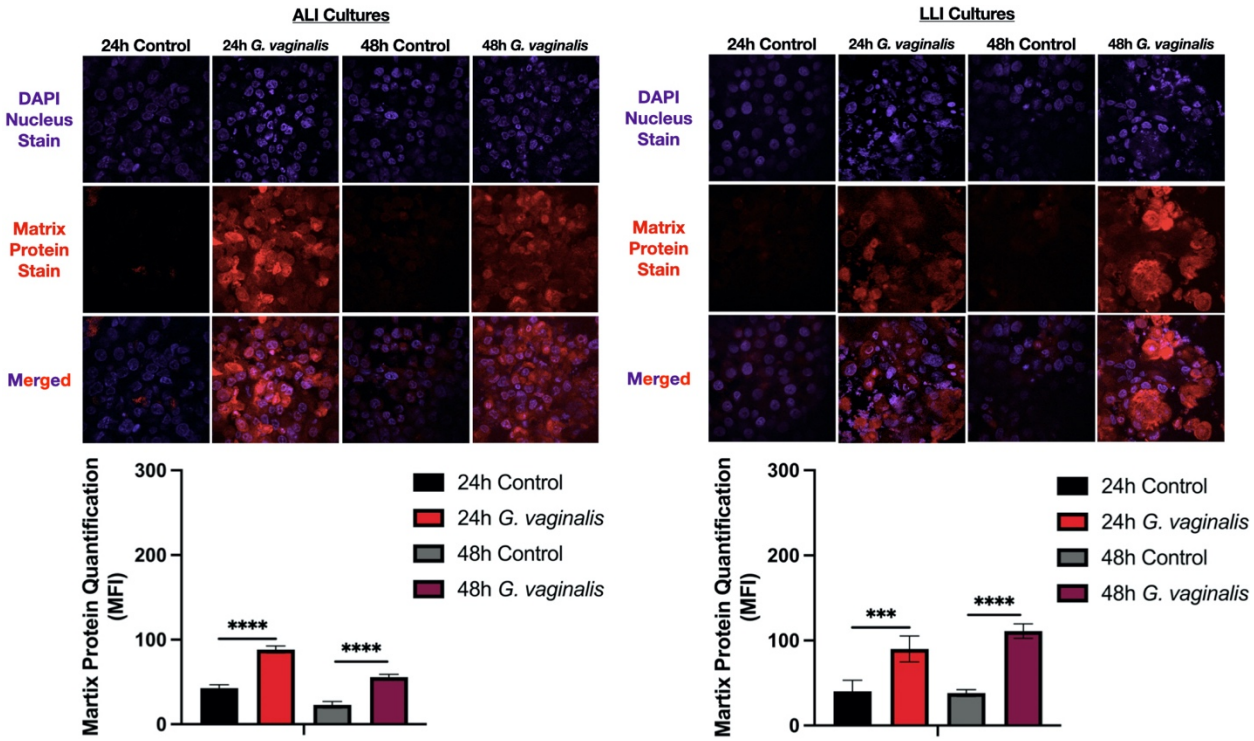

Figure 18. *G. vaginalis* shows significant biofilm production in Vk2 cell co-cultures as compared to Vk2 cells with no bacteria when stained for biofilm matrix proteins. *G. vaginalis* at MOI of 100 were incubated anaerobically with ALI and LLI Vk2 cell cultures, grown under aerobic condition for 6 days, for 24 and 48 h. The cultures were then stained with FilmTracerTM SYPRO® Ruby to visualize biofilm matrix proteins (red) on Nikon eclipse Ti2 confocal laser scanning microscope. Mean Fluorescence Intensity (MFI) for 24 and 48 h *G. vaginalis* growth on both ALI and LLI cultures determined by mean gray area quantification of duplicate representative images from a singular well on imageJ. Representative of N=3 separate experiments. Data was analyzed with one-way ANOVA, with Bonferroni test to correct for multiple comparisons. ****p<0.0001, ***p=0.0005.

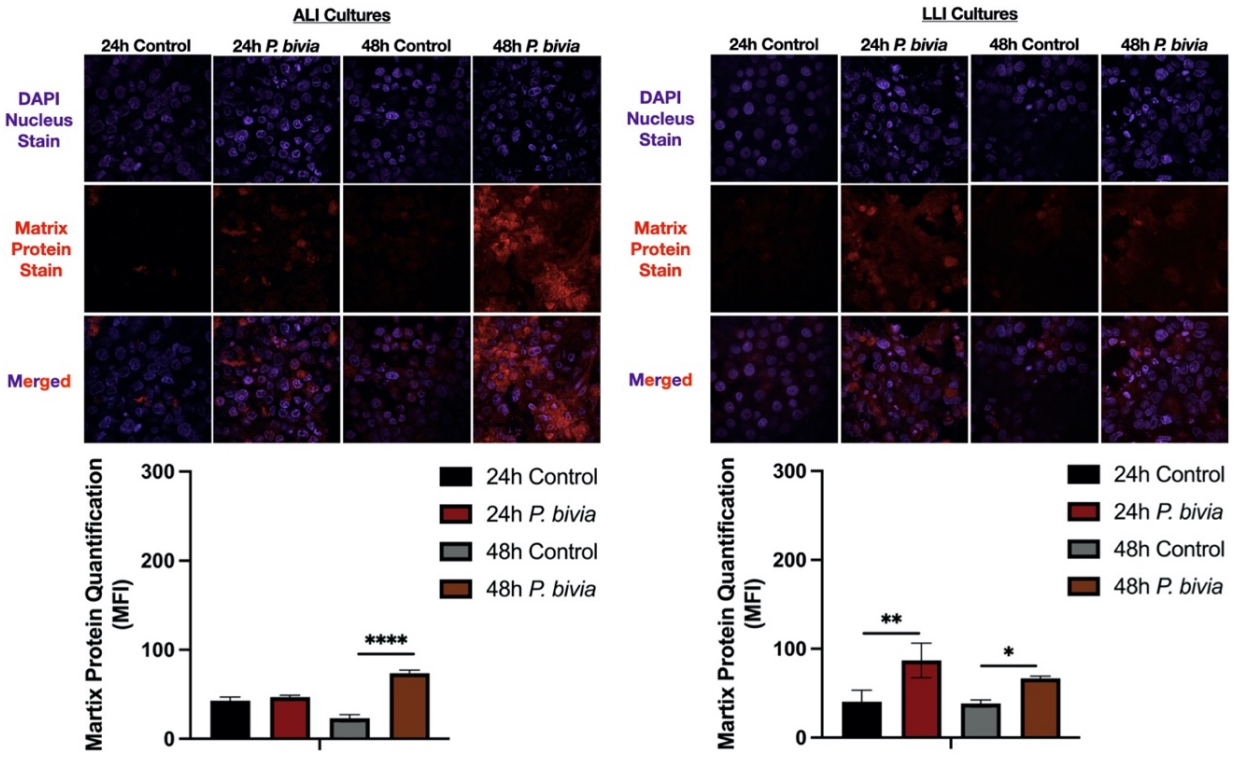

Figure 19. *P. bivia* shows significant biofilm production in Vk2 cell co-cultures as compared to Vk2 cells with no bacteria when stained for biofilm matrix proteins. *P. bivia* at MOI of 100 were incubated anaerobically with ALI and LLI Vk2 cell cultures, grown under aerobic condition for 6 days, for 24 and 48 h. The cultures were then stained with FilmTracerTM SYPRO® Ruby to visualize biofilm matrix proteins (red) on Nikon eclipse Ti2 confocal laser scanning microscope. Mean Fluorescence Intensity (MFI) for 24 and 48 h *P. bivia* growth on both ALI and LLI cultures determined by mean gray area quantification of duplicate representative images from a singular well on imageJ. Representative of N=3 separate experiments. Data was analyzed with one-way ANOVA, with Bonferroni test to correct for multiple comparisons. ****p<0.0001, **p=0.0021, *p=0.0302.

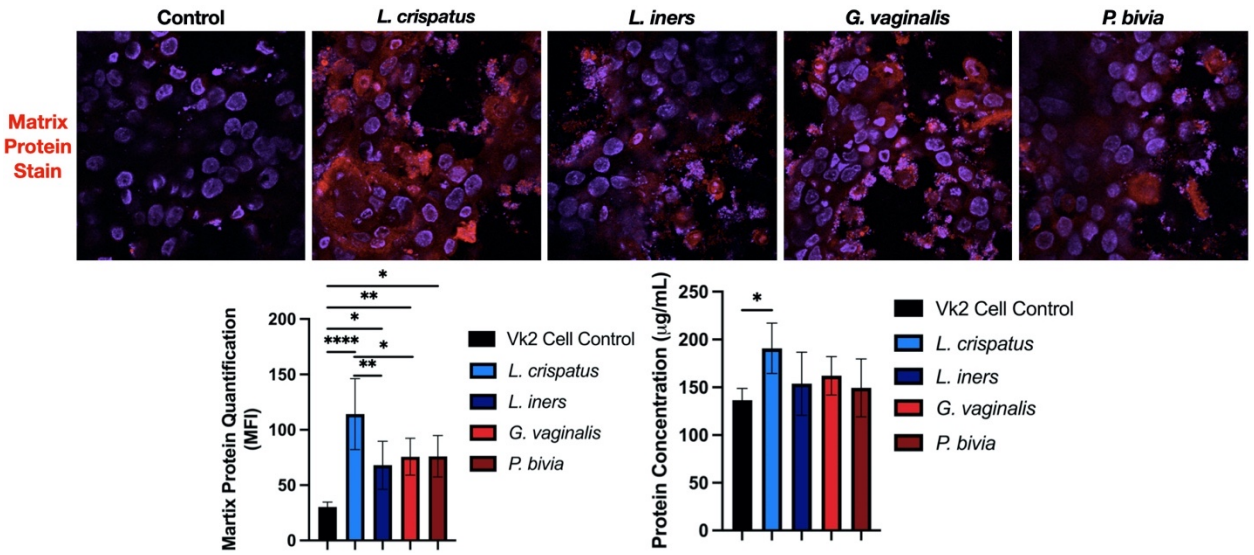

Figure 20. Protein quantification of biofilm growth using BCA assay shows similar trends as matrix protein staining. Vk2 cells were grown for 6-days in LLI cultures and *L. crispatus*, *L. iners*, *G. vaginalis* or *P. bivia* were added. Bacteria and Vk2 cell co-cultures were incubated in anaerobic conditions for 24 h. One set of wells was stained with FilmTracerTM SYPRO® Ruby to visualize biofilm matrix proteins (red) on Nikon eclipse Ti2 confocal laser scanning microscope. Mean Fluorescence Intensity (MFI) determined by mean grey area quantification of duplicate images on imageJ. Protein extraction and quantification was performed on another set of wells by BCA Assay according to manufacturer protocol (Thermo scientific, Cat. 23227). Representative of N=3 separate experiments. Data was analyzed with one-way ANOVA, with Bonferroni test to correct for multiple comparisons. ****p<0.0001, **p=0.0036, *p=0.0256.

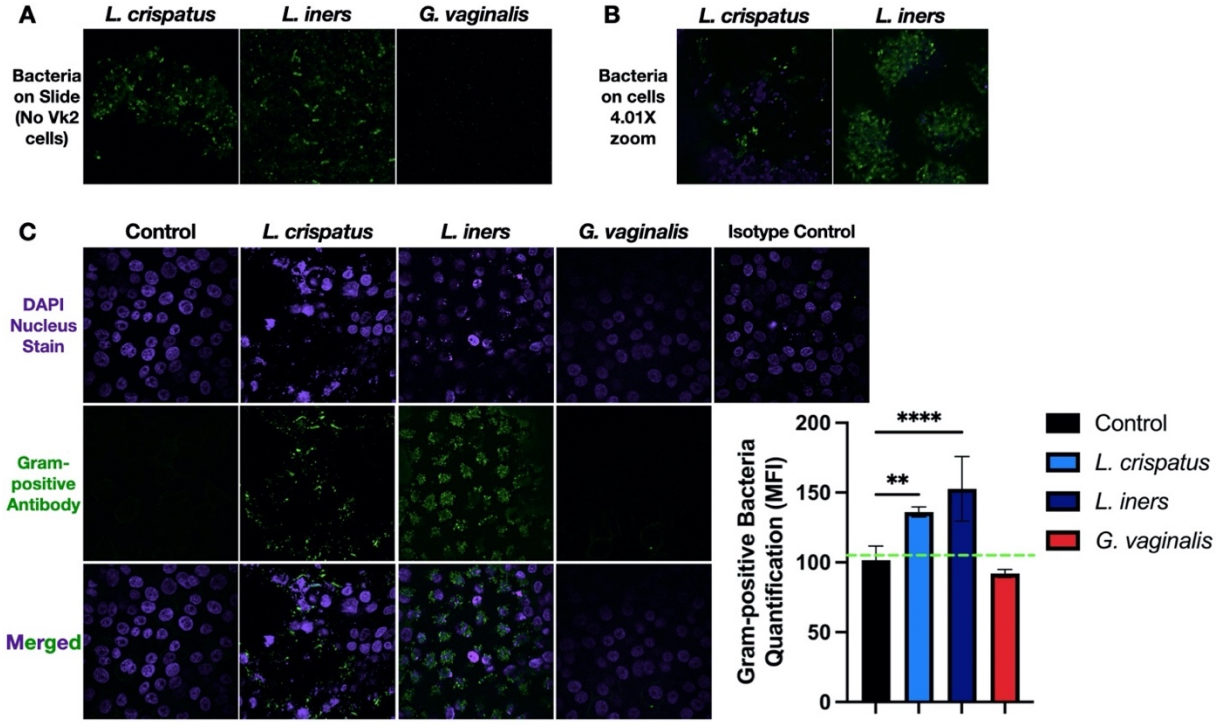

Figure 21. Gram-positive antibody against cell wall component LTA shows specific staining with *L. crispatus* and *L. iners* while there is no staining with *G. vaginalis.* A) *L. crispatus, L. iners* and *G. vaginalis* at exponential phase of growth was spread on glass slide, fixed with methanol and individually stained with mouse monoclonal anti-LTA (sc-58135) antibody to visualize Gram-positive bacteria (green). B-C) *L. crispatus, L. iners* and *G. vaginalis* at MOI of 100 were incubated anaerobically with LLI Vk2 cell cultures, grown under aerobic condition for 6 days, for 24 h then were stained with mouse monoclonal anti-LTA (sc-58135) antibody to visualize Gram-positive bacteria (green) on Nikon eclipse Ti2 confocal laser scanning microscope. B) Images are zoomed on confocal microscope at 4.01X. C) Mean Fluorescence Intensity (MFI) for 24-h bacteria growth on LLI cultures determined by mean grey area quantification of duplicate representative images from a singular well on imageJ. Baseline Fluorescence, represented by dotted green line, defined as the minimum quantification for green fluorescence intensity on imageJ. Representative of N=3 separate experiments. Data was analyzed with one-way ANOVA, with Bonferroni test to correct for multiple comparisons. ****p<0.0001, **p=0.0019.

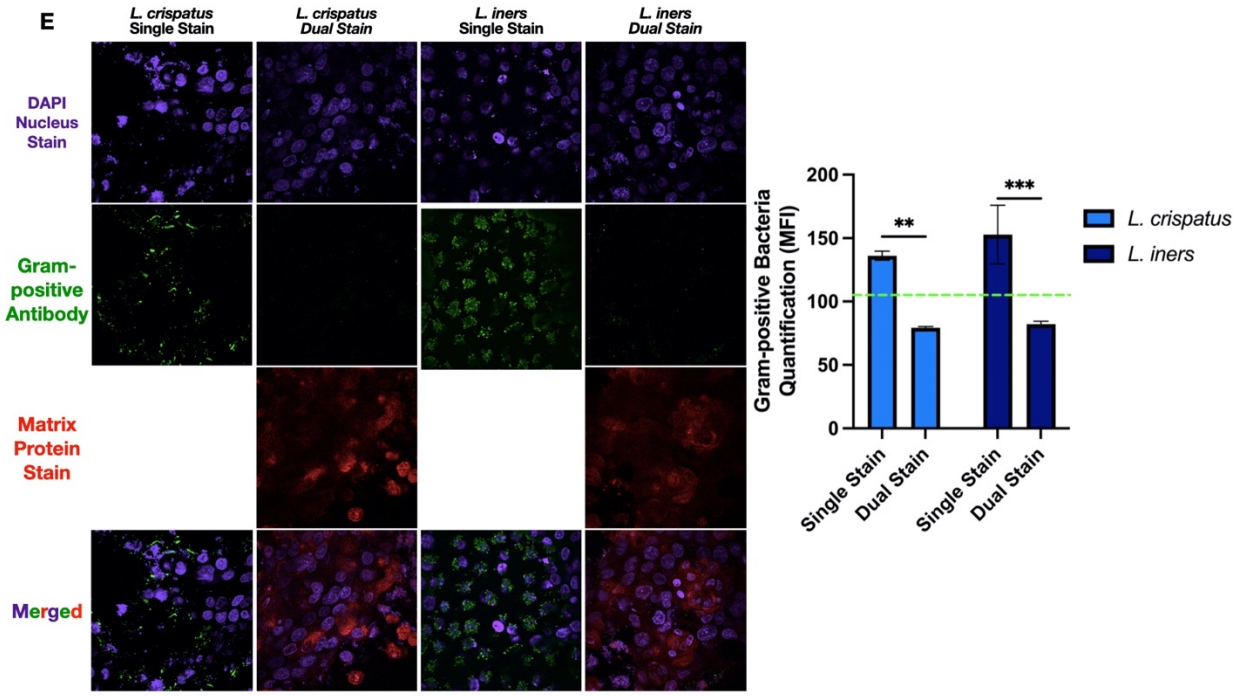

Figure 22. Gram-positive antibody staining of bacteria is significantly decreased in dual stain model with biofilm matrix protein stain. *L. crispatus* and *L. iners* at MOI of 100 were incubated anaerobically with LLI Vk2 cell cultures, grown under aerobic condition for 6 days, for 24 h, then were stained with mouse monoclonal anti-LTA (sc-58135) antibody to visualize Gram-positive bacteria (green) and FilmTracerTM SYPRO® Ruby to visualize biofilm matrix proteins (red) on Nikon eclipse Ti2 confocal laser scanning microscope. Mean Fluorescence Intensity (MFI) for 24 h bacteria growth on LLI cultures determined by mean gray area quantification of duplicate images on imageJ. Dual stain Gram-positive antibody fluorescence values were compared to the single Gram-positive antibody stain fluorescence values in the graph. Baseline Fluorescence, represented by dotted green line, defined as the minimum quantification for green fluorescence intensity on imageJ. Representative of N=3 separate experiments. Data was analyzed with two-way ANOVA, with Bonferroni test to correct for multiple comparisons. ***p=0.0004, **p=0.0020.

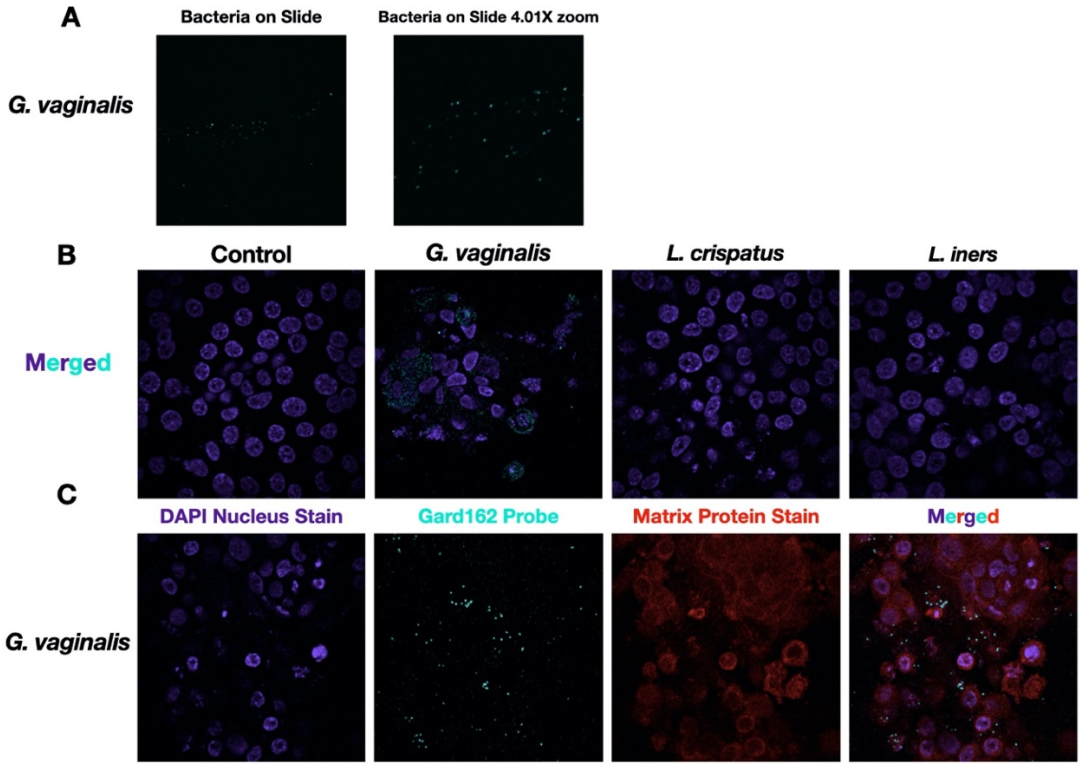

Figure 23. Gard162 probe and PNA FISH method shows *G. vaginalis* bacteria specific staining compared to control, *L. crispatus* and *L. iners*. A) *G. vaginalis* bacteria on slide (no Vk2 cells) was stained using Gard162 PNA FISH probe (Light blue). B) *G. vaginalis, L. crispatus* and *L. iners* at MOI of 100 were incubated anaerobically with LLI Vk2 cell cultures, grown under aerobic condition for 6 days, for 24 h, then were stained using Gard162 PNA FISH probe (Light blue) (detailed protocol in Materials and Methods). C) Dual staining with Gard162 PNA FISH probe (Light blue) and FilmTracerTM SYPRO® Ruby to visualize biofilm matrix proteins (red) was done. Images were captured on a Nikon eclipse Ti2 confocal laser scanning microscope. Representative of N=3 experiments.

Table 2. Optimization of biofilm growth on Vk2 cells for bacteria of interest in this project. Matrix protein stain is ideal biofilm matrix stain for all bacteria in this project. Gram- positive antibody stain in single staining conditions is ideal stain for *L. crispatus* and *L. iners* for bacterial detection on cells. Gard162 PNA probe and FISH protocol is ideal method for visualization of *G. vaginalis* bacteria on cells. Optimal culture conditions and growth time points were established for all bacteria in this project.

Bacteria	Optimal Staining	Optimal Vk2 Cell Culture Conditions	Optimal Bacteria Growth Time
L. crispatus	Single Matrix Protein Stain and Gram-positive Antibody	ALI and LLI	24h (Both) 48h (ALI)
L. iners	Single Matrix Protein Stain and Gram-positive Antibody	ALI and LLI	24h (Both) 48h (LLI)
G. vaginalis	Single Matrix Protein Stain and Gard162 PNA probe	ALI and LLI	24h (Both) 48h (Both)
P. bivia	Single Matrix Protein Stain	ALI and LLI	24h (LLI) 48h (Both)

4.2 Determine the effect of biofilm growth on vaginal epithelial cells and test different strategies for suppression of BV-associated biofilm growth and enhancement of *Lactobacillus* biofilm growth on cells.

BV-associated biofilm growth on the vaginal epithelium is the main mechanism of pathogenicity used to cause adverse health effects in the FGT such as increased susceptibility to HIV infection.[101] *G. vaginalis* biofilm is highly resistant to the main treatment for BV, the antibiotic metronidazole.[122] Studies have tested different strategies for *G. vaginalis* biofilm dissociation to combat BV.[124,126] However, many of these studies have only been conducted in a plate model. Also, the visualization and quantification of biofilm growth in the presence of different biofilm treatments has not been studied. Therefore, the second Aim of this project was to use novel treatment strategies that could enhance *Lactobacillus* biofilm formation and suppress BV-associated biofilm formation in the co-culture system optimized in Aim #1. The treatments used were hormone conditions, SCFA conditions, and the mucin-degrading enzyme sialidase.

4.2.1 Determine direct effect of biofilm growth on cells in-vitro.

The optimized model of biofilm growth on Vk2 cells established in the first aim was utilized to test how biofilm growth directly affects different aspects of Vk2 cells such as barrier integrity and cell cytotoxicity. First, we examined the effect of bacteria colonization and biofilm growth on barrier integrity of ALI and LLI Vk2 cells in co-culture with vaginal bacteria for 24 and 48 h by measuring TER (M&M 3.5). The results showed that LLI Vk2 cells grown in co-cultures with *G. vaginalis* and *P. bivia* for 24 and 48 h had significant decreases in percent pre-treatment TER when compared to control Vk2 cells with no bacteria as well as *L. crispatus* and *L. iners* Vk2 cell co-cultures (Figure 24). 24h ALI Vk2 cells grown in co-culture with *G. vaginalis* and *P. bivia* showed significant decreases in percent pre-treatment TER when compared to control Vk2 cells with no bacteria as well as *L. crispatus* and *L. iners* Vk2 cell co-cultures (Figure 24). 48h ALI Vk2 cells grown in co-culture with *G. vaginalis* showed significant decreases in percent pre-treatment TER when compared to Vk2 cells grown in co-culture with *L. crispatus* (Figure 24). The 24 h LLI cultures had the highest overall percent pre-treatment TER for all bacteria between all culture conditions, even with the significant decreases seen in *G. vaginalis* and *P. bivia*. Therefore, the negative effect on barrier integrity in this culture condition is reduced, and 24h LLI cultures were used for experiments testing strategies of biofilm modification to ensure that decreased barrier integrity does not have a significant impact of biofilm growth.

Next, we examined the effect of bacteria colonization and biofilm growth on cell cytotoxicity of ALI and LLI Vk2 cells in co-culture with vaginal bacteria for 24 and 48 h via LDH assays (M&M 3.6). LLI Vk2 cells grown in co-cultures with *P. bivia* for 24 and 48 h showed significant increases in LDH activity when compared to control Vk2 cells with no

bacteria, as well as *L. crispatus* and *L. iners* Vk2 cell co-cultures (Figure 25). LLI Vk2 cells grown in co-cultures with *G. vaginalis* for 48 h showed significant increases in LDH activity when compared *L. crispatus* and *L. iners* Vk2 cell co-cultures (Figure 25). Also, 24h ALI Vk2 cells grown in co-culture with *G. vaginalis* showed significant increases in LDH activity when compared to control Vk2 cells with no bacteria as well as *L. crispatus* and *L. iners* Vk2 cell co-cultures (Figure 25). The 48h ALI Vk2 cells grown in co-culture with *G. vaginalis* and *P. bivia* showed significant increases in LDH activity when compared to control Vk2 cells with no bacteria as well as Vk2 cells grown in co-culture with *L. crispatus* (Figure 25). None of the bacteria showed a cytotoxic effect comparable to positive control, which means none of the bacteria are having an extreme effect that results in complete cell lysis in culture (Figure 25). It is important to maintain some cell viability where biofilm can colonize when moving forward with experiments that are focused on altering biofilm formation in different conditions. The 24 h LLI Vk2 cell co-cultures had the lowest overall cytotoxicity for all bacteria between all culture conditions. Therefore, there was less cell cytotoxicity in this culture condition compared to the other conditions and this was considered for experiments testing strategies of biofilm modification.

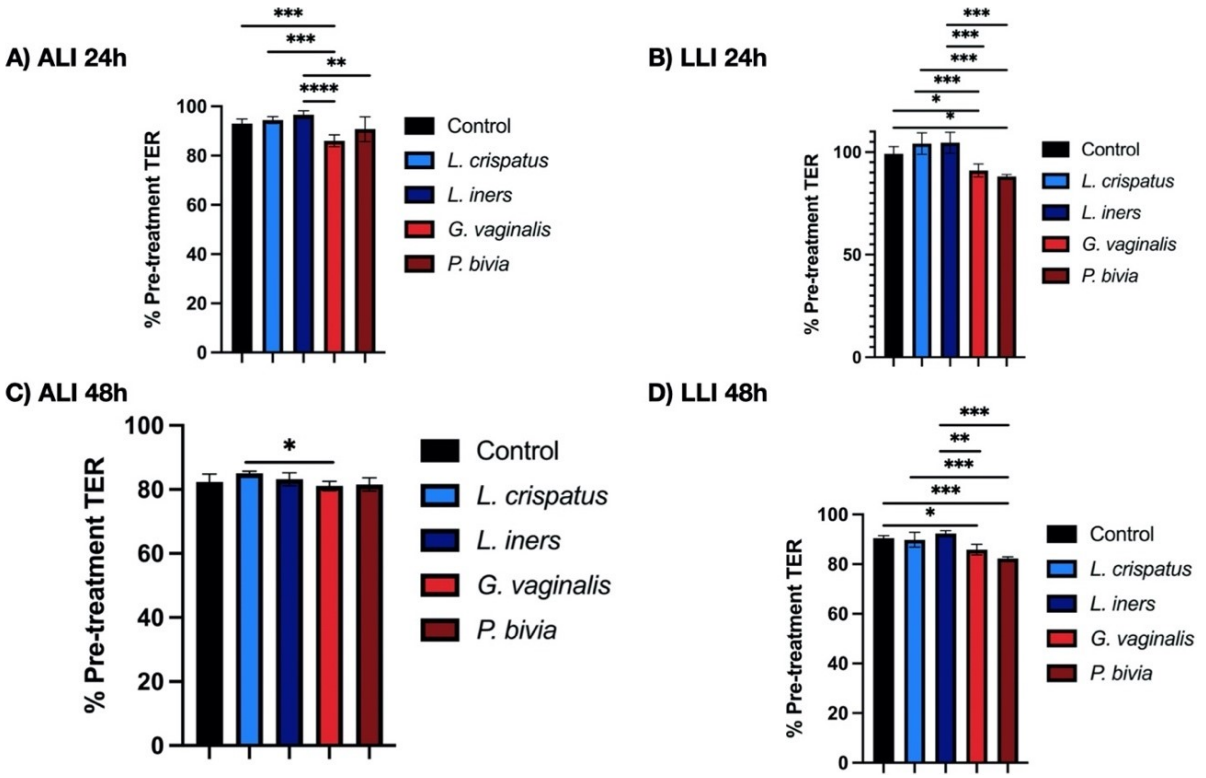

Figure 24. *G. vaginalis* and *P. bivia* show significant decrease in TER in Vk2 co-cultures. Vk2 cells were grown for 6-days in ALI and LLI cultures, and TER was measured before addition of bacteria. *L. crispatus*, *L. iners*, *G. vaginalis* or *P. bivia* were added to ALI (A & C) or LLI (B & D) cultures and the bacteria and Vk2 cell co-cultures were incubated in anaerobic conditions for 24 h (A & B) or 48 h (C & D). After both time points, TER of the co-cultures were measured. The effect of bacteria on Vk2 cells is determined by TER measurements and reported as % Pre- treatment: (TER of bacteria and Vk2 cell co-cultures / TER of the Day 6 Vk2 cell culture before bacteria was added)*100%. Representative of N=3 separate experiments. Data was analyzed with one-way ANOVA, with Bonferroni test to correct for multiple comparisons. ****p<0.0001, ***p=0.004, **p=0.0047, *p=0.0406.

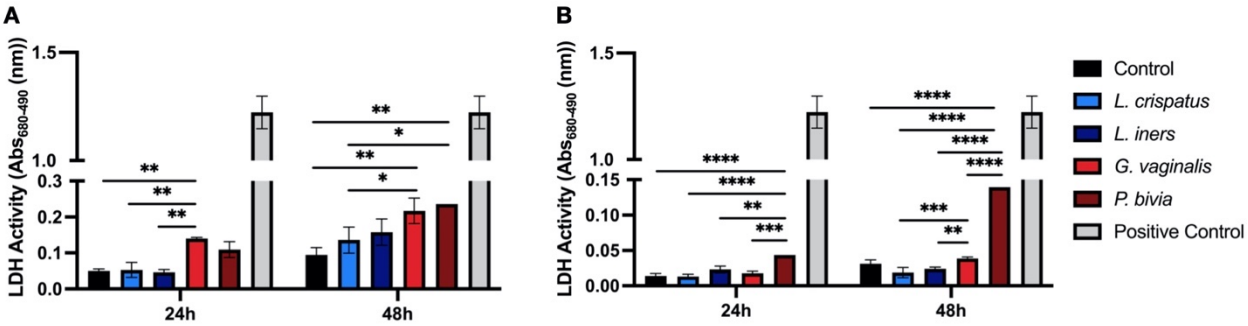

Figure 25. *G. vaginalis* and *P. bivia* show significant cytotoxicity in ALI and LLI Vk2 cell co-culture conditions. Vk2 cells were grown for 6-days in ALI and LLI cultures. *L. crispatus*, *L. iners*, *G. vaginalis* or *P. bivia* were added to ALI (A) or LLI (B) cultures and the bacteria and Vk2 cell co-cultures were incubated in anaerobic conditions for 24 h or 48 h. After both time points, supernatants of the co-cultures were collected for LDH assay. Cell viability was determined by comparing the LDH activity of bacteria and cell co-cultures supernatants to the

LDH activity of the control (Vk2 cells with no bacteria). Representative of N=3 separate experiments. Data was analyzed with two-way ANOVA, with Bonferroni test to correct for multiple comparisons. ****p<0.0001, ***p=0.0004, **p=0.0047, *p=0.0247.

4.2.2 Test the effect of different female sex hormones on biofilm growth to determine if certain hormones can promote *Lactobacillus* biofilm growth and decrease biofilm growth of BV-associated bacteria.

Endogenous sex hormones, as well as hormonal contraceptives, can significantly influence the composition of the VMB *in vivo*.[3] Therefore, hormone conditions were tested as a potential strategy of *Lactobacillus* biofilm enhancement on Vk2 cells, with the hypothesis that estradiol conditions would enhance biofilm growth.

Estradiol (E2) and progesterone (P4) supplemented KSFM media were used in comparison to no hormone (NH) containing KSFM media (M&M 3.18). LLI Vk2 cells grown in co-culture with *L. crispatus* for 24 h had significant biofilm growth in E2 hormone conditions compared to LLI Vk2 cell co-cultures in NH and progesterone conditions (Figure 26). LLI Vk2 cells grown in co-culture with *L. iners* did not have significant differences in biofilm growth among NH, E2 and P4 hormone conditions (Figure 27). LLI Vk2 cells grown in co-culture with *G. vaginalis* for 24 h demonstrated significant biofilm growth in P4 conditions compared to LLI Vk2 cell co-cultures in NH and E2 hormone conditions (Figure 28). LLI Vk2 cells grown in co-culture with *P. bivia* did not have significant differences in biofilm growth among NH, E2 and P4 hormone conditions (Figure 29).

When comparing staining between each bacterium in the different hormone conditions, *L. crispatus* co-cultures show significant biofilm staining compared to all other bacteria co-cultures in the E2 condition (Figure 30). This bacterium also shows significantly greater biofilm growth than *L. iners* and *G. vaginalis* in the no hormone condition (Figure 30). However, in P4 conditions *G. vaginalis* biofilm outgrew all other bacteria (Figure 30).

The impact of biofilm on the barrier integrity and cytotoxicity of cells in NH, E2 and P4 conditions was also analyzed. TER measurements and LDH assays were conducted, (M&M 3.5 & 3.6), to determine if the NH, E2 and P4 conditions stimulate increases or decreases in cell viability and barrier integrity for specific bacteria. LLI Vk2 cells grown in co-cultures with *G. vaginalis* and *P. bivia* for 24 h showed significant decreases in percent pre-treatment TER when compared to *L. crispatus* and *L. iners* Vk2 cell co-cultures in NH, E2 and P4 conditions, except there was no significant difference between *L. iners* and *P. bivia* Vk2 cell co-cultures in P4 conditions (Figure 31). LLI Vk2 cells grown in co-cultures with *L. crispatus* and *L. iners* in P4 hormone conditions for 24 h show significant decreases in percent pre-treatment TER when compared to E2 hormone conditions and NH conditions for *L. crispatus* (Figure 31).

The P4 hormone condition stimulated a significant increase in LDH activity in LLI Vk2 cells grown in co-cultures with *G. vaginalis* when compared to control Vk2 cells with no bacteria as well as *L. crispatus* and *L. iners* Vk2 cell co-cultures (Figure 32). LLI Vk2 cells grown in co-cultures with *P. bivia* also showed significantly increased cytotoxicity compared to the no bacteria control, *L. crispatus* and *L. iners* co-cultures in NH, E2 and P4 hormone conditions, but is upregulated in the P4 hormone condition (Figure 32).

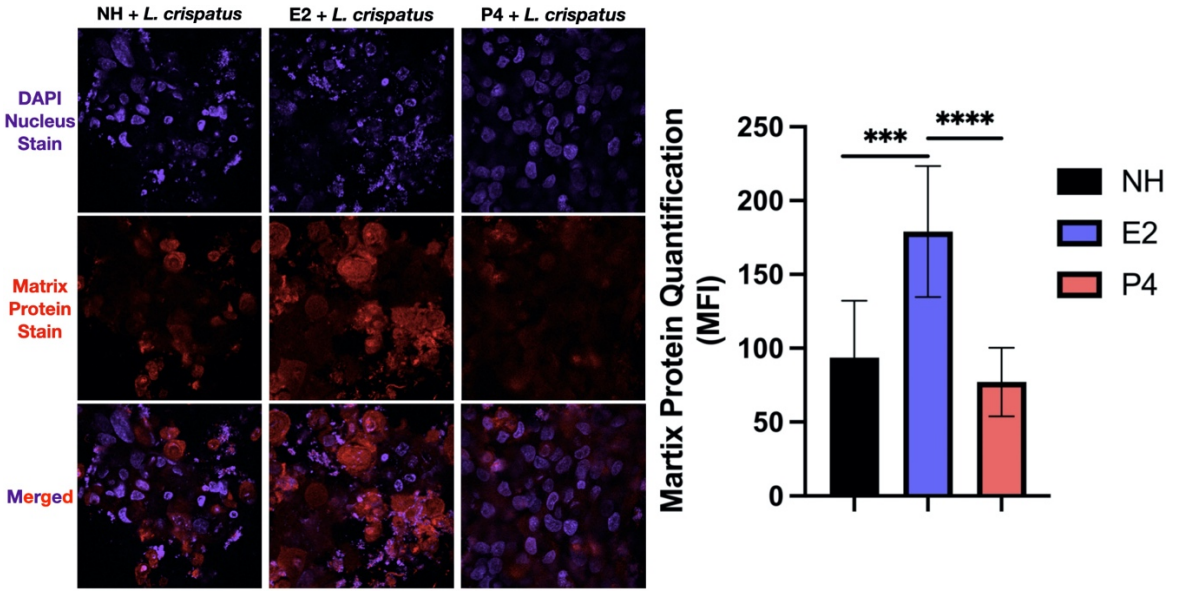

Figure 26. *L. crispatus* biofilm growth is significant in E2 hormone conditions compared to NH and P4 hormone conditions. *L. crispatus* at MOI of 100 were incubated anaerobically with LLI Vk2 cell cultures, grown under aerobic condition for 6 days, for 24 h with hormones E2 (10^{-9} M) or P4 (10^{-7} M). Fixed cultures were stained with FilmTracerTM SYPRO® Ruby to visualize biofilm matrix proteins (red) on Nikon eclipse Ti2 confocal laser scanning microscope. Mean Fluorescence Intensity (MFI) for 24 h *L. crispatus* biofilm growth on LLI cultures with hormones determined by mean grey area quantification of duplicate representative images from a singular well on imageJ. Representative of N=3 separate experiments. Data was analyzed with one- way ANOVA, with Bonferroni test to correct for multiple comparisons. ****p<0.0001, ***p=0.0003.

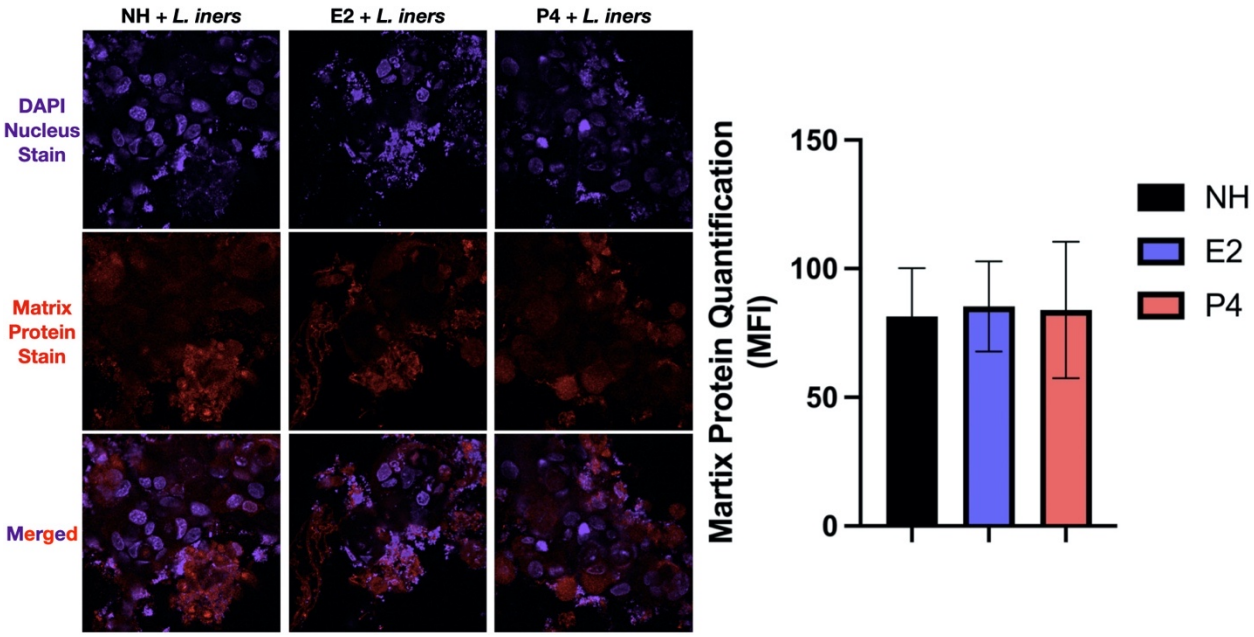

Figure 27. *L. iners* grows similarly in NH, E2 and P4 hormone conditions. *L. iners* at MOI of 100 were incubated anaerobically with LLI Vk2 cell cultures, grown under aerobic condition for 6 days, for 24 h with hormones E2 (10^{-9} M) or P4 (10^{-7} M). Fixed cultures were stained with FilmTracerTM SYPRO® Ruby to visualize biofilm matrix proteins (red) on Nikon eclipse Ti2 confocal laser scanning microscope. Mean Fluorescence Intensity (MFI) for 24 h *L. iners* biofilm growth on LLI cultures with hormones determined by mean gray area quantification of duplicate representative images from a singular well on imageJ. Representative of N=3 separate experiments. Data was analyzed with one-way ANOVA, with Bonferroni test to correct for multiple comparisons.

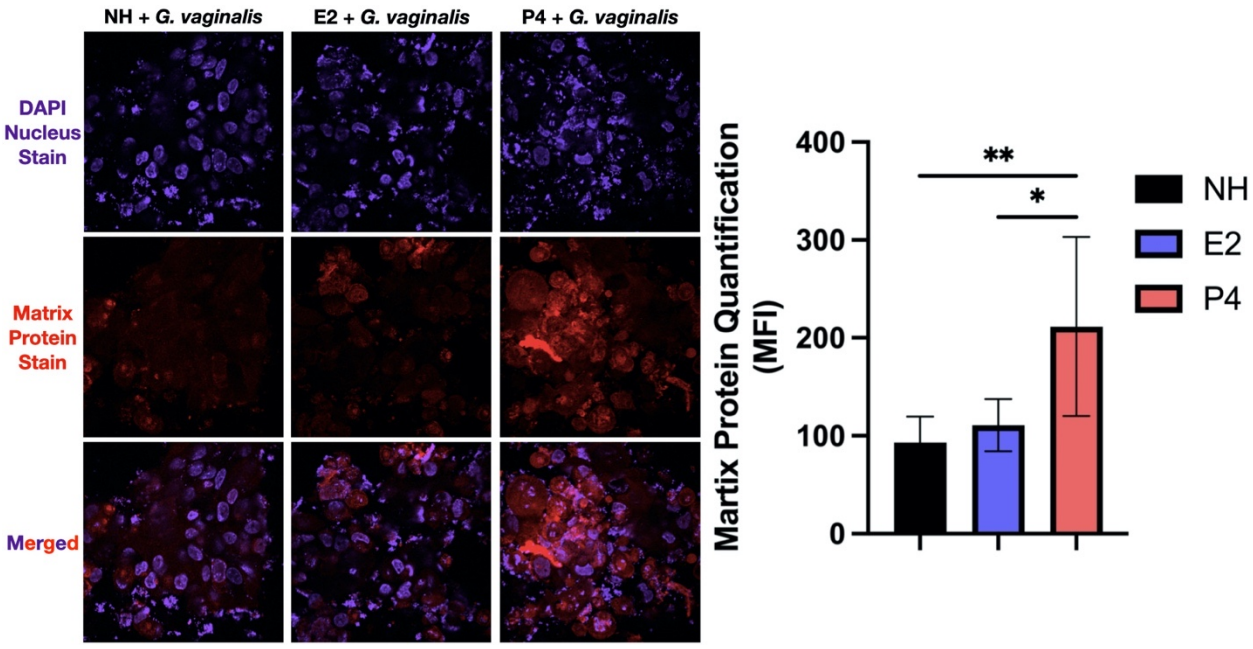

Figure 28. *G. vaginalis* biofilm growth is significant in P4 hormone conditions compared to NH and E2 hormone conditions. *G. vaginalis* at MOI of 100 were incubated anaerobically with LLI Vk2 cell cultures, grown under aerobic condition for 6 days, for 24 h with hormones E2 (10^{-9} M) or P4 (10^{-7} M). Fixed cultures were stained with FilmTracerTM SYPRO® Ruby to visualize biofilm matrix proteins (red) on Nikon eclipse Ti2 confocal laser scanning microscope. Mean Fluorescence Intensity (MFI) for 24 h *G. vaginalis* biofilm growth on LLI cultures with hormones determined by mean gray area quantification of duplicate representative images from a singular well on imageJ. Representative of N=3 separate experiments. Data was analyzed with one- way ANOVA, with Bonferroni test to correct for multiple comparisons. **p=0.0060, *p=0.0153.

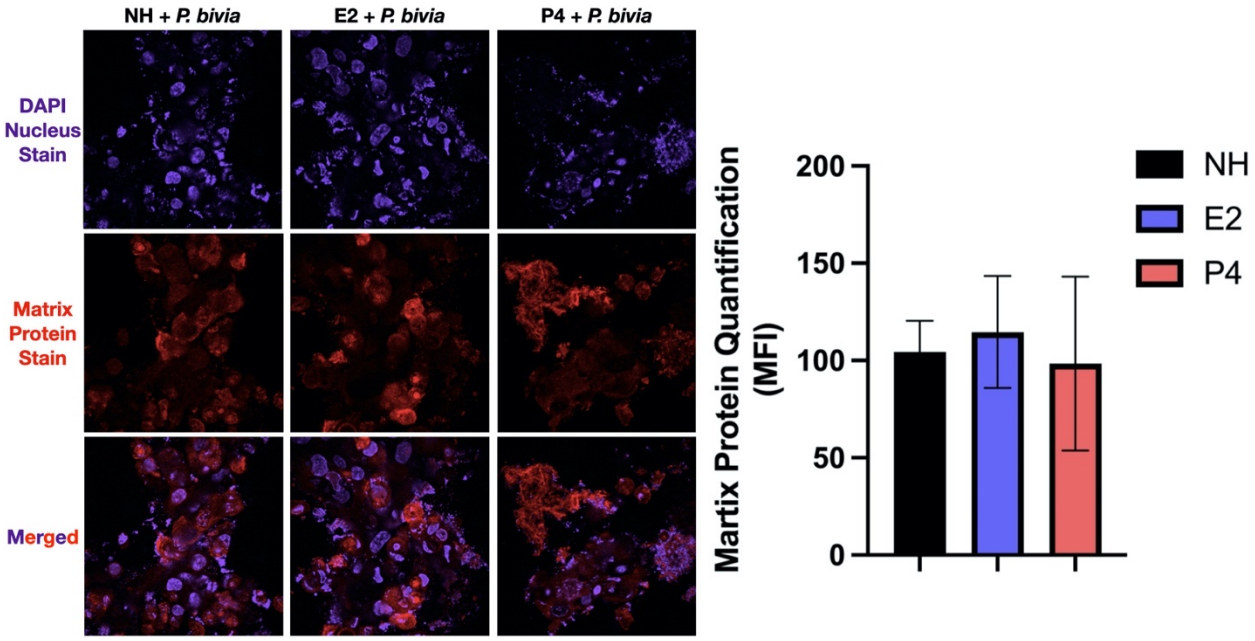

Figure 29. *P. bivia* grows similarly in NH, E2 and P4 hormone conditions. *P. bivia* at MOI of 100 were incubated anaerobically with LLI Vk2 cell cultures, grown under aerobic condition for 6 days, for 24 h with hormones E2 (10^{-9} M) or P4 (10^{-7} M). Fixed cultures were stained with FilmTracerTM SYPRO® Ruby to visualize biofilm matrix proteins (red) on Nikon eclipse Ti2 confocal laser scanning microscope. Mean Fluorescence Intensity (MFI) for 24 h *P. bivia* biofilm growth on LLI cultures with hormones determined by mean gray area quantification of duplicate representative images from a singular well on imageJ. Representative of N=3 separate experiments. Data was analyzed with one-way ANOVA, with Bonferroni test to correct for multiple comparisons.

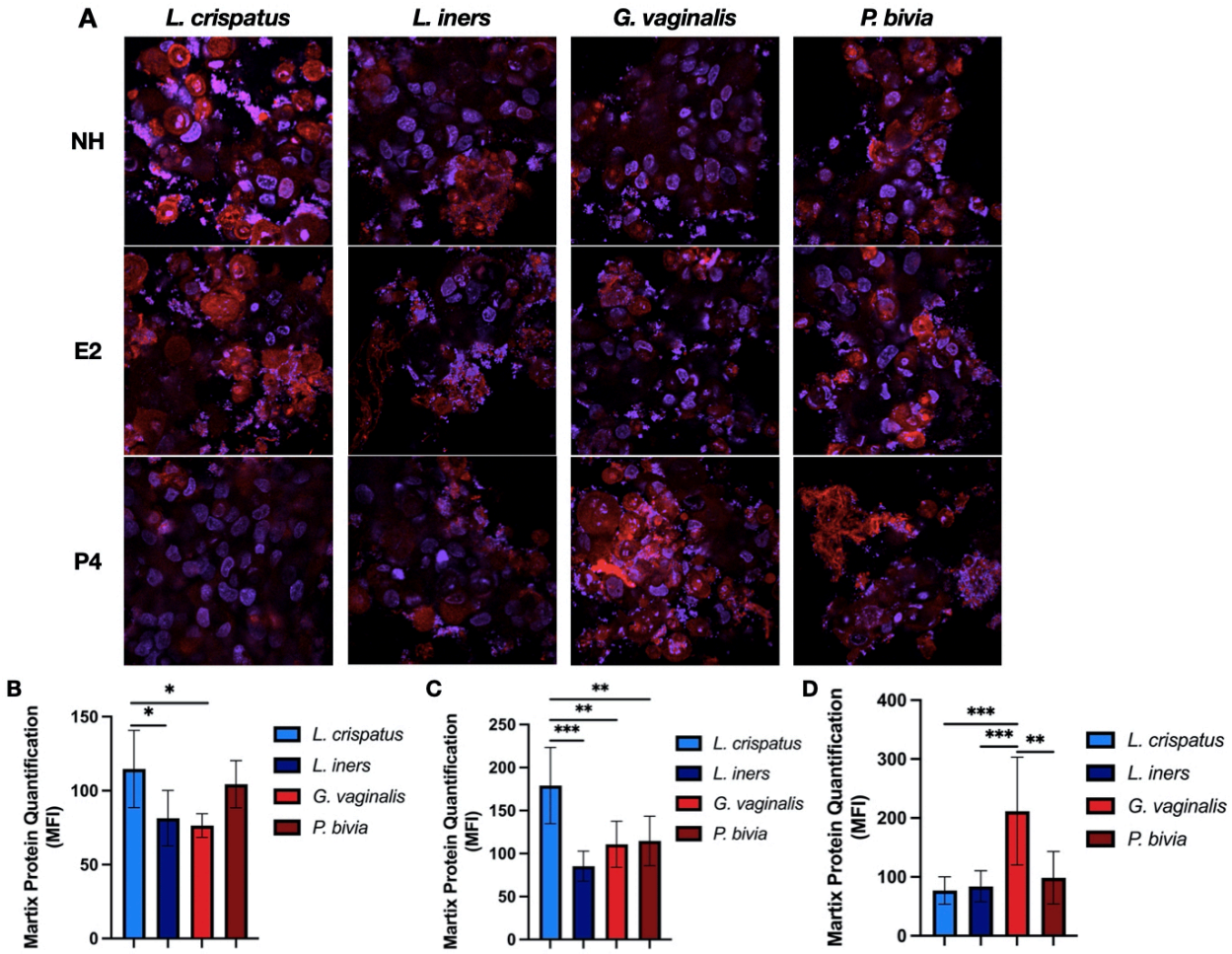

Figure 30. Biofilm growth comparison of all bacteria in NH, E2 and P4 hormone conditions. Bacteria at MOI of 100 were incubated anaerobically with LLI Vk2 cell cultures, grown under aerobic condition for 6 days, for 24 h with hormones E2 (10^{-9} M) or P4 (10^{-7} M). Fixed cultures were stained with FilmTracerTM SYPRO® Ruby to visualize biofilm matrix proteins (red) on Nikon eclipse Ti2 confocal laser scanning microscope (A). Mean Fluorescence Intensity (MFI) for 24 h growth on LLI cultures with no hormone conditions (B), E2 conditions (C) and P4 conditions (D) determined by mean gray area quantification of duplicate representative images from a singular well on imageJ. Representative of N=3 separate experiments. Data was analyzed with one-way ANOVA, with Bonferroni test to correct for multiple comparisons. ****p<0.0001, ***p=0.0004, **p=0.0026, *p=0.0132.

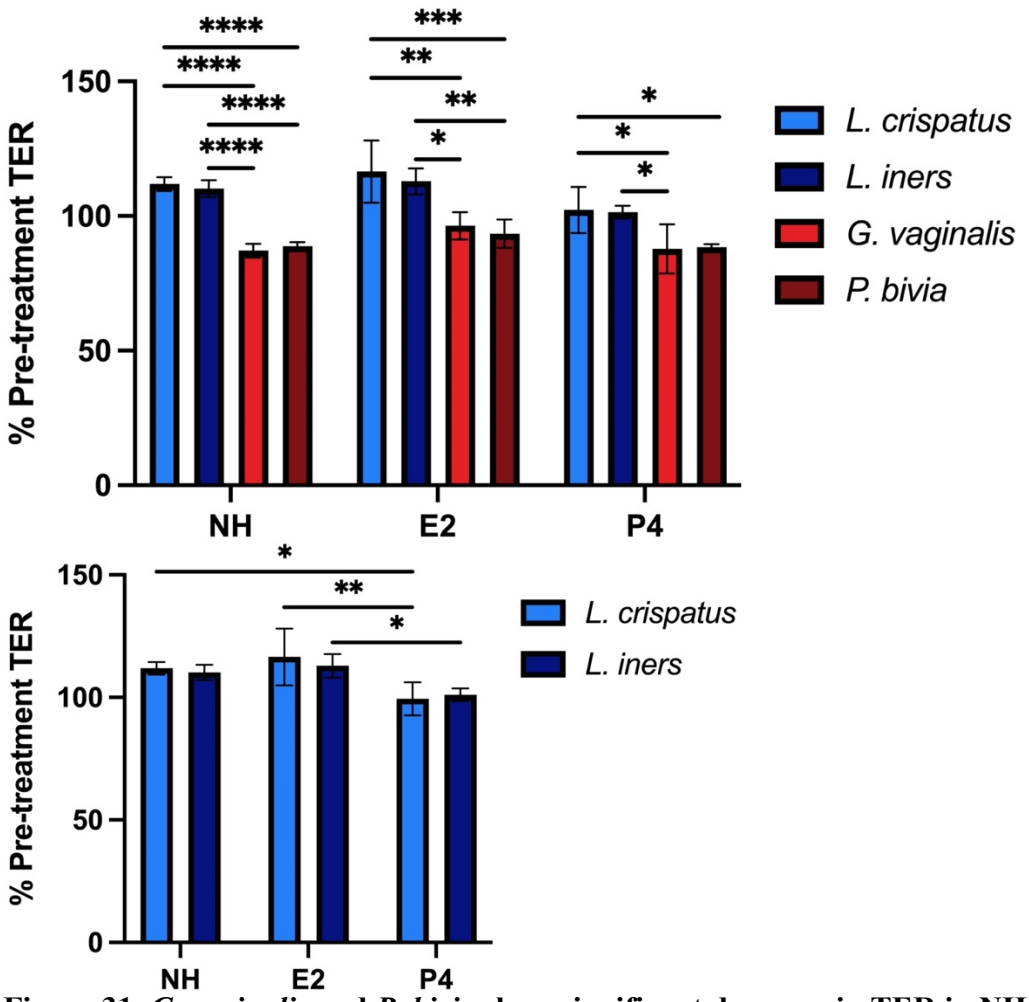

Figure 31. *G. vaginalis* and *P. bivia* show significant decrease in TER in NH, E2 and P4 hormone conditions in 24h LLI Vk2 cell co-cultures compared to *L. crispatus* and *L. iners*. Vk2 cells were grown for 6-days in LLI cultures in various hormone conditions, and TER was measured before addition of bacteria. *L. crispatus*, *L. iners*, *G. vaginalis* or *P. bivia* were added to cultures and the bacteria and Vk2 cell co-cultures were incubated in anaerobic conditions for 24 h. After both time points, TER of the co-cultures were measured. The effect of bacteria on the Vk2 cells is determined by TER measurements and reported as % Pre- treatment: (TER of bacteria and Vk2 cell co-cultures / TER of the Day 6 Vk2 cell culture before bacteria was added)*100%. Representative of N=3 separate experiments. Data was analyzed with two-way ANOVA, with Bonferroni test to correct for multiple comparisons. ****p<0.0001, ***p=0.0007, **p=0.033, *p=0.0387.

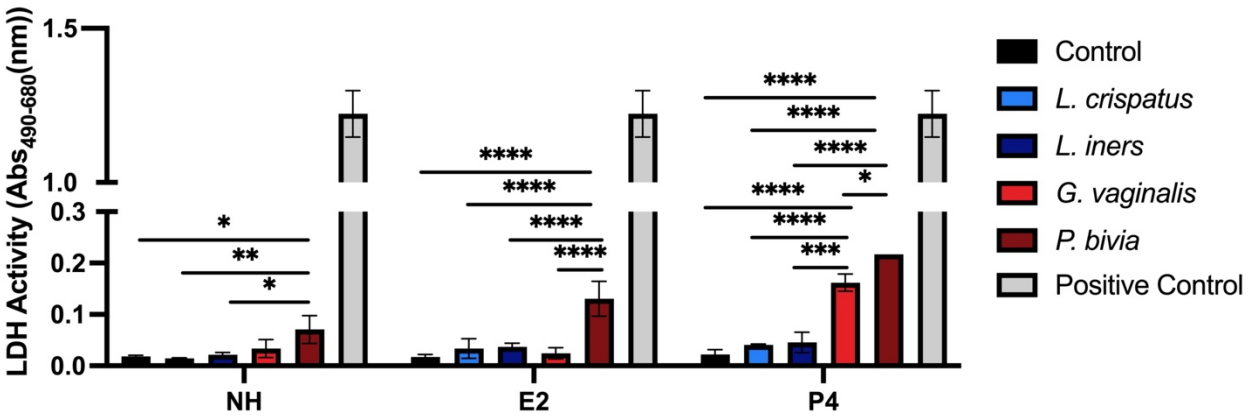

Figure 32. P4 hormone conditions enhance *G. vaginalis* and *P. bivia* cytotoxic effect on Vk2 cell co-cultures. Vk2 cells were grown for 6-days in LLI cultures in various hormone conditions. *L. crispatus*, *L. iners*, *G. vaginalis* or *P. bivia* were added to cultures and the bacteria and Vk2 cell co-cultures were incubated in anaerobic conditions for 24 h. After both time points, supernatants of the co-cultures were collected for LDH assay. Cell viability was determined by comparing the LDH activity of bacteria and cell co-cultures supernatants to the LDH activity of the control (Vk2 cells with no bacteria). Representative of N=3 separate experiments. Data was analyzed with two-way ANOVA, with Bonferroni test to correct for multiple comparisons. ****p<0.0001, ***p=0.0004, **p=0.0030, *p=0.0200.

4.2.3 Test the effect of eubiotic and dysbiotic short-chain fatty acid (SCFA) conditions on biofilm growth to determine if SFCA similar to that seen in eubiotic conditions can promote *Lactobacillus* biofilm growth and decrease biofilm growth of BV-associated bacteria.

Preliminary experiments for this sub-aim were first conducted in biofilm growth in a plate to determine if SCFA have any effect on bacteria growth in the absence of Vk2 cells. SCFA-supplemented bacteria growth medium that mimics either eubiotic or dysbiotic conditions based on the findings of the systemic review conducted in this lab were used in comparison to normal bacteria growth media.[90] It was determined that in a plate model, SCFA conditions can have varying effects on biofilm growth. *L. crispatus* had significant biofilm growth in normal and dysbiotic conditions compared to eubiotic conditions (Figure 33). This is unexpected as *Lactobacillus* is favoured in eubiotic conditions. However, the absence of Vk2 cells may have varying effects on how bacteria are growing biofilm. SCFA conditions had no effect on *L. iners* biofilm growth (Figure 34). *G. vaginalis* had significant biofilm growth in normal and dysbiotic

conditions compared to eubiotic conditions (Figure 35). *P. bivia* had significant biofilm growth in dysbiotic conditions compared to eubiotic and normal conditions (Figure 36).

This experiment was then conducted in bacteria and Vk2 cell co-cultures with SCFA supplemented media mimicking eubiotic or dysbiotic conditions (M&M 3.19). The results of this experiment were unexpected. Image analysis on confocal microscopy revealed that the SCFA conditions caused increased permeability and entry of matrix protein staining into the cells (Figure 37-40). This was determined by the apparent intracellular staining seen with the red matrix protein stain after separation of colour channels in each confocal image. Compared to the no SCFA condition, both eubiotic and dysbiotic conditions showed this unusual cell staining. It was also interesting to observe the variation in the DAPI cell staining in each condition. The nucleus staining in the dysbiotic condition looks very different than in the normal and eubiotic conditions, indicating that the metabolite conditions may be causing cells to enter varying stages of their life cycle. The impact that metabolite conditions are having on Vk2 cells, and the implications for biofilm growth need to be investigated further.

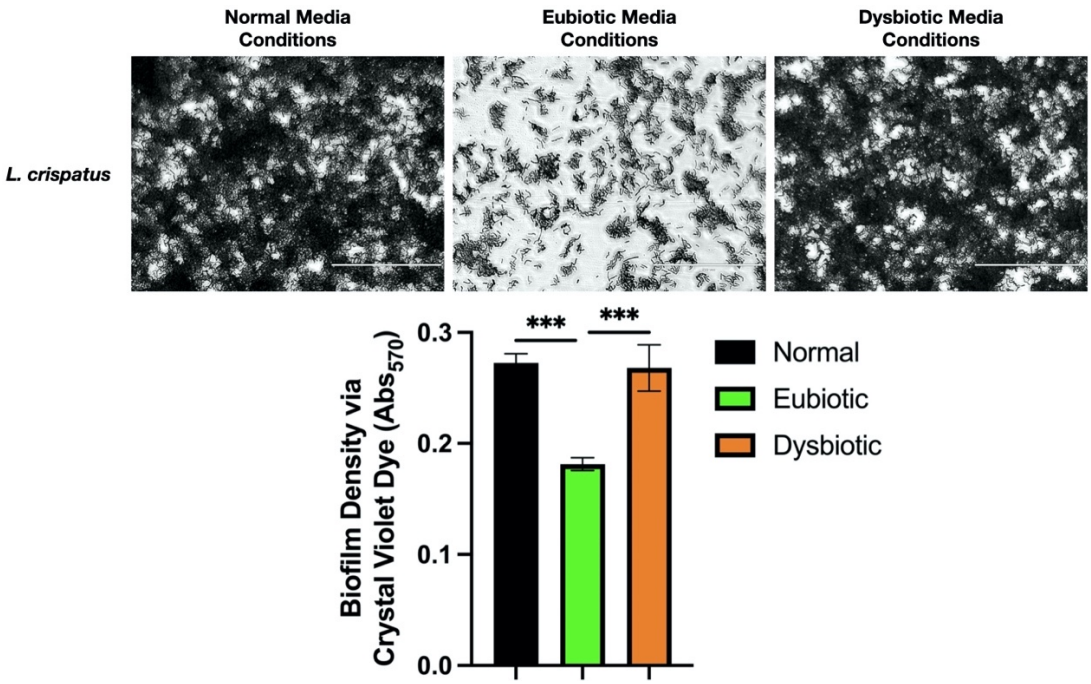

Figure 33. *L. crispatus* shows significant biofilm formation in normal and dysbiotic SCFA conditions compared to eubiotic SCFA conditions in a plate model of biofilm growth. Freshly grown *L. crispatus* was plated into 24-well plate and grown anaerobically at 37°C for 48 h. Images were captured on EVOS FL microscope (Life Technology). Biofilm was visualized with crystal violet. Bacteria biofilm grown in 96-well plates were stained with 0.1% crystal violet dye and Abs570 measured to determine the strength of biofilm by comparison of bacteria culture Abs to ODc (ODc = average Abs of negative control + (3xSD of negative control)). Representative of N=3 separate experiments, with triplicate wells quantified by Abs570 in each experiment. Data was analyzed with one-way ANOVA, with Bonferroni test to correct for multiple comparisons. ***p=0.0005.

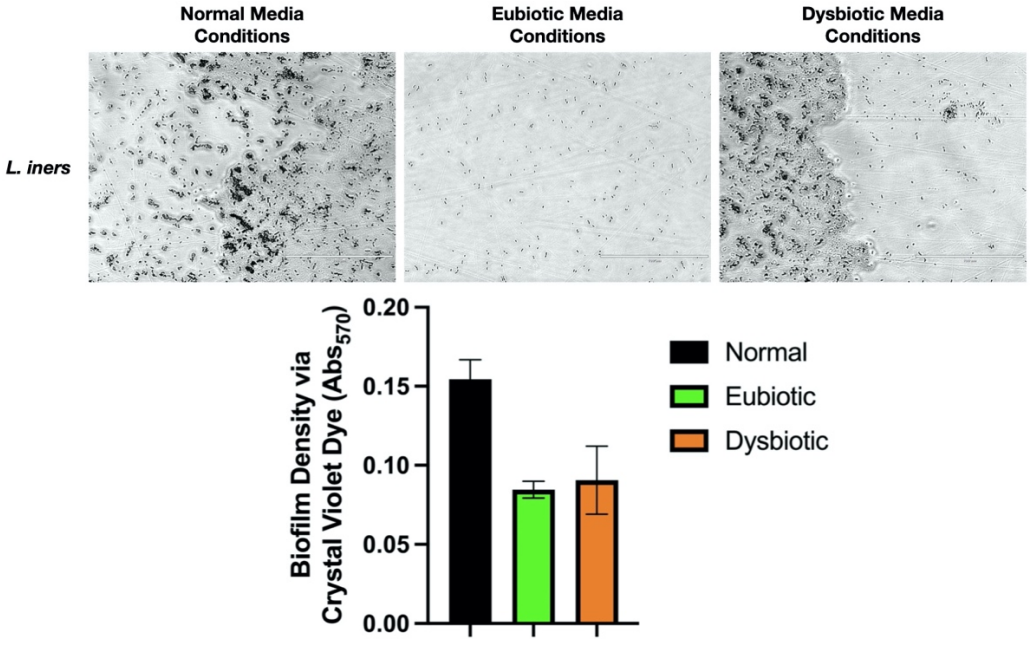

Figure 34. *L. iners* does not show significant differences in biofilm growth in normal, eubiotic or dysbiotic SCFA conditions in a plate model of biofilm growth. Freshly grown *L. iners* was plated into 24-well plate and grown anaerobically at 37°C for 48 h. Images were captured on EVOS FL microscope (Life Technology). Biofilm was visualized with crystal violet. Bacteria biofilm grown in 96-well plates were stained with 0.1% crystal violet dye and Abs570 measured to determine the strength of biofilm by comparison of bacteria culture Abs to ODc (ODc = average Abs of negative control + (3xSD of negative control)). Representative of N=3 separate experiments, with triplicate wells quantified by Abs570 in each experiment. Data was analyzed with one-way ANOVA, with Bonferroni test to correct for multiple comparisons.

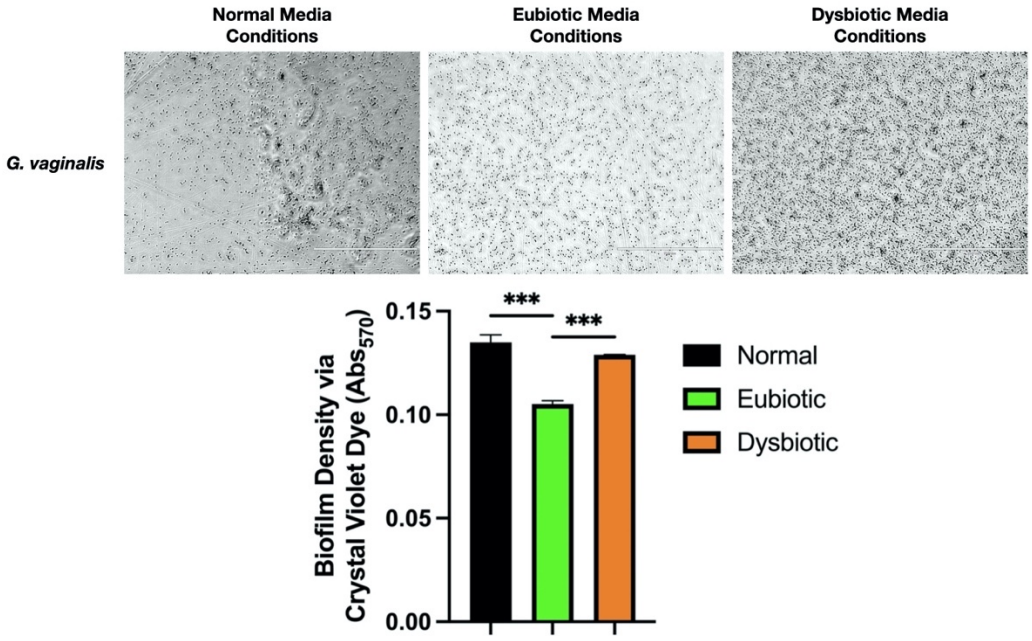

Figure 35. *G. vaginalis* shows significant biofilm growth in normal and dysbiotic SCFA conditions compared to eubiotic SCFA conditions in a plate model of biofilm growth. Freshly grown *G. vaginalis* was plated into 24-well plate and grown anaerobically at 37°C for 48 h. Images were captured on EVOS FL microscope (Life Technology). Biofilm was visualized with crystal violet. Bacteria biofilm grown in 96-well plates were stained with 0.1% crystal violet dye and Abs570 measured to determine the strength of biofilm by comparison of bacteria culture Abs to ODc (ODc = average Abs of negative control + (3xSD of negative control)). Representative of N=3 separate experiments, with triplicate wells quantified by Abs570 in each experiment. Data was analyzed with one-way ANOVA, with Bonferroni test to correct for multiple comparisons. ***p=0.0003.

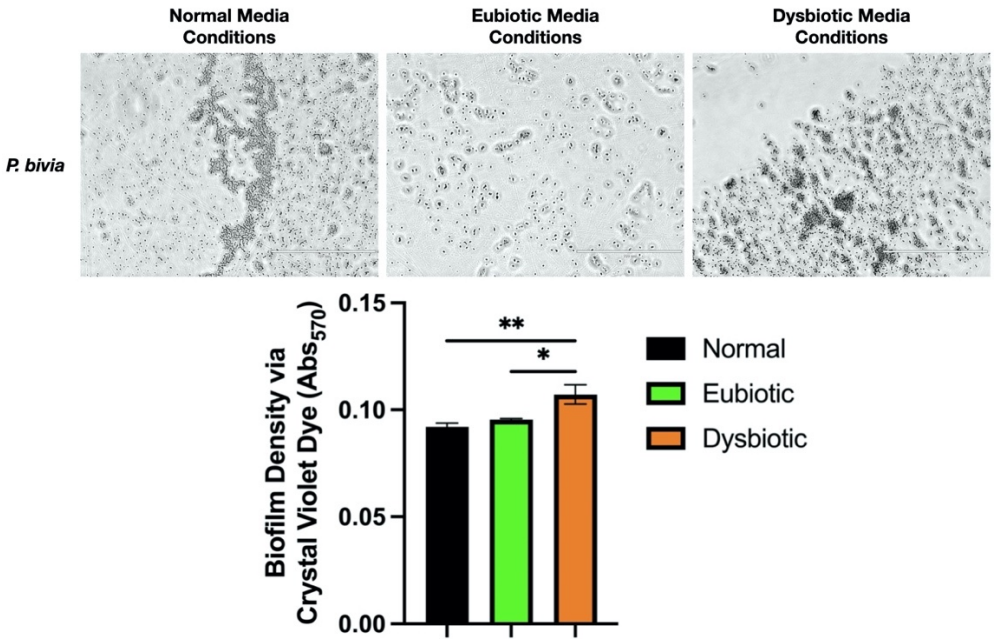

Figure 36. *P. bivia* shows significant biofilm growth in dysbiotic SCFA conditions compared to normal and eubiotic SCFA conditions in a plate model of biofilm growth. Freshly grown *P. bivia* was plated into 24-well plate and grown anaerobically at 37°C for 48 h. Images were captured on EVOS FL microscope (Life Technology). Biofilm was visualized with crystal violet. Bacteria biofilm grown in 96-well plates were stained with 0.1% crystal violet dye and Abs570 measured to determine the strength of biofilm by comparison of bacteria culture Abs to ODc (ODc = average Abs of negative control + (3xSD of negative control)). Representative of N=3 separate experiments, with triplicate wells quantified by Abs570 in each experiment. Data was analyzed with one-way ANOVA, with Bonferroni test to correct for multiple comparisons. **p=0.0095, *p=0.0323.

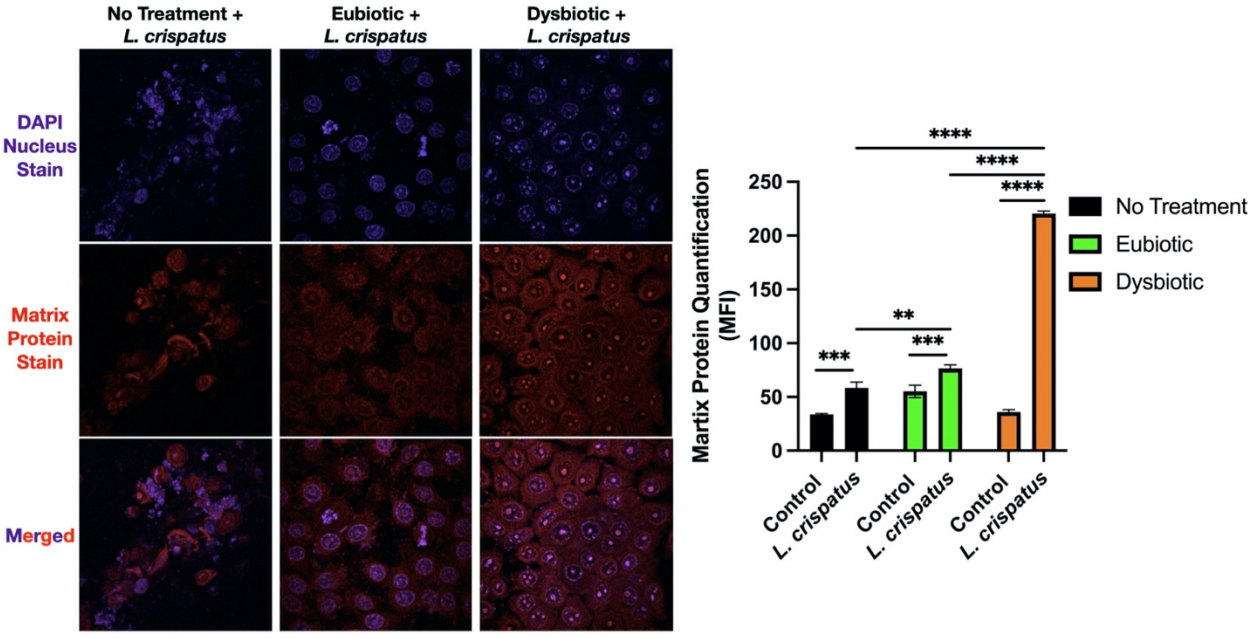

Figure 37. *L. crispatus* biofilm growth is significant in dysbiotic SCFA conditions compared to normal and eubiotic SCFA conditions. *L. crispatus* at MOI of 100 were incubated anaerobically with LLI Vk2 cell cultures, grown under aerobic condition for 6 days, for 24 h with eubiotic or dysbiotic metabolites. Fixed cultures were stained with FilmTracerTM SYPRO® Ruby to visualize biofilm matrix proteins (red) on Nikon eclipse Ti2 confocal laser scanning microscope. Mean Fluorescence Intensity (MFI) for 24 h *L. crispatus* biofilm growth on LLI cultures with eubiotic or dysbiotic metabolites determined by mean grey area quantification of duplicate representative images from a singular well on imageJ. Representative of N=3 separate experiments. Data was analyzed with two-way ANOVA, with Bonferroni test to correct for multiple comparisons. ****p<0.0001, ***p=0.0002, **p=0.0026.

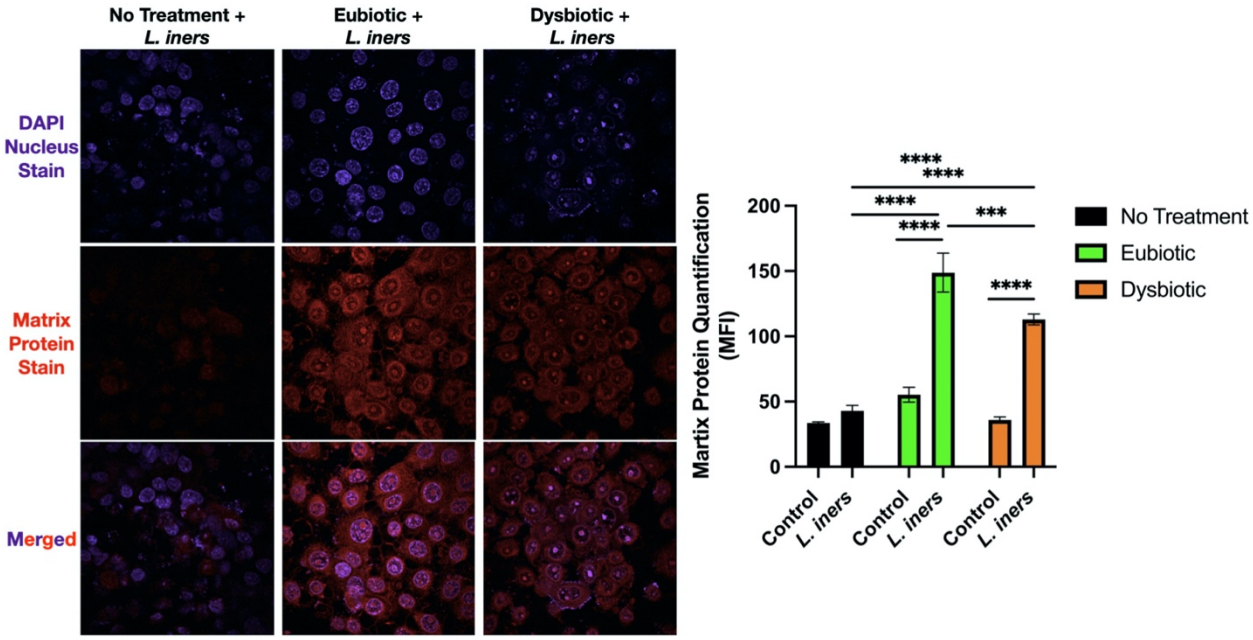

Figure 38. *L. iners* biofilm growth is significant in eubiotic SCFA conditions compared to normal and dysbiotic SCFA conditions. *L. iners* at MOI of 100 were incubated anaerobically with LLI Vk2 cell cultures, grown under aerobic condition for 6 days, for 24 h with eubiotic or dysbiotic metabolites. Fixed cultures were stained with FilmTracerTM SYPRO® Ruby to visualize biofilm matrix proteins (red) on Nikon eclipse Ti2 confocal laser scanning microscope. Mean Fluorescence Intensity (MFI) for 24 h *L. iners* biofilm growth on LLI cultures with eubiotic or dysbiotic metabolites determined by mean grey area quantification of duplicate representative images from a singular well on imageJ. Representative of N=3 separate experiments. Data was analyzed with two-way ANOVA, with Bonferroni test to correct for multiple comparisons. ****p<0.0001, ***p=0.0001.

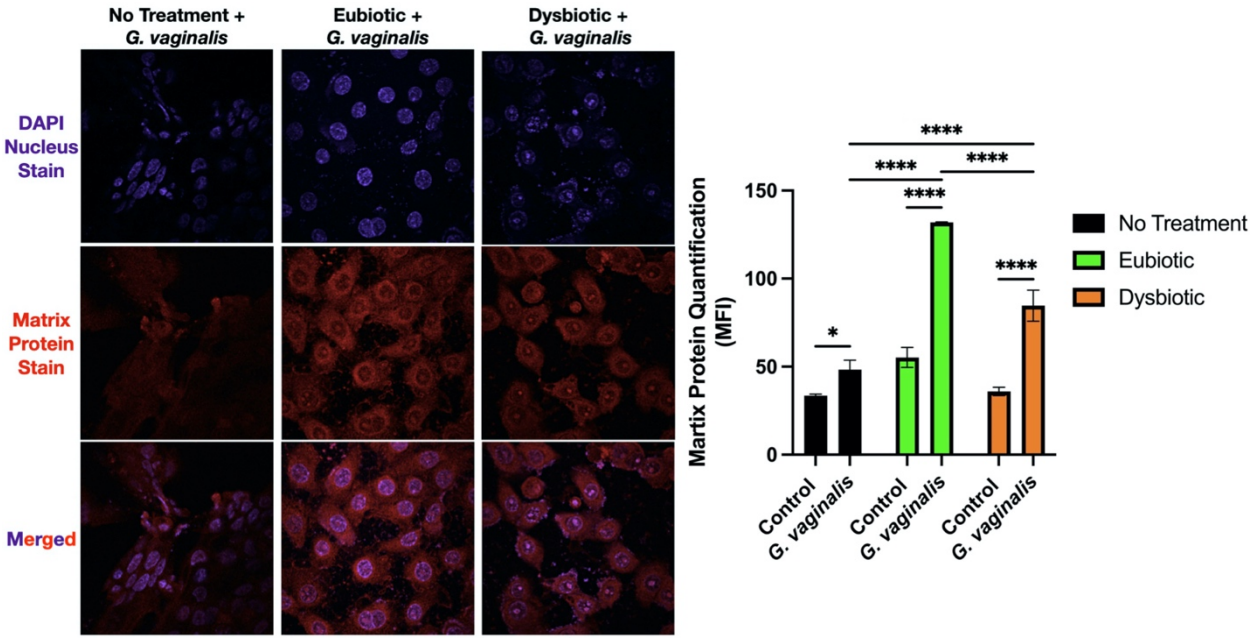

Figure 39. *G. vaginalis* biofilm growth is significant in eubiotic SCFA conditions compared to normal and dysbiotic SCFA conditions. *G. vaginalis* at MOI of 100 were incubated anaerobically with LLI Vk2 cell cultures, grown under aerobic condition for 6 days, for 24 h with eubiotic or dysbiotic metabolites. Fixed cultures were stained with FilmTracerTM SYPRO® Ruby to visualize biofilm matrix proteins (red) on Nikon eclipse Ti2 confocal laser scanning microscope. Mean Fluorescence Intensity (MFI) for 24 h *G. vaginalis* biofilm growth on LLI cultures with eubiotic or dysbiotic metabolites determined by mean grey area quantification of duplicate representative images from a singular well on imageJ. Representative of N=3 separate experiments. Data was analyzed with two-way ANOVA, with Bonferroni test to correct for multiple comparisons. ****p<0.0001, *p=0.0143.

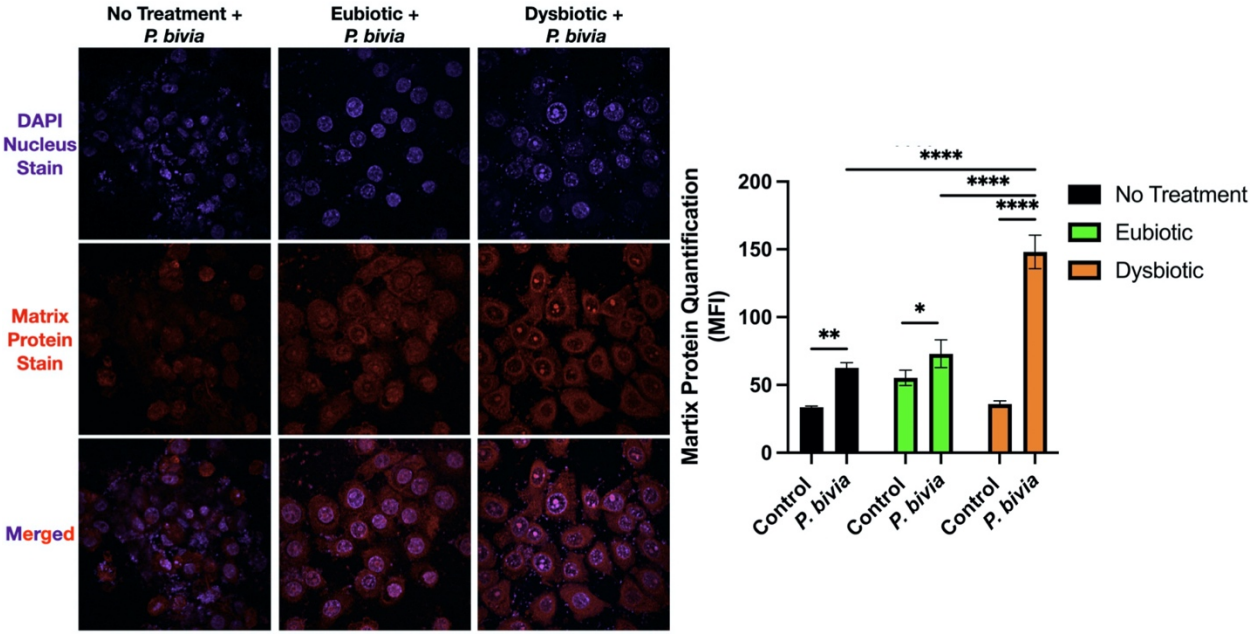

Figure 40. *P. bivia* biofilm growth is significant in dysbiotic SCFA conditions compared to normal and eubiotic SCFA conditions. *P. bivia* at MOI of 100 were incubated anaerobically with LLI Vk2 cell cultures, grown under aerobic condition for 6 days, for 24 h with eubiotic or dysbiotic metabolites. Fixed cultures were stained with FilmTracerTM SYPRO® Ruby to visualize biofilm matrix proteins (red) on Nikon eclipse Ti2 confocal laser scanning microscope. Mean Fluorescence Intensity (MFI) for 24 h *P. bivia* biofilm growth on LLI cultures with eubiotic or dysbiotic metabolites determined by mean grey area quantification of duplicate representative images from a singular well on imageJ. Representative of N=3 separate experiments. Data was analyzed with two-way ANOVA, with Bonferroni test to correct for multiple comparisons. ****$p<0.0001$, **$p=0.0010$, *$p=0.0322$.

4.2.4 Test the effect of mucin degrading enzyme sialidase on biofilm formation by different bacteria.

Due to the importance of mucin presence for biofilm growth *in vivo*, we used a sialidase enzyme to degrade mucin in the bacteria and Vk2 cell co-culture model to examine impact on biofilm growth.

Vk2 cell co-cultures were grown in the presence of sialidase before bacteria inoculation (M&M 3.20). Biofilm production was quantified by MFI of FilmTracerTM SYPRO® Ruby matrix protein stain and mucin-1 production was quantified by MFI of mouse anti-human MUC1 (CD227) antibody. Mucin-1 production in the control conditions, in the absence of bacteria, was significantly decreased in the E2 condition when sialidase was added (Figure 41).

L. crispatus biofilm growth in 24 h LLI Vk2 cell co-cultures in the no sialidase condition aligns with previous results from section 4.2.2 which showed increased biofilm growth in E2 compared to NH and P4 (Figure 42A). When sialidase was used to degrade mucin-1, there was a significant decrease in biofilm growth in the E2 condition (Figure 42A). The amount of biofilm growth quantified in the E2 and sialidase condition was consistent with the negative control, indicating that in a mucin-deficient system, *L. crispatus* biofilm growth in E2 conditions is reduced to none. When *L. crispatus* is present, mucin-1 production was significantly increased compared to the control in NH and E2 conditions (Figure 42B). Also, when comparing mucin-1

production in *L. crispatus* conditions, production was significantly decreased in the NH, E2 and P4 conditions when sialidase was present (Figure 42B). These results suggest that *L. crispatus* bacteria is stimulating mucin-1 production in Vk2 cells. This was demonstrated by the increased mucin-1 quantification seen in NH and E2 conditions compared to controls. There were significant decreases in mucin-1 production in the normal vs sialidase bacteria conditions that was not seen in the NH and P4 condition without bacteria.

L. iners biofilm growth in 24 h LLI Vk2 cell co-cultures in the no sialidase condition aligns with previous results from section 4.2.2 which showed consistent biofilm growth in NH, E2 and P4 conditions (Figure 43A). When sialidase was used to degrade mucin-1, there were no significant decreases in biofilm growth in the NH, E2 and P4 conditions (Figure 43A), indicating that biofilm growth was not impacted by lack of mucin. When *L. iners* was present, mucin-1 production significantly increased compared to the control in E2 conditions (Figure 43B). Also, when comparing mucin-1 production when *L. iners* was present, production significantly decreased in E2 conditions with the use of sialidase (Figure 43B).

G. vaginalis biofilm growth in 24 h LLI Vk2 cell co-cultures in the no sialidase condition aligns with previous results from section 4.2.2 which showed increased biofilm growth in P4 compared to NH and E2 (Figure 44A). When sialidase was used to degrade mucin-1, there was a significant decrease in biofilm growth for *G. vaginalis* in the P4 condition (Figure 44A). When *G. vaginalis* was present, mucin-1 production significantly increased compared to the control in NH, E2 and P4 conditions and was significantly decreased in NH, E2 and P4 conditions when sialidase was present (Figure 44B).

P. bivia biofilm growth in 24 h LLI Vk2 cell co-cultures in the no sialidase condition aligns with previous results from section 4.2.2 which showed consistent biofilm growth in NH,

E2 and P4 conditions (Figure 45A). When sialidase was used to degrade mucin-1, there was a significant decrease in biofilm growth in the NH condition (Figure 45A). When *P. bivia* was present, mucin-1 production was significantly increased compared to the control in NH and E2 conditions and was significantly decreased when sialidase was present for NH and E2 conditions as well (Figure 45B).

To determine the quantity of bacteria that was present in each condition in this aim, a qPCR was conducted. First, standard curves for each bacterium were created by DNA extraction of grown bacteria cultures, qPCR quantification of collected DNA and comparison of CT value to CFU/mL of each culture (M&M 3.21) (Figure 46). Next, 24-h LLI Vk2 cell co-cultures with all bacteria of interest in hormone conditions and sialidase conditions were used for DNA extraction. An enzymatic lysis buffer was used to release bacterial DNA in culture, which was then collected and used for real-time qPCR determination. Bacteria quantification through standard curve extrapolation was done for each bacterium and Vk2 cell co-culture in the various conditions tested (M&M 3.22) (Figure 47). Unexpectedly, for most bacteria the sialidase condition showed higher bacteria quantification than no sialidase condition for NH, E2 and P4 conditions (Figure 47). These are preliminary results and will be explored further in future experiments.

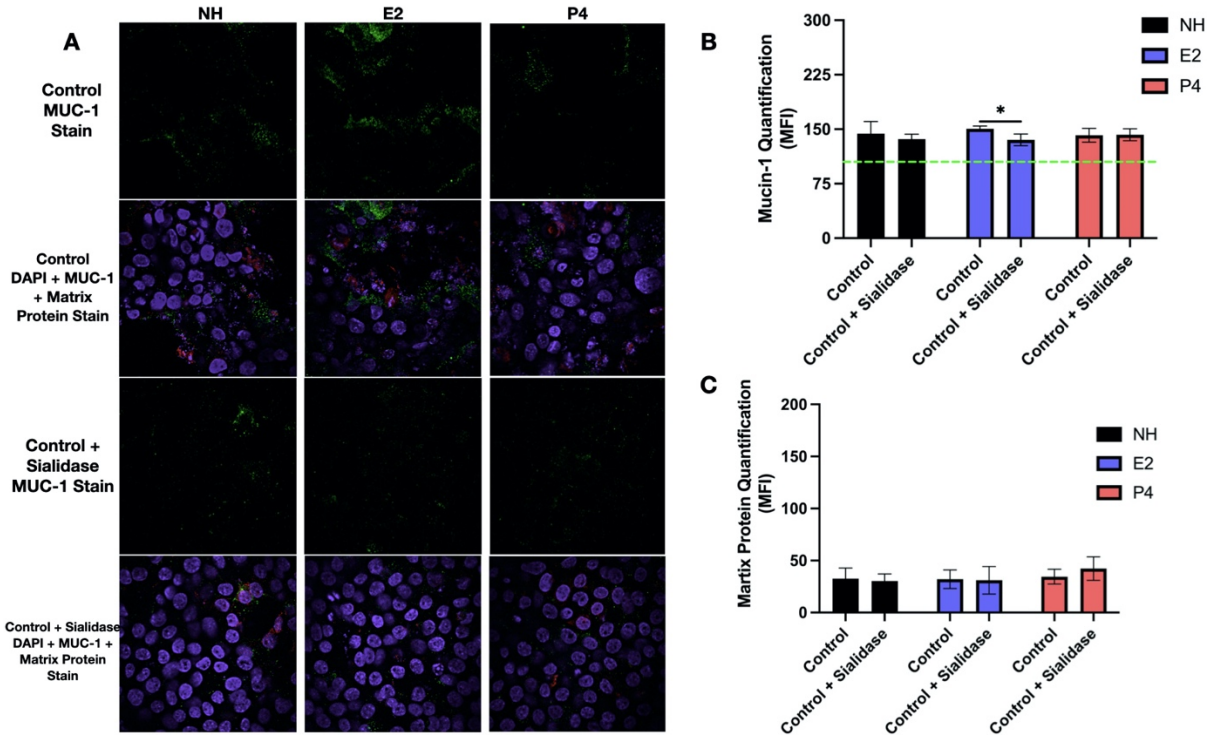

Figure 41. Mucin degrading enzyme, Sialidase significantly decreases mucin production in E2 hormone conditions. Vk2 cells were grown for 6-days in LLI cultures in various hormone conditions. Sialidase was added to cells for 2 h prior to bacteria inoculation then removed. Vk2 cell controls with no bacteria were incubated in anaerobic conditions for 24 h. A) Fixed cultures were stained with FilmTracerTM SYPRO® Ruby to visualize biofilm matrix proteins (red) (separate matrix protein stain channel not shown on image) and mouse anti-human MUC1 (CD227) antibody (green) on Nikon eclipse Ti2 confocal laser scanning microscope. Mean Fluorescence Intensity (MFI) of MUC-1 staining (B) and matrix protein stain (C) for 24-h control LLI cultures with hormones determined by mean gray area quantification of duplicate representative images from a singular well on imageJ. Baseline Fluorescence, represented by dotted green line, defined as the minimum quantification for green fluorescence intensity on imageJ. Representative of N=3 separate experiments. Data was analyzed with two-way ANOVA, with Bonferroni test to correct for multiple comparisons. *p=0.0171.

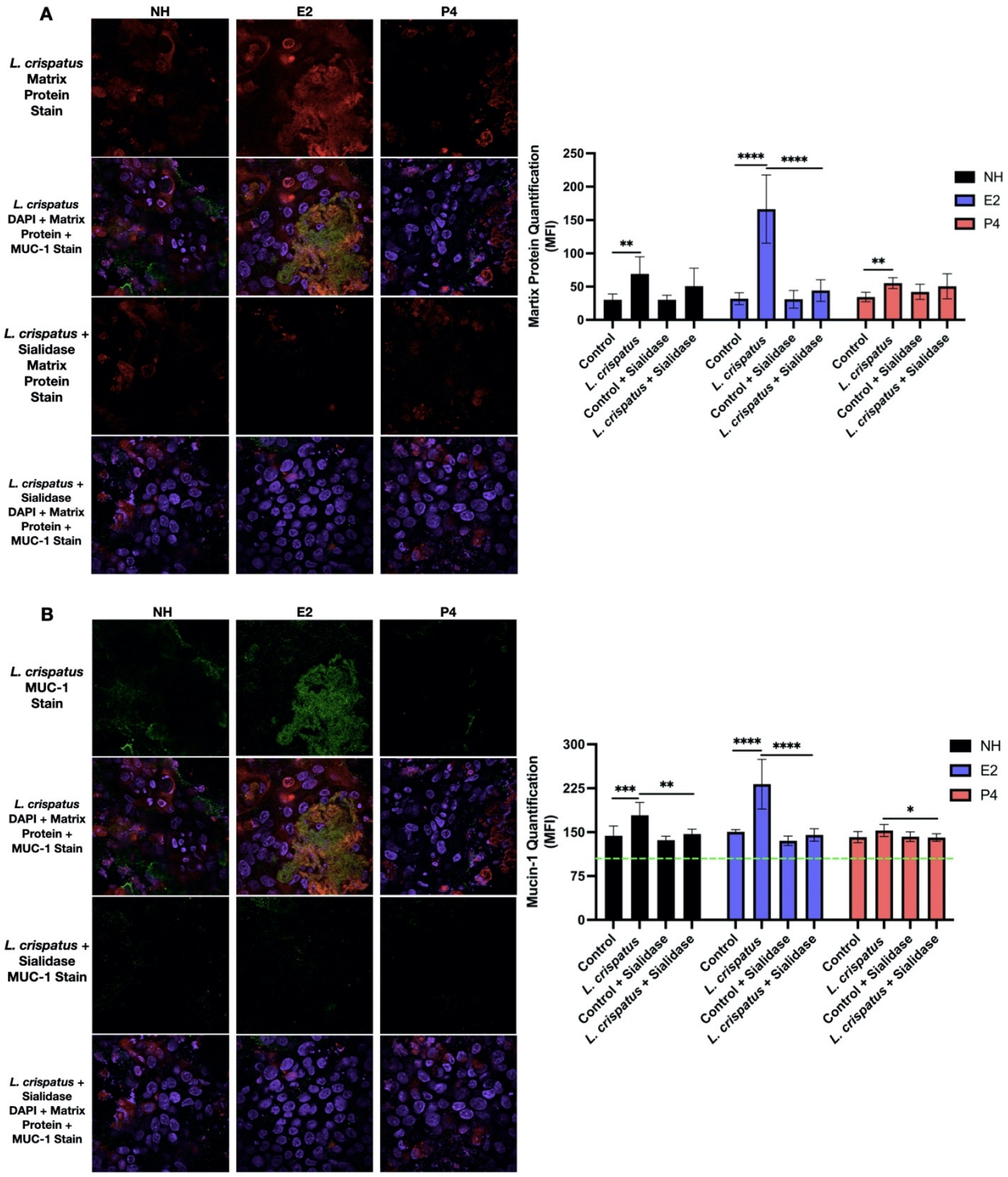

Figure 42. Mucin degrading enzyme, Sialidase in *L. crispatus* and Vk2 cell co-cultures significantly decreases biofilm formation in E2 hormone conditions and mucin production in NH, E2 and P4 hormone conditions. Vk2 cells were grown for 6-days in LLI cultures in various hormone conditions. Sialidase was added to cells for 2 h prior to bacteria inoculation then removed. *L. crispatus* was added to cultures and bacteria and Vk2 cell co-cultures incubated in anaerobic conditions for 24 h. Fixed cultures were stained with FilmTracerTM SYPRO®

Ruby to visualize biofilm matrix proteins (red) and mouse anti-human MUC1 (CD227) antibody (green) on Nikon eclipse Ti2 confocal laser scanning microscope. Mean Fluorescence Intensity (MFI) of matrix protein staining (A) and MUC-1 staining (B) for 24-h *L. crispatus* and LLI Vk2 cell co-cultures with hormones determined by mean gray area quantification of duplicate representative images from a singular well on imageJ. Baseline Fluorescence, represented by dotted green line, defined as the minimum quantification for green fluorescence intensity on imageJ. Representative of N=3 separate experiments. Data was analyzed with two-way ANOVA, with Bonferroni test to correct for multiple comparisons. ****p<0.0001, ***p=0.0008, **p=0.0012, *p=0.0322.

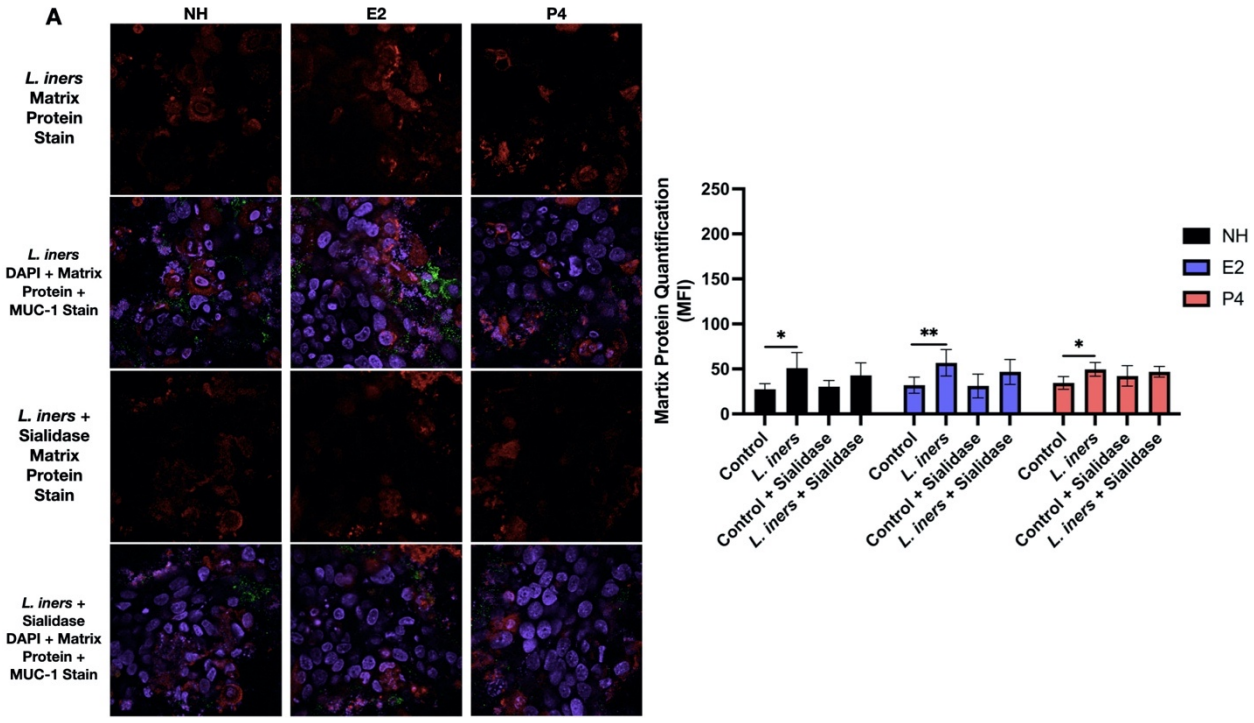

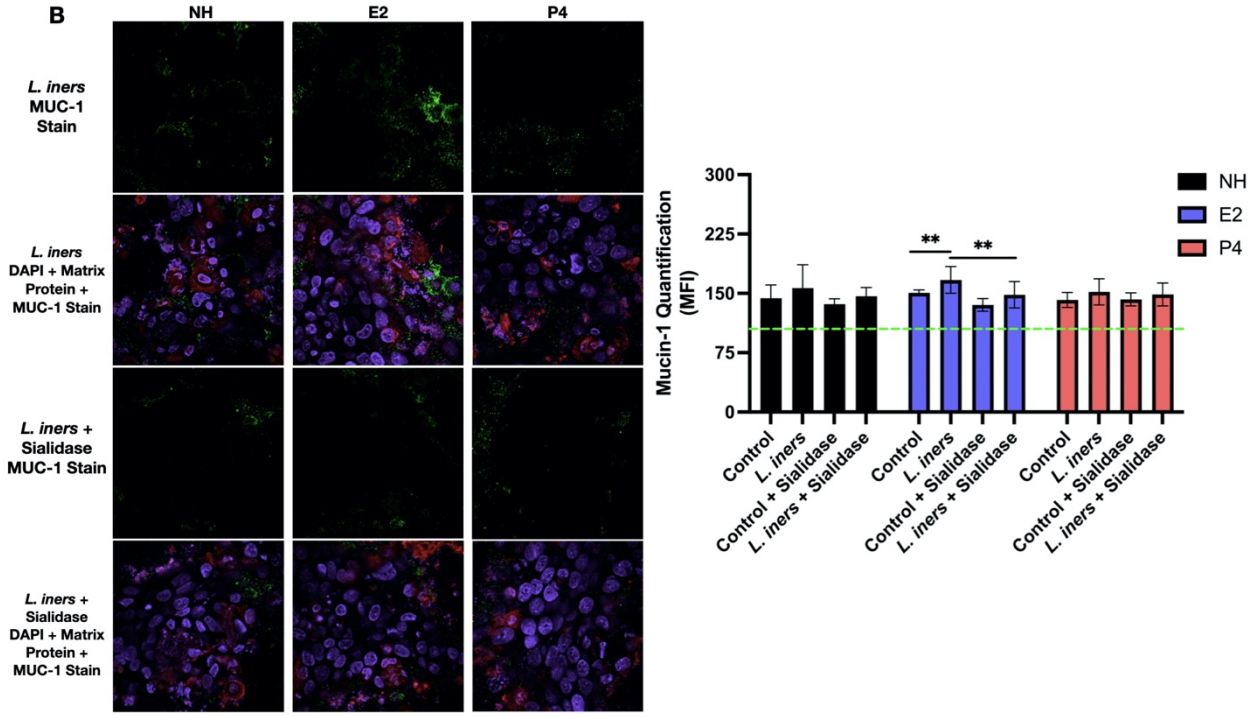

Figure 43. Mucin degrading enzyme, Sialidase in *L. iners* and Vk2 cell co-cultures significantly decreases mucin production in E2 hormone conditions. Vk2 cells were grown for 6-days in LLI cultures in various hormone conditions. Sialidase was added to cells for 2 h prior to bacteria inoculation then removed. *L. iners* was added to cultures and bacteria and Vk2 cell co-cultures incubated in anaerobic conditions for 24 h. Fixed cultures were stained with FilmTracerTM SYPRO® Ruby to visualize biofilm matrix proteins (red) and mouse anti-human MUC1 (CD227) antibody (green) on Nikon eclipse Ti2 confocal laser scanning microscope. Mean Fluorescence Intensity (MFI) of matrix protein staining (A) and MUC-1 staining (B) for 24-h *L. iners* and LLI Vk2 cell co-cultures with hormones determined by mean gray area quantification of duplicate representative images from a singular well on imageJ. Baseline Fluorescence, represented by dotted green line, defined as the minimum quantification for green fluorescence intensity on imageJ. Representative of N=3 separate experiments. Data was analyzed with two-way ANOVA, with Bonferroni test to correct for multiple comparisons. **p=0.0019, *p=0.0207.

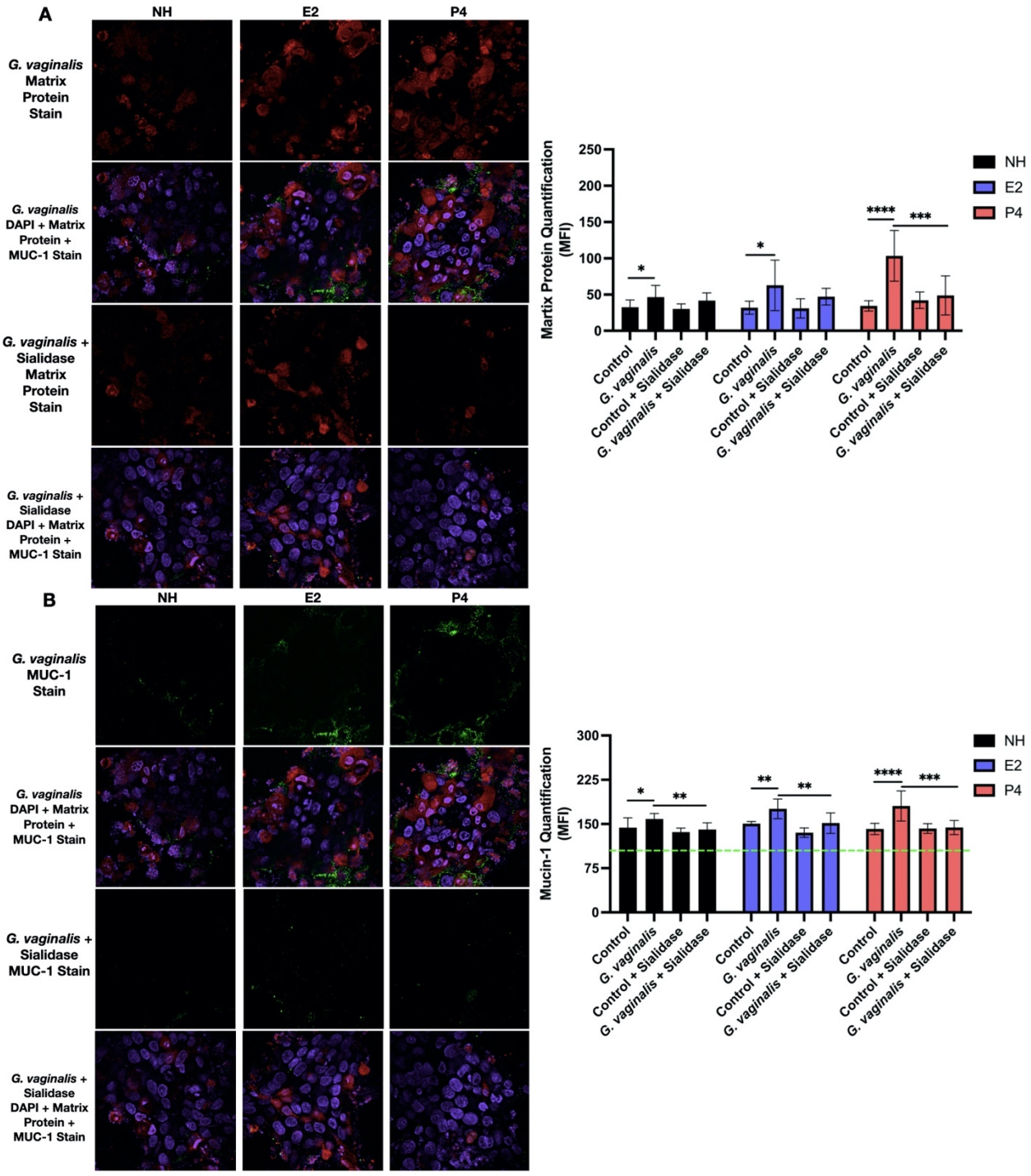

Figure 44. Mucin degrading enzyme, Sialidase in *G. vaginalis* and Vk2 cell co-cultures significantly decreases biofilm formation in P4 hormone conditions and mucin production in NH, E2 and P4 hormone conditions. Vk2 cells were grown for 6-days in LLI cultures in various hormone conditions. Sialidase was added to cells for 2 h prior to bacteria inoculation then removed. *G. vaginalis* was added to cultures and bacteria and Vk2 cell co-cultures incubated in anaerobic conditions for 24 h. Fixed cultures were stained with FilmTracerTM SYPRO® Ruby to visualize biofilm matrix proteins (red) and mouse anti-human MUC1

(CD227) antibody (green) on Nikon eclipse Ti2 confocal laser scanning microscope. Mean Fluorescence Intensity (MFI) of matrix protein staining (A) and MUC-1 staining (B) for 24-h *G. vaginalis* and LLI Vk2 cell co-cultures with hormones determined by mean gray area quantification of duplicate representative images from a singular well on imageJ. Baseline Fluorescence, represented by dotted green line, defined as the minimum quantification for green fluorescence intensity on imageJ. Representative of N=3 separate experiments. Data was analyzed with two-way ANOVA, with Bonferroni test to correct for multiple comparisons. ****p<0.0001, ***p=0.0001, **p=0.0014, *p=0.0362.

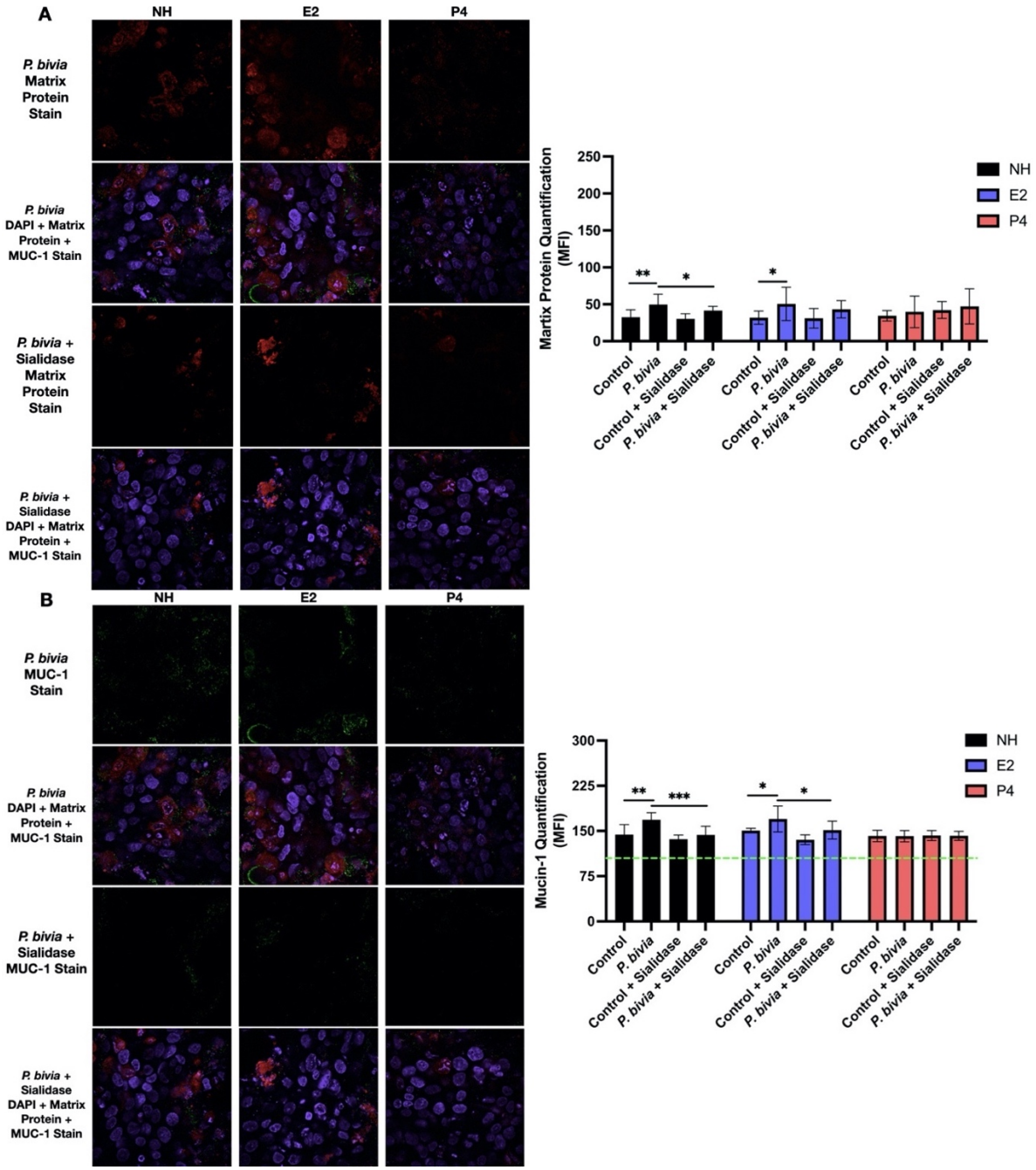

Figure 45. Mucin degrading enzyme, Sialidase in *P. bivia* and Vk2 cell co-cultures significantly decrease biofilm formation in normal media conditions and significantly decreases mucin production in NH and E2 hormone conditions. Vk2 cells were grown for 6-days in LLI cultures in various hormone conditions. Sialidase was added to cells for 2 h prior to bacteria inoculation then removed. *P. bivia* was added to cultures and bacteria and Vk2 cell co-cultures incubated in anaerobic conditions for 24 h. Fixed cultures were stained with FilmTracerTM SYPRO® Ruby to visualize biofilm matrix proteins (red) and mouse anti-human MUC1 (CD227) antibody (green) on Nikon eclipse Ti2 confocal laser scanning microscope. Mean Fluorescence Intensity (MFI) of matrix protein staining (A) and MUC-1 staining (B) for 24-h *P. bivia* and LLI Vk2 cell co-cultures with hormones determined by mean gray area quantification of duplicate representative images from a singular well on imageJ. Baseline Fluorescence, represented by dotted green line, defined as the minimum quantification for green fluorescence intensity on imageJ. Representative of N=3 separate experiments. Data was analyzed with two-way ANOVA, with Bonferroni test to correct for multiple comparisons. ***p=0.0009, **p=0.0021, *p=0.0380.

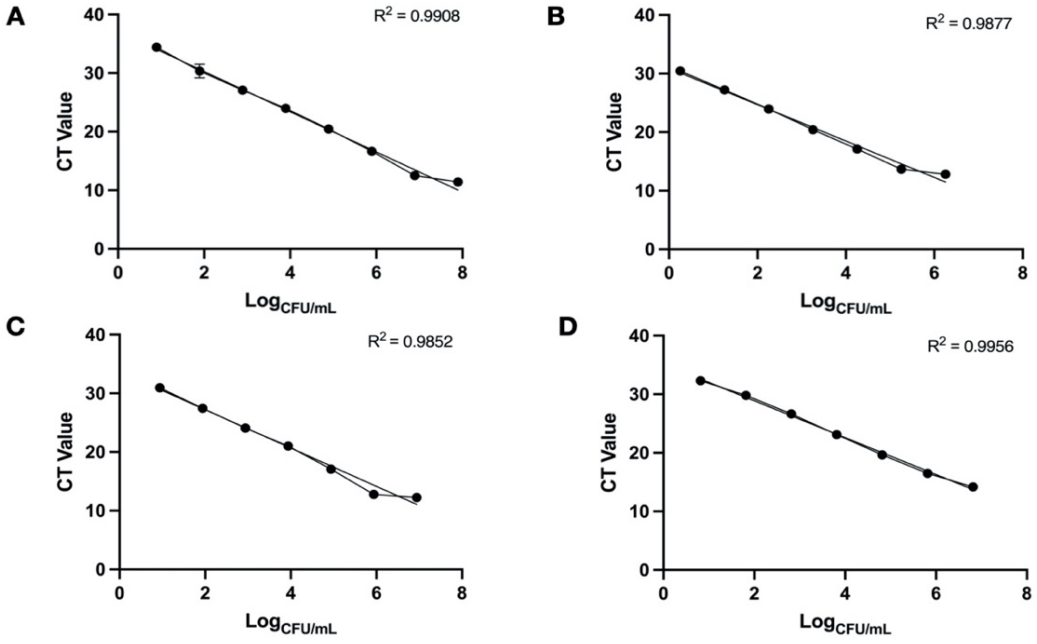

Figure 46. qPCR standard curve quantification of each bacteria of interest. *L. crispatus* (A)*, L. iners* (B), *G. vaginalis* (C) *and P. bivia* (D) cultures of 1 mL quantity were grown to their exponential phase of growth as determined by "Bacterial Growth Curve". CFU/mL of each culture was determined using the standard method. Cultures were pelleted and re-suspended with 180 µL of Enzymatic Lysis Buffer and incubated for 30 min at 37°C. DNA was extracted from each sample using the DNeasy® Blood & Tissue Kit (Qiagen, Cat. 69506) protocol. Next, 6-7 10-fold dilutions of stock extracted DNA for each bacterium was made depending on the starting culture CFU/mL. Real-time qPCR was performed as specified in "Materials and Methods". Standard curve plotted at CT value and $Log_{CFU/mL}$. Used for extrapolation of CFU values for each bacterium in future experiments.

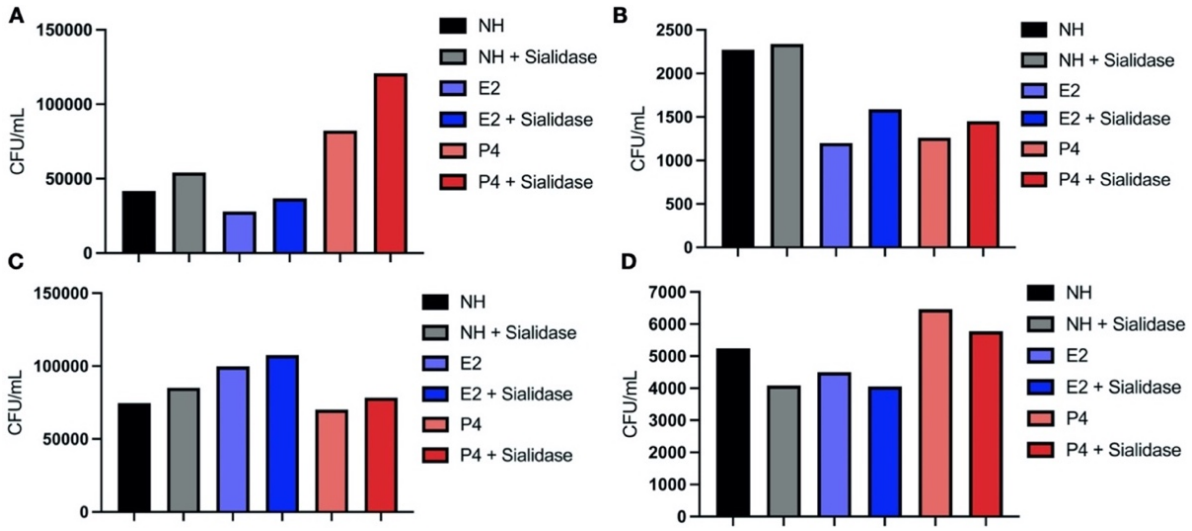

Figure 47. qPCR quantification of bacteria in NH, E2 and P4 hormone conditions with sialidase. Vk2 cells were grown for 6-days in LLI cultures in various hormone conditions. Sialidase was added to cells for 2 h prior to bacteria inoculation then removed. *L. crispatus* (A), *L. iners* (B), *G. vaginalis* (C) *and P. bivia* (D) was added to cultures and bacteria + cell cultures incubated in anaerobic conditions for 24 h. In culture wells, 180 µL of Enzymatic Lysis Buffer was added and plates incubated for 30 min at 37°C. DNA was pooled and extracted from each sample using the DNeasy® Blood & Tissue Kit (Qiagen, Cat. 69506) protocol. Real-time qPCR was performed as specified in "Materials and Methods". Standard curve used for extrapolation of CFU values for each bacterium in each condition. Representative of N=1 separate experiment.

CHAPTER 5: DISCUSSION

5.1 Discussion

The first aim of this thesis was establishing an *in vitro* model of biofilm formation on vaginal epithelial cells which could be visualized and quantified. As a first step we characterized the ideal conditions to model the vaginal epithelium. The Vk2 cell line grown as both ALI and LLI cultures was used in this project (Results 4.1.1). Improvements to this model, including assessment of viability in anaerobic conditions and the visualization and quantification of mucin-1 production for both ALI and LLI cultures, were completed as examining these factors of Vk2 cells had not been examined previously (Results 4.1.1). Next, both beneficial and pathogenic VMB associated bacteria were studied in this model, as it was important to assess the differences in biofilm formation and effect on epithelial cells. *L. crispatus* is the most common beneficial *Lactobacillus* species in the VMB[34], *L. iners* has an unclear role in dysbiosis and pathogenesis[52], *G. vaginalis* is a strong biofilm forming bacteria highly correlated with dysbiosis and BV conditions[29,101], and *P. bivia* plays a supporting role in *G. vaginalis* pathogenesis and biofilm formation[112,114], therefore these four bacteria were chosen. Different visualization strategies for biofilm production by these bacteria in the Vk2 cell co-culture model were tested (Results 4.1.3&4.1.4). The FilmTracerTM SYPRO® Ruby Biofilm Matrix protein stain was determined to be the best visualization method of those tested, as it clearly stained the biofilm matrix with little background in the control wells and could be accurately correlated to protein quantification via a BCA assay. Visualization strategies for identifying individual bacterial cells were optimized for *L. crispatus* and *L. iners* using a Gram-positive specific antibody and for *G. vaginalis* using a PNA FISH probe (Results 4.1.4). This will be useful for future multi-species biofilm growth assays conducted in this model.

The second aim of this thesis was to utilize the *in vitro* model of biofilm formation in Vk2 cell co-cultures, to test how each specific biofilm was impacting cell function (Results 4.2.1) and then to test strategies to dissociate BV-associated biofilm and enhance *Lactobacillus* biofilm (Results 4.2.2-4.2.4). To assess biofilm impact on cell function, TER was measured to determine the effect on epithelial barrier function, and LDH assays were conducted to determine the cytotoxic effect of biofilm on epithelial cells (Results 4.2.1). The next objective in this aim was testing different strategies for biofilm manipulation. Our laboratory has conducted extensive research on the influence of endogenous sex hormones on susceptibility to infections like HIV and HSV-2, and it was speculated that NH, E2 and P4 conditions may also impact biofilm growth *in vitro* (Results 4.2.2). Estradiol conditions enhanced *L. crisaptus* biofilm growth and progesterone conditions enhanced *G. vaginalis* biofilm growth in this model. The use of SCFA combinations mimicking eubiosis or dysbiosis was chosen because our laboratory has conducted studies showing that these SCFA conditions can influence barrier integrity and inflammation in Vk2 cell cultures, and it was speculated that these conditions may also influence biofilm growth *in vitro* (Results 4.2.3). The effect of SCFA conditions on Vk2 cells were not clear and will be discussed in more depth below. Lastly, the mucin-degrading enzyme sialidase was chosen because it was speculated that the loss of the mucus layer on Vk2 cells would inhibit growth of bacteria like *G. vaginalis* and *P. bivia* that use mucin-degradation for colonization and biofilm growth (Results 4.2.4). Mucin degradation by sialidase had an impact on *L. crispatus*, *G. vaginalis* and *P. bivia* biofilm growth in certain hormone conditions.

One aspect of Vk2 cell cultures not explored in previous projects is the presence of mucin. The cervicovaginal mucus layer is an important component of the vaginal epithelium, and its presence in *in vitro* co-cultures would further mimic *in vivo* conditions. Studies have

identified *in vitro* models of mucin production in different cell lines, including respiratory and intestinal epithelial cell lines.[166] Another study used a novel 3D human vaginal epithelial cell model created in a rotating wall vessel bioreactor and found high levels of MUC1 and MUC4 production.[167] However, the visualization and quantification of mucin production in Vk2 epithelial cells in both ALI and LLI culture systems and in anaerobic conditions had not been established. The findings of this project show that mucin-1 production is present in both ALI and LLI Vk2 cell cultures in aerobic and anaerobic conditions (Figure 2-3). LLI cultures had more consistency in mucin production in anaerobic conditions, possibly do to its single layered nature which remains unchanged during anaerobic culture. ALI cultures had slightly more LDH activity in aerobic and anaerobic conditions when compared to LLI cultures, although the difference was not significant. Due to the multilayered nature of ALI cultures, anaerobic conditions may cause some cytotoxicity and cell death of the topmost layers. Therefore, this may cause the decrease in mucin production in ALI cultures after extended anaerobic incubation. To ensure these results more closely align with *in vivo* conditions, endogenous sex hormones were added to culture media to mimic fluctuations in hormone presence seen in the menstrual cycle. Estradiol (E2) increased mucin production in both ALI and LLI cultures, but the effect was more pronounced in ALI cultures (Figure 4). This could be due to less variation in mucin production in LLI cultures in since the density of epithelial monolayer formed is less variable across culture conditions.

The optimal biofilm visualization strategy tested was FilmTracerTM SYPRO® Ruby Biofilm Matrix stain for staining different classes of proteins in the biofilm matrix that are otherwise difficult to stain individually, including phosphoproteins and fibrillar proteins among others. Extracellular matrix proteins make up a large component of the biofilm matrix.[92] They are important in the structural aspects and architecture of the biofilm matrix.[92] Some studies have

utilized this staining method to visualize biofilm growth.[165,168] In this project, this stain generated best results among the different stains tested, showing significant staining for all bacteria in most of the culture conditions tested, and very little non-specific background staining of Vk2 cells (Figure 16-19). To ensure the accuracy of the matrix protein stain for the quantification of biofilm, staining results were compared to protein quantification with a BCA assay after extraction from bacteria and Vk2 cell co-cultures (Figure 20). Similar trends were seen in protein quantification as seen with staining, and it was determined that matrix protein staining was an accurate method for both visualization and quantification. Therefore, this stain worked well for the purposes of this project and this biofilm visualization strategy will make this model more useful for future studies.

Aim #2 began with utilizing the optimized bacteria and Vk2 cell co-culture model to assess the effect that biofilm formation has on vaginal epithelial cells. Previous research in our laboratory showed that addition of vaginal bacteria on Vk2 cells had varying effects on certain aspects of cell viability.[45] Dupont, H. A (2020) found that *L. crispatus* bacteria had beneficial effects on Vk2 cells, by maintaining barrier integrity, not inducing cell cytotoxicity and limiting production of pro-inflammatory cytokines. That project also found that *L. iners* and BV-associated bacteria such as *G. vaginalis* and *P. bivia* had harmful effects on Vk2 cells through decreasing barrier integrity and increasing cell cytotoxicity and production of pro-inflammatory cytokines. My project found that *L. crispatus,* in co-culture with Vk2 cells, maintained barrier integrity and did not induce cell cytotoxicity (Figure 24-25). This is aligned with literature outlining the beneficial effects of this bacteria on barrier integrity and cell viability of the vaginal epithelium and with previous research in our laboratory showing neutral effects of *L. crispatus* when using the same assays.[45] This project also found that *G. vaginalis* and *P. bivia* in co-culture

with Vk2 cells decreased barrier integrity and increased cytotoxicity (Figure 24-25). This is aligned with literature highlighting the harmful effects of this bacteria and the results previously observed in our laboratory showing the negative effects of *G. vaginalis* and *P. bivia* on barrier integrity and cytotoxicity of cells using similar assays.[45] The neutral effects on barrier integrity and cytotoxicity of Vk2 cells seen with *L. iners* co-cultures in this project varies from previous research in our laboratory.[45] A recent systemic review determined that *L. iners* bacteria has shown inconsistency in its effect on the vaginal epithelium and in its relation to BV diagnosis and increased susceptibility to STI's, and may be a transitional species that colonizes the VMB after disruptions in the microenvironment.[51] An *L. iners* dominant VMB has been cited as a predictor of BV onset since this bacteria has the capability of co-existing with dysbiotic bacteria, discovered through its detection during BV conditions.[51] However, this bacterium is part of the *Lactobacillus* family and is closely related to *L. crispatus* and may also share some similar beneficial characteristics.[48] This could be the reason for inconsistencies in the *L. iners* effect seen between projects, but remains an unresolved phenomenon that should be investigated further in future experiments. Overall, general trends seen with each bacterium align with literature and with previous research in our laboratory.

The main objective of Aim #2 was to utilize the optimized model of biofilm formation on Vk2 cells to test different strategies of *Lactobacillus* biofilm enhancement and BV-associated biofilm dispersion, starting with the use of endogenous sex hormones. Our laboratory has studied and reviewed the effect of endogenous sex hormones and hormonal contraceptives on susceptibility to infections like HIV and HSV-2 in depth.[3,12,13,15,79,145,169] Therefore, with the body of work conducted in our laboratory showing the variable effects of hormone treatments on genital epithelial cells, these same treatments were examined to determine if differential effects

can be seen in Vk2-bacteria cell co-cultures. The enhancement of *L. crispatus* biofilm growth in E2 conditions aligns with literature stating that estrogen presence enhances *Lactobacillus* growth (Figure 26). There was a significant increase in TER measurements in E2 conditions when compared to P4 conditions for *L. crispatus* and Vk2 cell co-cultures (Figure 31). This could be due to increased *L. crispatus* biofilm growth having a greater positive impact on barrier strength and the estradiol in culture exhibiting barrier strengthening capabilities, as seen previously in other studies in our laboratory,.[12] NH, E2 and P4 conditions did not have a significant impact on *L. iners* (Figure 27). One study analyzing VMB composition of women using an estrogen-containing hormonal contraceptive vaginal ring found increased presence of H_2O_2-producing *Lactobacillus* species, while H_2O_2-negative *Lactobacillus* species presence remained the same.[84] This may explain why *L. iners* biofilm growth remains consistent in the NH, E2 and P4 hormone conditions and is not increased in E2 since it does not produce H_2O_2. The enhancement of *G. vaginalis* biofilm growth in P4 (Figure 28) is aligned with literature showing progesterone-high conditions such as use of progestin-containing hormonal contraceptives can shift the VMB from *Lactobacillus* dominance to dysbiosis.[24] The impact of enhanced *G. vaginalis* growth in P4 conditions was evident in the increased cytotoxicity of cells in P4 when co-cultured with *G. vaginalis*, which was not seen in the other NH and E2 conditions (Figure 32). NH, E2 and P4 conditions did not have a significant impact on *P. bivia* biofilm growth, as seen by similar growth in all conditions (Figure 29). *P. bivia* biofilm growth in P4 conditions is not as significant as *G. vaginalis*, possibly due to the fact that *P. bivia* is considered a secondary pathogen in a dysbiotic VMB and may not respond to progesterone presence as significantly as *G. vaginalis*. Therefore, the use of endogenous sex hormones in this culture system worked well and produced results aligned with the hypothesis.

The second biofilm treatment strategy tested in Aim #2 was the use of combination of SCFAs to mimic eubiosis and dysbiosis in culture and determine the effect on biofilm growth. Results in our laboratory using these SCFA conditions have shown that the dysbiotic concentrations of SCFA cause decreased TER measurements and increased TNF-α production through the NFkB pathway in Vk2 cells (Ingrid Schwecht, unpublished data). Therefore, we hypothesized that these SCFA conditions could be utilized in my project to manipulate biofilm growth. The results generated with bacteria and Vk2 cell co-cultures in SCFA containing media were not what we had expected. The obvious nuclear staining with the matrix protein stain in the eubiotic and dysbiotic conditions, and the unusual DAPI nuclear staining in dysbiotic conditions were indications that these SCFA may have unknown effects on Vk2 cells that need to be studied further (Figure 37-40). It can be speculated that the SCFA are influencing different inflammatory responses not seen with the bacteria co-cultures in other conditions and it is resulting in the unexpected staining. One study looked at the pro- and anti-inflammatory effects that eubiotic and BV-associated metabolites have on Vk2 cells and found that eubiotic metabolites, like lactic acid, have anti-inflammatory effects while BV-associated SCFA showed pro-inflammatory cytokine stimulation after prolonged and sustained treatment.[89] Therefore, the unclear impact of SCFA conditions simulating eubiosis and dysbiosis on vaginal epithelial cells remains an unresolved issue in this project and needs to be investigated further to determine the cause of the unusual DAPI nuclear staining, and the permeability of cells allowing matrix protein staining of the nucleus.

The last biofilm treatment strategy tested in Aim #2 was the use of the mucin-degrading enzyme sialidase. The use of sialidase as a mechanism for BV-associated biofilm dispersal has not been investigated. When bacteria were inoculated in Vk2 cells in different hormone

conditions and mucin presence was quantified, some interesting trends were observed (Figure 42-45). All bacteria stimulated significant mucin-1 production compared to the no bacteria controls in at least one hormone condition. *L. crispatus* up-regulated mucin-1 production in NH and E2 conditions, *L. iners* up-regulated mucin-1 production in E2 conditions, *G. vaginalis* upregulated mucin-1 production in NH, E2 and P4 conditions and *P. bivia* up-regulated mucin-1 production in NH and E2 conditions (Figure 42-45). This suggests that vaginal bacteria may be interacting with vaginal epithelial cells on a molecular level to stimulate upregulation of key cellular factors needed for biofilm growth. Determination of the specific mechanisms behind these results remains unresolved but would be an interesting phenomenon to explore further. One speculation for the increase in mucin-1 production seen with *G. vaginalis* and *P. bivia* is that there is increased mucin production response by Vk2 cells to compensate for mucin being degraded by these known sialidase producing bacteria.

The use of sialidase on Vk2 cells resulted in dramatic decreases in biofilm formation for most bacteria tested. *L. crispatus* had significant decreases in biofilm formation in the E2 media condition (Figure 42), and *G. vaginalis* had significant decreases in biofilm formation in the P4 media condition (Figure 44). *L. crispatus* and *G. vaginalis* both grow their most significant biofilm in E2 and P4 respectively, so it is expected that the most dramatic decrease in biofilm formation in the presence of sialidase would be in these conditions. *P. bivia* had significant decreases in biofilm formation in the NH condition (Figure 45). *P. bivia* grows its most stable biofilm in NH conditions, as indicated by less biofilm quantification variability in this condition, and this could explain the decrease in biofilm formation in this condition which is not seen in E2 or P4 conditions. *L. iners* did not show significant decreases in biofilm formation when the sialidase enzyme was used (Figure 43). This could be because *L. iners* biofilm growth is not

significantly amplified in any of the hormone conditions, as seen with *L. crispatus* in E2 conditions. The quantification of bacteria in this experiment by qPCR was conducted to determine if the decrease in biofilm formation seen is a result of decreased bacteria growth. Interestingly, bacteria quantification in the sialidase conditions was higher than in the no sialidase conditions for most bacteria (Figure 47). One possible explanation could be that biofilm does not grow as well when sialidase is added, and less bacteria are encapsulated in biofilm making them easier to lyse, then the extraction of bacterial DNA from lysed cells would be amplified and result in higher qPCR quantification. However, this remains unresolved and needs to be repeated to confirm these results.

5.2 Strengths and Limitations

A major strength of this project was the optimization of novel aspects of the Vk2 *in vitro* culture system which have not been included in other studies before, like the presence of mucin in ALI and LLI Vk2 cultures and the viability of both cell culture systems in oxygen deficient conditions. However, this model still has limitations since it was unable to capture the full extent of fundamental features found *in vivo* which may impact the translation of results generated in this project. Lacking in our model is the presence of immune cells and other vaginal epithelium factors, such as proteins, carbohydrates, lipids, enzymes, and more that may influence bacteria growth and biofilm formation. Therefore, *in vivo* biofilm growth may look different than what was modelled in this *in vitro* system where the presence and influence of these various factors was not analyzed in depth. The use of confocal microscopy for most images taken in this project was a strength of the experimental design. This allowed for detailed images to be captured which included different aspects like Vk2 cell staining and biofilm staining together, generation of 3D images, and allowed for multiple biofilm and bacteria stains to be tested in conjunction.

However, a limitation of the experimental design for biofilm visualization was the fact that only two biofilm matrix stains were tested. Once the matrix protein stain was determined to be effective and it was used moving forward in the project. Staining for other aspects of the biofilm matrix would allow a more complete picture of biofilm visualization. Another limitation in the experimental design is the single species biofilm model which was utilized in this project. The VMB *in vivo* is colonized by a variety of species, even in a *Lactobacillus*-dominant VMB where other bacteria species are present in smaller quantities. The multi-species bacteria interactions influence the way bacteria grow and the way biofilm is formed. It would be beneficial to use the currently established model with multi-species bacteria co-cultures to determine how this would affect biofilm growth. Also, incorporating different VMB associated bacteria or various strains of the bacteria used in this project would broaden the scope of the model. It is known that various strains of vaginal bacteria have variable genetic profiles and biofilm forming capabilities, therefore using different strains may change the generalized outcomes detailed for each species in this project. A major strength of Aim #2 was the biofilm manipulation strategies tested. The use of endogenous sex hormone supplemented media worked very well to enhance biofilm growth, and E2 conditions were confirmed to greatly enhance *Lactobacillus* biofilm growth as hypothesized. Also, the use of sialidase to degrade mucin and influence biofilm growth was unique to this project and worked well to dissociate biofilm. The only limitation to this strategy was the fact that most bacteria experienced this effect, and it was not exclusive to BV-associated biofilm. Therefore, using this dissociation strategy in combination with strategies for *Lactobacillus* biofilm enhancement should be investigated.

5.3 Future Directions

This project established a novel *in vitro* model for visualization and quantification of biofilm growth on Vk2 cells. The determination of mucin production in this system, as well as the treatment methods utilized to manipulate biofilm growth are novel aspects of this project. However, addressing the limitations discussed above would further improve this model. Including more relevant *in vivo* factors, like proteins, carbohydrates, lipids, enzymes present in the vaginal microenvironment, and ensuring cell were cultured in normal vaginal pH conditions would be prioritized in the future to gain a more accurate picture of the dynamics between the vaginal epithelium and the VMB. Then, re-assessing the effect of biofilm growth in this co-culture model once more *in vivo* factors are included could strengthen the conclusions drawn here and lead to a better understanding of the mechanisms being utilized to generate these effects. Also, future studies could investigate more aspects of cell viability to further elucidate mechanisms of biofilm protection or pathogenicity. For example, samples of bacteria and Vk2 cell co-cultures in different conditions collected throughout this project will be analyzed for cytokine and chemokine production. This is similar to previous research in our laboratory which found anti-inflammatory effects of *L. crispatus* bacteria on Vk2 cells and pro-inflammatory effects of *G. vaginalis*, *P. bivia* and *L. iners* bacteria on Vk2 cells.[45] This analysis will lead to a better understanding of the inflammatory state that biofilm formation in the VMB generates. The creation of multi-species biofilms in this model is another area of interest which will be pursued in the future. Establishing staining methods to distinguish individual bacteria cells in Vk2 cell co-cultures was a key objective in this project. While we did successfully optimize the Gram-positive antibody staining for visualization of *L. crispatus* and *L. iners*, and the Gard162 PNA FISH probe for *G. vaginalis*, individual staining methods for *P. bivia* bacteria still need to be

determined. Once all individual staining methods are optimized, they can be used to examine multi-species models. This would create a more accurate representation of the VMB *in vivo* as it is composed of more than one species of bacteria. It would also be valuable to determine how these bacteria interact with each other in co-culture to either enhance or dissociate biofilm. Although novel methods of biofilm enhancement or dissociation were tested in this project, exploring other treatment options, alone or in combination, is another future aim. There are many new developments in biofilm treatment that would be interesting to test for dysbiotic biofilm dissociation in this model. New treatments for BV specifically focus on dissociation of *G. vaginalis* biofilm and would be valuable to test in this cell model, including plant derived compounds, natural antimicrobials and small molecules, and other dissociative enzymes which have all been studied previously in plate models.[119,126,170,171] Other antibiotic strategies with broader biological activity, like thiopeptides, would also be interesting to study in this model.[118] Lastly, using combinations of treatment strategies to enhance *Lactobacillus* biofilm growth and suppress BV-associated biofilm growth could be tested. The limitation with using sialidase was the non-specific biofilm dissociation results generated for all bacteria. However, using sialidase with bacteria co-cultures, like *L. crispatus* and *G. vaginalis*, may supress *G. vaginalis* biofilm growth and allow *L. crispatus* biofilm to prosper. Also using probiotic *Lactobacillus* species in this model may lead to increased *Lactobacillus* biofilm growth. These conditions can be explored in future experiments. Overall, this model system provided a strong basis for the study of biofilm interactions in the vaginal epithelium. Future investigations into mechanisms of protection or pathogenicity by the VMB, and the enhancement or dissociation of biofilm on vaginal epithelial cells would advance our understanding of the VMB and could lead to prevention strategies for infections such an BV and HIV-1.

5.4 Significance

The most important achievement in this project was the optimization of a novel model of biofilm formation in Vk2 cell co-cultures with different VMB-associated bacteria, and the establishment of novel aspects of the Vk2 cell line used, including presence of mucin-1 in culture and viability in anaerobic conditions (Figure 1-4). This expanded on work done previously in our laboratory in this cell line and improved this model which can be used in the future to advance the field of *in vitro* cell work. This project is also the first time the FilmTracerTM SYPRO® Ruby stain to visualize biofilm matrix proteins was used in a model of biofilm formation on Vk2 vaginal epithelial cells (Figure 16-19). This staining option worked very effectively not only to visualize biofilm growth, but to accurately quantify biofilm matrix proteins as well (Figure 20). These results could be clinically significant as detection and quantification of biofilm in clinical samples could be done using this visualization strategy. This project is also the first time that individual bacteria staining options, such as the Gram-positive bacteria antibody staining and the Gard162 PNA FISH probe was used to effectively visualize individual *L. crispatus*, *L. iners* and *G. vaginalis* bacteria respectively on Vk2 cells.

This project expanded on previous results from our laboratory by investigating aspects of vaginal epithelial cells that may be impacted by biofilm growth, including barrier integrity and cell cytotoxicity. The results showed that *L. crispatus* elicits positive effects through maintenance of barrier integrity and cell viability (Figure 24-25). It was also determined that *G. vaginalis* and *P. bivia* elicit negative effects through decreasing barrier integrity and increasing cytotoxicity of epithelial cells (Figure 24-25). Determining how the vaginal epithelial is influenced by biofilm formation contributes to the growing body of literature which sets out to understand the mechanisms behind the beneficial health effects in the FGT associated with

Lactobacillus dominant biofilm and the harmful effects in the FGT related to BV-associated bacteria biofilm presence.

Lastly, this project tested novel treatments for biofilm formation on vaginal epithelial cells. The use of estrogen hormone treatment to enhance *Lactobacillus* growth *in vivo* is being investigated currently as a treatment option for BV. This study has shown that estradiol treatment can enhance *L. crispatus* biofilm growth *in vitro* and may be a viable method to conserve *Lactobacillus* dominance in the VMB or shift a dysbiotic VMB to that of *Lactobacillus* dominance. This has clinical relevance when testing strategies for BV treatment in women. The use of the mucin-degrading enzyme sialidase to inhibit BV-associated biofilm growth is a novel treatment method that was utilized in this project. It was found to inhibit strong biofilm growth by *G. vaginalis* in progesterone conditions and *P. bivia* biofilm growth in normal culture conditions. However, this treatment also significantly inhibited *L. crispatus* biofilm growth in estradiol conditions. Therefore, this treatment option needs to be investigated further, potentially in combination with other treatments, to ensure that only pathogenic bacteria biofilm is being dissociated and *Lactobacillus* biofilm remains intact.

The development of novel treatment strategies for BV are needed to combat this common adverse condition in the FGT. The presence of BV leads to many harmful health outcomes, with one of the most concerning being increased susceptibility to HIV acquisition. With the increased burden of HIV infection in women worldwide, developing ways to decrease susceptibility to this infection is extremely important. The results of this project can be built upon to continue understanding VMB interactions with the vaginal epithelium and how they relate to infection in

the FGT. This project can also be expanded to develop more treatment options for BV, which would ultimately lead to better protection from HIV infection in women.

5.5 Conclusions

Women carry a disproportionately high burden of new HIV infections worldwide. Over 50% of cases in 2021 were in women. With 40% of annual HIV transmission occurring in the FGT, understanding factors that result in the increased susceptibility to HIV infection in the FGT is critical. A major contributor to the protection against infection or increase in susceptibility to infection in the FGT is the VMB. This project set out to establish an *in vitro* model of VMB associated biofilm formation on vaginal epithelial cells to study the specific mechanisms that the VMB use to elicit either beneficial or harmful effects on the vaginal epithelium. A novel model of VMB associated bacteria biofilm formation on Vk2 vaginal epithelial cells was created which could be visualized and quantified. The model recapitulated novel *in vivo* aspects which have not been established in this *in vitro* model previously and utilized a novel biofilm visualization and quantification strategy which will contribute to advancements in VMB biofilm research. This model was then used to investigate mechanisms of protection or pathogenicity biofilm uses on the vaginal epithelium. This will contribute to the field of research investigating how the VMB influences FGT health. Lastly, this model was used to test strategies of beneficial *Lactobacillus* biofilm enhancement and harmful BV-associated biofilm dispersal. Novel strategies, like the use of endogenous sex hormones and the mucin-degrading enzyme sialidase, were used and showed promising results for biofilm manipulation. This model can be used to investigate different strategies for the treatment of BV, a condition which causes increased susceptibility to HIV infection. Using this model to discover effective treatments for BV can combat the development

of adverse health conditions and high risk of HIV infection, which would have major implications in improving women's health.

References

1 Unaids.org. *Global HIV & Aids Statistics - Fact Sheet*, <https://www.unaids.org/en/resources/fact-sheet> (2022).

2 Haase, A. T. Targeting early infection to prevent HIV-1 mucosal transmission. *Nature* **464**, 217-223, doi:10.1038/nature08757 (2010).

3 Wessels, J. M., Felker, A. M., Dupont, H. A. & Kaushic, C. The relationship between sex hormones, the vaginal microbiome and immunity in HIV-1 susceptibility in women. *Dis Model Mech* **11**, doi:10.1242/dmm.035147 (2018).

4 Kaushic, C. HIV-1 infection in the female reproductive tract: role of interactions between HIV-1 and genital epithelial cells. *Am J Reprod Immunol* **65**, 253-260, doi:10.1111/j.1600-0897.2010.00965.x (2011).

5 Hladik, F. & Hope, T. J. HIV infection of the genital mucosa in women. *Curr HIV/AIDS Rep* **6**, 20-28, doi:10.1007/s11904-009-0004-1 (2009).

6 Miller, C. J. & Shattock, R. J. Target cells in vaginal HIV transmission. *Microbes Infect* **5**, 59-67, doi:10.1016/s1286-4579(02)00056-4 (2003).

7 Kaushic, C., Ferreira, V. H., Kafka, J. K. & Nazli, A. HIV infection in the female genital tract: discrete influence of the local mucosal microenvironment. *Am J Reprod Immunol* **63**, 566-575, doi:10.1111/j.1600-0897.2010.00843.x (2010).

8 Reis Machado, J. *et al.* Mucosal immunity in the female genital tract, HIV/AIDS. *Biomed Res Int* **2014**, 350195, doi:10.1155/2014/350195 (2014).

9 Nguyen, P. V., Kafka, J. K., Ferreira, V. H., Roth, K. & Kaushic, C. Innate and adaptive immune responses in male and female reproductive tracts in homeostasis and following HIV infection. *Cell Mol Immunol* **11**, 410-427, doi:10.1038/cmi.2014.41 (2014).

10 Nazli, A. *et al.* Exposure to HIV-1 directly impairs mucosal epithelial barrier integrity allowing microbial translocation. *PLoS Pathog* **6**, e1000852, doi:10.1371/journal.ppat.1000852 (2010).

11 Reed, B. G. & Carr, B. R. in *Endotext* (eds K. R. Feingold *et al.*) (MDText.com, Inc. Copyright © 2000-2022, MDText.com, Inc., 2000).

12 Dizzell, S., Nazli, A., Reid, G. & Kaushic, C. Protective Effect of Probiotic Bacteria and Estrogen in Preventing HIV-1-Mediated Impairment of Epithelial Barrier Integrity in Female Genital Tract. *Cells* **8**, doi:10.3390/cells8101120 (2019).

13 Vitali, D., Wessels, J. M. & Kaushic, C. Role of sex hormones and the vaginal microbiome in susceptibility and mucosal immunity to HIV-1 in the female genital tract. *AIDS Res Ther* **14**, 39, doi:10.1186/s12981-017-0169-4 (2017).

14 Wira, C. R., Rodriguez-Garcia, M., Shen, Z., Patel, M. & Fahey, J. V. The role of sex hormones and the tissue environment in immune protection against HIV in the female reproductive tract. *Am J Reprod Immunol* **72**, 171-181, doi:10.1111/aji.12235 (2014).

15 Kaushic, C., Roth, K. L., Anipindi, V. & Xiu, F. Increased prevalence of sexually transmitted viral infections in women: the role of female sex hormones in regulating susceptibility and immune responses. *J Reprod Immunol* **88**, 204-209, doi:10.1016/j.jri.2010.12.004 (2011).

16 Dupont, H. A., Lam, J., Woods, M. W., Zahoor, M. A. & Kaushic, C. Hormonal influence on HIV-1 transmission in the female genital tract: New insights from systems biology. *Am J Reprod Immunol* **80**, e13019, doi:10.1111/aji.13019 (2018).
17 Vishwanathan, S. A. *et al.* High susceptibility to repeated, low-dose, vaginal SHIV exposure late in the luteal phase of the menstrual cycle of pigtail macaques. *J Acquir Immune Defic Syndr* **57**, 261-264, doi:10.1097/QAI.0b013e318220ebd3 (2011).
18 Blaskewicz, C. D., Pudney, J. & Anderson, D. J. Structure and function of intercellular junctions in human cervical and vaginal mucosal epithelia. *Biol Reprod* **85**, 97-104, doi:10.1095/biolreprod.110.090423 (2011).
19 Wagner, C. E., Wheeler, K. M. & Ribbeck, K. Mucins and Their Role in Shaping the Functions of Mucus Barriers. *Annu Rev Cell Dev Biol* **34**, 189-215, doi:10.1146/annurev-cellbio-100617-062818 (2018).
20 Carson, D. D. *et al.* Mucin expression and function in the female reproductive tract. *Hum Reprod Update* **4**, 459-464, doi:10.1093/humupd/4.5.459 (1998).
21 Ferreira, V. H., Kafka, J. K. & Kaushic, C. Influence of common mucosal co-factors on HIV infection in the female genital tract. *Am J Reprod Immunol* **71**, 543-554, doi:10.1111/aji.12221 (2014).
22 Miller, L. *et al.* Depomedroxyprogesterone-induced hypoestrogenism and changes in vaginal flora and epithelium. *Obstet Gynecol* **96**, 431-439, doi:10.1016/s0029-7844(00)00906-6 (2000).
23 Hild-Petito, S., Veazey, R. S., Larner, J. M., Reel, J. R. & Blye, R. P. Effects of two progestin-only contraceptives, Depo-Provera and Norplant-II, on the vaginal epithelium of rhesus monkeys. *AIDS Res Hum Retroviruses* **14 Suppl 1**, S125-130 (1998).
24 Smith, S. M. *et al.* Topical estrogen protects against SIV vaginal transmission without evidence of systemic effect. *Aids* **18**, 1637-1643, doi:10.1097/01.aids.0000131393.76221.cc (2004).
25 Moncla, B. J., Chappell, C. A., Debo, B. M. & Meyn, L. A. The Effects of Hormones and Vaginal Microflora on the Glycome of the Female Genital Tract: Cervical-Vaginal Fluid. *PLoS One* **11**, e0158687, doi:10.1371/journal.pone.0158687 (2016).
26 Monin, L., Whettlock, E. M. & Male, V. Immune responses in the human female reproductive tract. *Immunology* **160**, 106-115, doi:10.1111/imm.13136 (2020).
27 Rancez, M., Couëdel-Courteille, A. & Cheynier, R. Chemokines at mucosal barriers and their impact on HIV infection. *Cytokine Growth Factor Rev* **23**, 233-243, doi:10.1016/j.cytogfr.2012.05.010 (2012).
28 Ravel, J. *et al.* Vaginal microbiome of reproductive-age women. *Proc Natl Acad Sci U S A* **108 Suppl 1**, 4680-4687, doi:10.1073/pnas.1002611107 (2011).
29 McKinnon, L. R. *et al.* The Evolving Facets of Bacterial Vaginosis: Implications for HIV Transmission. *AIDS Res Hum Retroviruses* **35**, 219-228, doi:10.1089/AID.2018.0304 (2019).
30 Anahtar, M. N., Gootenberg, D. B., Mitchell, C. M. & Kwon, D. S. Cervicovaginal Microbiota and Reproductive Health: The Virtue of Simplicity. *Cell Host Microbe* **23**, 159-168, doi:10.1016/j.chom.2018.01.013 (2018).

31 Gosmann, C. *et al.* Lactobacillus-Deficient Cervicovaginal Bacterial Communities Are Associated with Increased HIV Acquisition in Young South African Women. *Immunity* **46**, 29-37, doi:10.1016/j.immuni.2016.12.013 (2017).

32 Munoz, A. *et al.* Modeling the temporal dynamics of cervicovaginal microbiota identifies targets that may promote reproductive health. *Microbiome* **9**, 163, doi:10.1186/s40168-021-01096-9 (2021).

33 Goldstein, E. J., Tyrrell, K. L. & Citron, D. M. Lactobacillus species: taxonomic complexity and controversial susceptibilities. *Clin Infect Dis* **60 Suppl 2**, S98-107, doi:10.1093/cid/civ072 (2015).

34 Petrova, M. I., Lievens, E., Malik, S., Imholz, N. & Lebeer, S. Lactobacillus species as biomarkers and agents that can promote various aspects of vaginal health. *Front Physiol* **6**, 81, doi:10.3389/fphys.2015.00081 (2015).

35 Ma, B., Forney, L. J. & Ravel, J. Vaginal microbiome: rethinking health and disease. *Annu Rev Microbiol* **66**, 371-389, doi:10.1146/annurev-micro-092611-150157 (2012).

36 Rose, W. A., 2nd *et al.* Commensal bacteria modulate innate immune responses of vaginal epithelial cell multilayer cultures. *PLoS One* **7**, e32728, doi:10.1371/journal.pone.0032728 (2012).

37 O'Hanlon, D. E., Moench, T. R. & Cone, R. A. Vaginal pH and microbicidal lactic acid when lactobacilli dominate the microbiota. *PLoS One* **8**, e80074, doi:10.1371/journal.pone.0080074 (2013).

38 France, M., Alizadeh, M., Brown, S., Ma, B. & Ravel, J. Towards a deeper understanding of the vaginal microbiota. *Nat Microbiol* **7**, 367-378, doi:10.1038/s41564-022-01083-2 (2022).

39 Graver, M. A. & Wade, J. J. The role of acidification in the inhibition of Neisseria gonorrhoeae by vaginal lactobacilli during anaerobic growth. *Ann Clin Microbiol Antimicrob* **10**, 8, doi:10.1186/1476-0711-10-8 (2011).

40 Conti, C., Malacrino, C. & Mastromarino, P. Inhibition of herpes simplex virus type 2 by vaginal lactobacilli. *J Physiol Pharmacol* **60 Suppl 6**, 19-26 (2009).

41 Boris, S., Suárez, J. E., Vázquez, F. & Barbés, C. Adherence of human vaginal lactobacilli to vaginal epithelial cells and interaction with uropathogens. *Infect Immun* **66**, 1985-1989, doi:10.1128/iai.66.5.1985-1989.1998 (1998).

42 Zarate, G. & Nader-Macias, M. E. Influence of probiotic vaginal lactobacilli on in vitro adhesion of urogenital pathogens to vaginal epithelial cells. *Lett Appl Microbiol* **43**, 174-180, doi:10.1111/j.1472-765X.2006.01934.x (2006).

43 Ojala, T. *et al.* Comparative genomics of Lactobacillus crispatus suggests novel mechanisms for the competitive exclusion of Gardnerella vaginalis. *BMC Genomics* **15**, 1070, doi:10.1186/1471-2164-15-1070 (2014).

44 Castro, J. *et al.* Reciprocal interference between Lactobacillus spp. and Gardnerella vaginalis on initial adherence to epithelial cells. *Int J Med Sci* **10**, 1193-1198, doi:10.7150/ijms.6304 (2013).

45 Dupont, H. A. *Examining abiotic and biotic factors influencing bacterial and host interactions in the female reproductive tract.* Master's of Science thesis, McMaster University, (2020).

46 Doerflinger, S. Y., Throop, A. L. & Herbst-Kralovetz, M. M. Bacteria in the vaginal microbiome alter the innate immune response and barrier properties of the human vaginal epithelia in a species-specific manner. *J Infect Dis* **209**, 1989-1999, doi:10.1093/infdis/jiu004 (2014).

47 Petrova, M. I., van den Broek, M., Balzarini, J., Vanderleyden, J. & Lebeer, S. Vaginal microbiota and its role in HIV transmission and infection. *FEMS Microbiol Rev* **37**, 762-792, doi:10.1111/1574-6976.12029 (2013).

48 Macklaim, J. M., Gloor, G. B., Anukam, K. C., Cribby, S. & Reid, G. At the crossroads of vaginal health and disease, the genome sequence of Lactobacillus iners AB-1. *Proc Natl Acad Sci U S A* **108 Suppl 1**, 4688-4695, doi:10.1073/pnas.1000086107 (2011).

49 Mendes-Soares, H., Suzuki, H., Hickey, R. J. & Forney, L. J. Comparative functional genomics of Lactobacillus spp. reveals possible mechanisms for specialization of vaginal lactobacilli to their environment. *J Bacteriol* **196**, 1458-1470, doi:10.1128/JB.01439-13 (2014).

50 Witkin, S. S. *et al.* Influence of vaginal bacteria and D- and L-lactic acid isomers on vaginal extracellular matrix metalloproteinase inducer: implications for protection against upper genital tract infections. *mBio* **4**, doi:10.1128/mBio.00460-13 (2013).

51 Zheng, N., Guo, R., Wang, J., Zhou, W. & Ling, Z. Contribution of Lactobacillus iners to Vaginal Health and Diseases: A Systematic Review. *Front Cell Infect Microbiol* **11**, 792787, doi:10.3389/fcimb.2021.792787 (2021).

52 Verstraelen, H. *et al.* Longitudinal analysis of the vaginal microflora in pregnancy suggests that L. crispatus promotes the stability of the normal vaginal microflora and that L. gasseri and/or L. iners are more conducive to the occurrence of abnormal vaginal microflora. *BMC Microbiology* **9**, 116, doi:10.1186/1471-2180-9-116 (2009).

53 Mtshali, A. *et al.* Temporal Changes in Vaginal Microbiota and Genital Tract Cytokines Among South African Women Treated for Bacterial Vaginosis. *Front Immunol* **12**, 730986, doi:10.3389/fimmu.2021.730986 (2021).

54 Yeoman, C. J. *et al.* Comparative genomics of Gardnerella vaginalis strains reveals substantial differences in metabolic and virulence potential. *PLoS One* **5**, e12411, doi:10.1371/journal.pone.0012411 (2010).

55 Cornejo, O. E., Hickey, R. J., Suzuki, H. & Forney, L. J. Focusing the diversity of Gardnerella vaginalis through the lens of ecotypes. *Evol Appl* **11**, 312-324, doi:10.1111/eva.12555 (2018).

56 Park, Y. J. & Lee, H. K. The Role of Skin and Orogenital Microbiota in Protective Immunity and Chronic Immune-Mediated Inflammatory Disease. *Front Immunol* **8**, 1955, doi:10.3389/fimmu.2017.01955 (2017).

57 Onderdonk, A. B., Delaney, M. L. & Fichorova, R. N. The Human Microbiome during Bacterial Vaginosis. *Clin Microbiol Rev* **29**, 223-238, doi:10.1128/cmr.00075-15 (2016).

58 Srinivasan, S. *et al.* Bacterial communities in women with bacterial vaginosis: high resolution phylogenetic analyses reveal relationships of microbiota to clinical criteria. *PLoS One* **7**, e37818, doi:10.1371/journal.pone.0037818 (2012).

59 Morrill, S., Gilbert, N. M. & Lewis, A. L. Gardnerella vaginalis as a Cause of Bacterial Vaginosis: Appraisal of the Evidence From in vivo Models. *Front Cell Infect Microbiol* **10**, 168, doi:10.3389/fcimb.2020.00168 (2020).

60 Paramel Jayaprakash, T., Schellenberg, J. J. & Hill, J. E. Resolution and characterization of distinct cpn60-based subgroups of Gardnerella vaginalis in the vaginal microbiota. *PLoS One* **7**, e43009, doi:10.1371/journal.pone.0043009 (2012).

61 Hardy, L. *et al.* The presence of the putative Gardnerella vaginalis sialidase A gene in vaginal specimens is associated with bacterial vaginosis biofilm. *PLoS One* **12**, e0172522, doi:10.1371/journal.pone.0172522 (2017).

62 Jung, H. S., Ehlers, M. M., Lombaard, H., Redelinghuys, M. J. & Kock, M. M. Etiology of bacterial vaginosis and polymicrobial biofilm formation. *Crit Rev Microbiol* **43**, 651-667, doi:10.1080/1040841X.2017.1291579 (2017).

63 Castro, J., Machado, D. & Cerca, N. Unveiling the role of Gardnerella vaginalis in polymicrobial Bacterial Vaginosis biofilms: the impact of other vaginal pathogens living as neighbors. *Isme j* **13**, 1306-1317, doi:10.1038/s41396-018-0337-0 (2019).

64 Machado, A., Jefferson, K. K. & Cerca, N. Interactions between Lactobacillus crispatus and bacterial vaginosis (BV)-associated bacterial species in initial attachment and biofilm formation. *Int J Mol Sci* **14**, 12004-12012, doi:10.3390/ijms140612004 (2013).

65 Machado, A. & Cerca, N. Influence of Biofilm Formation by Gardnerella vaginalis and Other Anaerobes on Bacterial Vaginosis. *J Infect Dis* **212**, 1856-1861, doi:10.1093/infdis/jiv338 (2015).

66 Hinderfeld, A. S., Phukan, N., Bär, A. K., Roberton, A. M. & Simoes-Barbosa, A. Cooperative Interactions between Trichomonas vaginalis and Associated Bacteria Enhance Paracellular Permeability of the Cervicovaginal Epithelium by Dysregulating Tight Junctions. *Infect Immun* **87**, doi:10.1128/iai.00141-19 (2019).

67 Lewis, W. G., Robinson, L. S., Gilbert, N. M., Perry, J. C. & Lewis, A. L. Degradation, foraging, and depletion of mucus sialoglycans by the vagina-adapted Actinobacterium Gardnerella vaginalis. *J Biol Chem* **288**, 12067-12079, doi:10.1074/jbc.M113.453654 (2013).

68 Briselden, A. M., Moncla, B. J., Stevens, C. E. & Hillier, S. L. Sialidases (neuraminidases) in bacterial vaginosis and bacterial vaginosis-associated microflora. *J Clin Microbiol* **30**, 663-666, doi:10.1128/jcm.30.3.663-666.1992 (1992).

69 Muzny, C. A. *et al.* An Updated Conceptual Model on the Pathogenesis of Bacterial Vaginosis. *J Infect Dis* **220**, 1399-1405, doi:10.1093/infdis/jiz342 (2019).

70 Torcia, M. G. Interplay among Vaginal Microbiome, Immune Response and Sexually Transmitted Viral Infections. *Int J Mol Sci* **20**, doi:10.3390/ijms20020266 (2019).

71 Gelber, S. E., Aguilar, J. L., Lewis, K. L. & Ratner, A. J. Functional and phylogenetic characterization of Vaginolysin, the human-specific cytolysin from Gardnerella vaginalis. *J Bacteriol* **190**, 3896-3903, doi:10.1128/jb.01965-07 (2008).

72 Patterson, J. L., Stull-Lane, A., Girerd, P. H. & Jefferson, K. K. Analysis of adherence, biofilm formation and cytotoxicity suggests a greater virulence potential of Gardnerella vaginalis relative to other bacterial-vaginosis-associated anaerobes. *Microbiology (Reading)* **156**, 392-399, doi:10.1099/mic.0.034280-0 (2010).

73 Anton, L. *et al.* Gardnerella vaginalis alters cervicovaginal epithelial cell function through microbe-specific immune responses. *Microbiome* **10**, 119, doi:10.1186/s40168-022-01317-9 (2022).

74 Fichorova, R. N. *et al.* The villain team-up or how Trichomonas vaginalis and bacterial vaginosis alter innate immunity in concert. *Sex Transm Infect* **89**, 460-466, doi:10.1136/sextrans-2013-051052 (2013).
75 Aroutcheva, A., Ling, Z. & Faro, S. Prevotella bivia as a source of lipopolysaccharide in the vagina. *Anaerobe* **14**, 256-260, doi:10.1016/j.anaerobe.2008.08.002 (2008).
76 Hickey, R. J. *et al.* Vaginal microbiota of adolescent girls prior to the onset of menarche resemble those of reproductive-age women. *mBio* **6**, doi:10.1128/mBio.00097-15 (2015).
77 Brotman, R. M. *et al.* Association between the vaginal microbiota, menopause status, and signs of vulvovaginal atrophy. *Menopause* **25**, 1321-1330, doi:10.1097/gme.0000000000001236 (2018).
78 Shen, J. *et al.* Effects of low dose estrogen therapy on the vaginal microbiomes of women with atrophic vaginitis. *Sci Rep* **6**, 24380, doi:10.1038/srep24380 (2016).
79 Hapgood, J. P., Kaushic, C. & Hel, Z. Hormonal Contraception and HIV-1 Acquisition: Biological Mechanisms. *Endocr Rev* **39**, 36-78, doi:10.1210/er.2017-00103 (2018).
80 Noguchi, L. M. *et al.* Risk of HIV-1 acquisition among women who use diff erent types of injectable progestin contraception in South Africa: a prospective cohort study. *Lancet HIV* **2**, e279-287, doi:10.1016/s2352-3018(15)00058-2 (2015).
81 Mitchell, C. M. *et al.* Long-term effect of depot medroxyprogesterone acetate on vaginal microbiota, epithelial thickness and HIV target cells. *J Infect Dis* **210**, 651-655, doi:10.1093/infdis/jiu176 (2014).
82 Wessels, J. M. *et al.* Medroxyprogesterone acetate alters the vaginal microbiota and microenvironment in women and increases susceptibility to HIV-1 in humanized mice. *Dis Model Mech* **12**, doi:10.1242/dmm.039669 (2019).
83 De Seta, F. *et al.* Effects of hormonal contraception on vaginal flora. *Contraception* **86**, 526-529, doi:10.1016/j.contraception.2012.02.012 (2012).
84 Huang, Y. *et al.* Effects of a One Year Reusable Contraceptive Vaginal Ring on Vaginal Microflora and the Risk of Vaginal Infection: An Open-Label Prospective Evaluation. *PLoS One* **10**, e0134460, doi:10.1371/journal.pone.0134460 (2015).
85 Borgogna, J. C. *et al.* The vaginal metabolome and microbiota of cervical HPV-positive and HPV-negative women: a cross-sectional analysis. *Bjog* **127**, 182-192, doi:10.1111/1471-0528.15981 (2020).
86 Srinivasan, S. *et al.* Metabolic signatures of bacterial vaginosis. *mBio* **6**, doi:10.1128/mBio.00204-15 (2015).
87 Aldunate, M. *et al.* Antimicrobial and immune modulatory effects of lactic acid and short chain fatty acids produced by vaginal microbiota associated with eubiosis and bacterial vaginosis. *Front Physiol* **6**, 164, doi:10.3389/fphys.2015.00164 (2015).
88 Hearps, A. C. *et al.* Vaginal lactic acid elicits an anti-inflammatory response from human cervicovaginal epithelial cells and inhibits production of pro-inflammatory mediators associated with HIV acquisition. *Mucosal Immunol* **10**, 1480-1490, doi:10.1038/mi.2017.27 (2017).
89 Delgado-Diaz, D. J. *et al.* Distinct Immune Responses Elicited From Cervicovaginal Epithelial Cells by Lactic Acid and Short Chain Fatty Acids Associated With Optimal and

Non-optimal Vaginal Microbiota. *Front Cell Infect Microbiol* **9**, 446, doi:10.3389/fcimb.2019.00446 (2019).

90 Ingrid Schwecht, T. D., Nuzhat Rahman, Chris Verschoor, Aisha Nazli and Charu Kaushic. *Changes in metabolic profile of lower female reproductive tract during health and disease: A systematic review and meta-analysis* (McMaster University, 2022.).

91 Sauer, K. *et al.* The biofilm life cycle: expanding the conceptual model of biofilm formation. *Nat Rev Microbiol*, doi:10.1038/s41579-022-00767-0 (2022).

92 Rabin, N. *et al.* Biofilm formation mechanisms and targets for developing antibiofilm agents. *Future Med Chem* **7**, 493-512, doi:10.4155/fmc.15.6 (2015).

93 Muhammad, M. H. *et al.* Beyond Risk: Bacterial Biofilms and Their Regulating Approaches. *Front Microbiol* **11**, 928, doi:10.3389/fmicb.2020.00928 (2020).

94 Tolker-Nielsen, T. Biofilm Development. *Microbiol Spectr* **3**, MB-0001-2014, doi:10.1128/microbiolspec.MB-0001-2014 (2015).

95 Toyofuku, M. *et al.* Environmental factors that shape biofilm formation. *Biosci Biotechnol Biochem* **80**, 7-12, doi:10.1080/09168451.2015.1058701 (2016).

96 Hengge, R. Principles of c-di-GMP signalling in bacteria. *Nature Reviews Microbiology* **7**, 263-273, doi:10.1038/nrmicro2109 (2009).

97 Schlafer, S. & Meyer, R. L. Confocal microscopy imaging of the biofilm matrix. *J Microbiol Methods* **138**, 50-59, doi:10.1016/j.mimet.2016.03.002 (2017).

98 van der Veer, C. *et al.* Comparative genomics of human Lactobacillus crispatus isolates reveals genes for glycosylation and glycogen degradation: implications for in vivo dominance of the vaginal microbiota. *Microbiome* **7**, 49, doi:10.1186/s40168-019-0667-9 (2019).

99 Parolin, C. *et al.* Lactobacillus Biofilms Influence Anti-Candida Activity. *Front Microbiol* **12**, 750368, doi:10.3389/fmicb.2021.750368 (2021).

100 Wei, X. Y., Zhang, R., Xiao, B. B. & Liao, Q. P. Biofilms of vaginal Lactobacillus in vitro test. *J Obstet Gynaecol* **37**, 69-73, doi:10.1080/01443615.2016.1217508 (2017).

101 Castro, J. *et al.* Comparative transcriptomic analysis of Gardnerella vaginalis biofilms vs. planktonic cultures using RNA-seq. *npj Biofilms and Microbiomes* **3**, 3, doi:10.1038/s41522-017-0012-7 (2017).

102 Swidsinski, A. *et al.* Adherent biofilms in bacterial vaginosis. *Obstet Gynecol* **106**, 1013-1023, doi:10.1097/01.AOG.0000183594.45524.d2 (2005).

103 Garcia, E. M., Kraskauskiene, V., Koblinski, J. E. & Jefferson, K. K. Interaction of Gardnerella vaginalis and Vaginolysin with the Apical versus Basolateral Face of a Three-Dimensional Model of Vaginal Epithelium. *Infect Immun* **87**, doi:10.1128/iai.00646-18 (2019).

104 Castro, J. *et al.* Using an in-vitro biofilm model to assess the virulence potential of bacterial vaginosis or non-bacterial vaginosis Gardnerella vaginalis isolates. *Sci Rep* **5**, 11640, doi:10.1038/srep11640 (2015).

105 Patterson, J. Characterization of adherence, cytotoxicity and biofilm formation by Gardnerella vaginalis. (2010).

106 Alves, P., Castro, J., Sousa, C., Cereija, T. B. & Cerca, N. Gardnerella vaginalis outcompetes 29 other bacterial species isolated from patients with bacterial vaginosis,

using in an in vitro biofilm formation model. *J Infect Dis* **210**, 593-596, doi:10.1093/infdis/jiu131 (2014).
107 Machado, A., Salgueiro, D., Harwich, M., Jefferson, K. K. & Cerca, N. Quantitative analysis of initial adhesion of bacterial vaginosis-associated anaerobes to ME-180 cells. *Anaerobe* **23**, 1-4, doi:10.1016/j.anaerobe.2013.07.007 (2013).
108 Campisciano, G. *et al.* Vaginal microbiota dysmicrobism and role of biofilm-forming bacteria. *Front Biosci (Elite Ed)* **10**, 528-536, doi:10.2741/e839 (2018).
109 Hardy, L. *et al.* Unravelling the Bacterial Vaginosis-Associated Biofilm: A Multiplex Gardnerella vaginalis and Atopobium vaginae Fluorescence In Situ Hybridization Assay Using Peptide Nucleic Acid Probes. *PLoS One* **10**, e0136658, doi:10.1371/journal.pone.0136658 (2015).
110 Randis, T. M. & Ratner, A. J. Gardnerella and Prevotella: Co-conspirators in the Pathogenesis of Bacterial Vaginosis. *J Infect Dis* **220**, 1085-1088, doi:10.1093/infdis/jiy705 (2019).
111 Ilhan, Z. E., Laniewski, P., Tonachio, A. & Herbst-Kralovetz, M. M. Members of Prevotella Genus Distinctively Modulate Innate Immune and Barrier Functions in a Human Three-Dimensional Endometrial Epithelial Cell Model. *J Infect Dis* **222**, 2082-2092, doi:10.1093/infdis/jiaa324 (2020).
112 Pybus, V. & Onderdonk, A. B. Evidence for a commensal, symbiotic relationship between Gardnerella vaginalis and Prevotella bivia involving ammonia: potential significance for bacterial vaginosis. *J Infect Dis* **175**, 406-413, doi:10.1093/infdis/175.2.406 (1997).
113 Muzny, C. A. *et al.* Identification of Key Bacteria Involved in the Induction of Incident Bacterial Vaginosis: A Prospective Study. *J Infect Dis* **218**, 966-978, doi:10.1093/infdis/jiy243 (2018).
114 Gilbert, N. M. *et al.* Gardnerella vaginalis and Prevotella bivia Trigger Distinct and Overlapping Phenotypes in a Mouse Model of Bacterial Vaginosis. *J Infect Dis* **220**, 1099-1108, doi:10.1093/infdis/jiy704 (2019).
115 Zhang, K., Li, X., Yu, C. & Wang, Y. Promising Therapeutic Strategies Against Microbial Biofilm Challenges. *Front Cell Infect Microbiol* **10**, 359, doi:10.3389/fcimb.2020.00359 (2020).
116 Jiang, Y., Geng, M. & Bai, L. Targeting Biofilms Therapy: Current Research Strategies and Development Hurdles. *Microorganisms* **8**, doi:10.3390/microorganisms8081222 (2020).
117 Yaeger, L. N., Coles, V. E., Chan, D. C. K. & Burrows, L. L. How to kill Pseudomonas-emerging therapies for a challenging pathogen. *Ann N Y Acad Sci* **1496**, 59-81, doi:10.1111/nyas.14596 (2021).
118 Chan, D. C. K. & Burrows, L. L. Thiopeptides: antibiotics with unique chemical structures and diverse biological activities. *J Antibiot (Tokyo)* **74**, 161-175, doi:10.1038/s41429-020-00387-x (2021).
119 Turovskiy, Y. *et al.* Susceptibility of Gardnerella vaginalis biofilms to natural antimicrobials subtilosin, epsilon-poly-L-lysine, and lauramide arginine ethyl ester. *Infect Dis Obstet Gynecol* **2012**, 284762, doi:10.1155/2012/284762 (2012).
120 Algburi, A., Volski, A. & Chikindas, M. L. Natural antimicrobials subtilosin and lauramide arginine ethyl ester synergize with conventional antibiotics clindamycin and

metronidazole against biofilms of Gardnerella vaginalis but not against biofilms of healthy vaginal lactobacilli. *Pathog Dis* **73**, doi:10.1093/femspd/ftv018 (2015).

121 Gottschick, C. *et al.* Screening of Compounds against Gardnerella vaginalis Biofilms. *PLoS One* **11**, e0154086, doi:10.1371/journal.pone.0154086 (2016).

122 Li, T. *et al.* Antimicrobial Susceptibility Testing of Metronidazole and Clindamycin against Gardnerella vaginalis in Planktonic and Biofilm Formation. *Can J Infect Dis Med Microbiol* **2020**, 1361825, doi:10.1155/2020/1361825 (2020).

123 Kaplan, J. B. Therapeutic potential of biofilm-dispersing enzymes. *Int J Artif Organs* **32**, 545-554, doi:10.1177/039139880903200903 (2009).

124 Thellin, O. *et al.* Lysozyme as a cotreatment during antibiotics use against vaginal infections: An in vitro study on Gardnerella vaginalis biofilm models. *Int Microbiol* **19**, 101-107, doi:10.2436/20.1501.01.268 (2016).

125 Hukic, M. *et al.* The Effect of Lysozyme on Reducing Biofilms by Staphylococcus aureus, Pseudomonas aeruginosa, and Gardnerella vaginalis: An In Vitro Examination. *Microb Drug Resist* **24**, 353-358, doi:10.1089/mdr.2016.0303 (2018).

126 Hymes, S. R., Randis, T. M., Sun, T. Y. & Ratner, A. J. DNase inhibits Gardnerella vaginalis biofilms in vitro and in vivo. *J Infect Dis* **207**, 1491-1497, doi:10.1093/infdis/jit047 (2013).

127 Ginkel, P. D., Soper, D. E., Bump, R. C. & Dalton, H. P. Vaginal flora in postmenopausal women: the effect of estrogen replacement. *Infect Dis Obstet Gynecol* **1**, 94-97, doi:10.1155/S1064744993000225 (1993).

128 Christina L. Hayes, J. R., Junic Wokuri, Gregor Reid, Rupert Kaul, Jesleen Rana, Muna Alkhaifi, Wangari Tharao, Fiona Smaill, & Charu Kaushic. in *IAIDS Conference 2022.*

129 Reid, G. *et al.* Oral use of Lactobacillus rhamnosus GR-1 and L. fermentum RC-14 significantly alters vaginal flora: randomized, placebo-controlled trial in 64 healthy women. *FEMS Immunol Med Microbiol* **35**, 131-134, doi:10.1016/s0928-8244(02)00465-0 (2003).

130 Breshears, L. M., Edwards, V. L., Ravel, J. & Peterson, M. L. Lactobacillus crispatus inhibits growth of Gardnerella vaginalis and Neisseria gonorrhoeae on a porcine vaginal mucosa model. *BMC Microbiol* **15**, 276, doi:10.1186/s12866-015-0608-0 (2015).

131 Castro, J., Martins, A. P., Rodrigues, M. E. & Cerca, N. Lactobacillus crispatus represses vaginolysin expression by BV associated Gardnerella vaginalis and reduces cell cytotoxicity. *Anaerobe* **50**, 60-63, doi:10.1016/j.anaerobe.2018.01.014 (2018).

132 Herbst-Kralovetz, M. M., Pyles, R. B., Ratner, A. J., Sycuro, L. K. & Mitchell, C. New Systems for Studying Intercellular Interactions in Bacterial Vaginosis. *J Infect Dis* **214 Suppl 1**, S6-S13, doi:10.1093/infdis/jiw130 (2016).

133 Nazli, A. *et al.* HIV-1 gp120 induces TLR2- and TLR4-mediated innate immune activation in human female genital epithelium. *J Immunol* **191**, 4246-4258, doi:10.4049/jimmunol.1301482 (2013).

134 Nazli, A. *et al.* Interferon-β induced in female genital epithelium by HIV-1 glycoprotein 120 via Toll-like-receptor 2 pathway acts to protect the mucosal barrier. *Cellular & Molecular Immunology* **16**, 178-194, doi:10.1038/cmi.2017.168 (2019).

135 Shen, Z., Rodriguez-Garcia, M., Patel, M. V. & Wira, C. R. Direct and Indirect endocrine-mediated suppression of human endometrial CD8+T cell cytotoxicity. *Sci Rep* **11**, 1773, doi:10.1038/s41598-021-81380-8 (2021).
136 Patel, M. V., Shen, Z., Rossoll, R. M. & Wira, C. R. Estradiol-regulated innate antiviral responses of human endometrial stromal fibroblasts. *Am J Reprod Immunol* **80**, e13042, doi:10.1111/aji.13042 (2018).
137 Rohan, L. C. *et al.* In vitro and ex vivo testing of tenofovir shows it is effective as an HIV-1 microbicide. *PLoS One* **5**, e9310, doi:10.1371/journal.pone.0009310 (2010).
138 Kala, S., Dunk, C., Acosta, S. & Serghides, L. Periconceptional exposure to lopinavir, but not darunavir, impairs decidualization: a potential mechanism leading to poor birth outcomes in HIV-positive pregnancies. *Hum Reprod* **35**, 1781-1796, doi:10.1093/humrep/deaa151 (2020).
139 Fichorova, R. N., Yamamoto, H. S., Delaney, M. L., Onderdonk, A. B. & Doncel, G. F. Novel vaginal microflora colonization model providing new insight into microbicide mechanism of action. *mBio* **2**, e00168-00111, doi:10.1128/mBio.00168-11 (2011).
140 Squier, C. A., Mantz, M. J., Schlievert, P. M. & Davis, C. C. Porcine vagina ex vivo as a model for studying permeability and pathogenesis in mucosa. *J Pharm Sci* **97**, 9-21, doi:10.1002/jps.21077 (2008).
141 Schaller, M., Korting, H. C., Borelli, C., Hamm, G. & Hube, B. Candida albicans-secreted aspartic proteinases modify the epithelial cytokine response in an in vitro model of vaginal candidiasis. *Infect Immun* **73**, 2758-2765, doi:10.1128/iai.73.5.2758-2765.2005 (2005).
142 Grammen, C. *et al.* Development and in vitro evaluation of a vaginal microbicide gel formulation for UAMC01398, a novel diaryltriazine NNRTI against HIV-1. *Antiviral Res* **101**, 113-121, doi:10.1016/j.antiviral.2013.11.005 (2014).
143 Abdel-Motal, U. M. *et al.* Anti-gp120 minibody gene transfer to female genital epithelial cells protects against HIV-1 virus challenge in vitro. *PLoS One* **6**, e26473, doi:10.1371/journal.pone.0026473 (2011).
144 Fichorova, R. N., Rheinwald, J. G. & Anderson, D. J. Generation of papillomavirus-immortalized cell lines from normal human ectocervical, endocervical, and vaginal epithelium that maintain expression of tissue-specific differentiation proteins. *Biol Reprod* **57**, 847-855, doi:10.1095/biolreprod57.4.847 (1997).
145 Lee, Y. *et al.* Effects of Female Sex Hormones on Susceptibility to HSV-2 in Vaginal Cells Grown in Air-Liquid Interface. *Viruses* **8**, doi:10.3390/v8090241 (2016).
146 Africander, D., Louw, R., Verhoog, N., Noeth, D. & Hapgood, J. P. Differential regulation of endogenous pro-inflammatory cytokine genes by medroxyprogesterone acetate and norethisterone acetate in cell lines of the female genital tract. *Contraception* **84**, 423-435, doi:10.1016/j.contraception.2011.06.006 (2011).
147 Saha, D., Koli, S., Patgaonkar, M. & Reddy, K. V. Expression of hemoglobin-α and β subunits in human vaginal epithelial cells and their functional significance. *PLoS One* **12**, e0171084, doi:10.1371/journal.pone.0171084 (2017).
148 Mossop, H., Linhares, I. M., Bongiovanni, A. M., Ledger, W. J. & Witkin, S. S. Influence of lactic acid on endogenous and viral RNA-induced immune mediator production by

vaginal epithelial cells. *Obstet Gynecol* **118**, 840-846, doi:10.1097/AOG.0b013e31822da9e9 (2011).

149 Mikamo, H. *et al.* High glucose-mediated overexpression of ICAM-1 in human vaginal epithelial cells increases adhesion of Candida albicans. *J Obstet Gynaecol* **38**, 226-230, doi:10.1080/01443615.2017.1343810 (2018).

150 Fanibunda, S. E., Modi, D. N., Gokral, J. S. & Bandivdekar, A. H. HIV gp120 binds to mannose receptor on vaginal epithelial cells and induces production of matrix metalloproteinases. *PLoS One* **6**, e28014, doi:10.1371/journal.pone.0028014 (2011).

151 Kinlock, B. L., Wang, Y., Turner, T. M., Wang, C. & Liu, B. Transcytosis of HIV-1 through vaginal epithelial cells is dependent on trafficking to the endocytic recycling pathway. *PLoS One* **9**, e96760, doi:10.1371/journal.pone.0096760 (2014).

152 Machado, R. M., Palmeira-de-Oliveira, A., Breitenfeld, L., Martinez-de-Oliveira, J. & Palmeira-de-Oliveira, R. Optimization and Application of In Vitro and Ex Vivo Models for Vaginal Semisolids Safety Evaluation. *J Pharm Sci* **108**, 3289-3301, doi:10.1016/j.xphs.2019.05.026 (2019).

153 Herbst-Kralovetz, M. M. *et al.* Quantification and comparison of toll-like receptor expression and responsiveness in primary and immortalized human female lower genital tract epithelia. *Am J Reprod Immunol* **59**, 212-224, doi:10.1111/j.1600-0897.2007.00566.x (2008).

154 Plesniarski, A., Siddik, A. B. & Su, R. C. The Microbiome as a Key Regulator of Female Genital Tract Barrier Function. *Front Cell Infect Microbiol* **11**, 790627, doi:10.3389/fcimb.2021.790627 (2021).

155 Chen, S. & Schoen, J. Air-liquid interface cell culture: From airway epithelium to the female reproductive tract. *Reprod Domest Anim* **54 Suppl 3**, 38-45, doi:10.1111/rda.13481 (2019).

156 Rosca, A. S., Castro, J. & Cerca, N. Evaluation of different culture media to support in vitro growth and biofilm formation of bacterial vaginosis-associated anaerobes. *PeerJ* **8**, e9917, doi:10.7717/peerj.9917 (2020).

157 Castro, J., Rosca, A. S., Cools, P., Vaneechoutte, M. & Cerca, N. Gardnerella vaginalis Enhances Atopobium vaginae Viability in an in vitro Model. *Front Cell Infect Microbiol* **10**, 83, doi:10.3389/fcimb.2020.00083 (2020).

158 Miles, A. A., Misra, S. S. & Irwin, J. O. The estimation of the bactericidal power of the blood. *J Hyg (Lond)* **38**, 732-749, doi:10.1017/s002217240001158x (1938).

159 Hill, D. R. *et al.* In vivo assessment of human vaginal oxygen and carbon dioxide levels during and post menses. *J Appl Physiol (1985)* **99**, 1582-1591, doi:10.1152/japplphysiol.01422.2004 (2005).

160 Place, T. L., Domann, F. E. & Case, A. J. Limitations of oxygen delivery to cells in culture: An underappreciated problem in basic and translational research. *Free Radical Biology and Medicine* **113**, 311-322, doi:https://doi.org/10.1016/j.freeradbiomed.2017.10.003 (2017).

161 Schwebke, J. R., Muzny, C. A. & Josey, W. E. Role of Gardnerella vaginalis in the pathogenesis of bacterial vaginosis: a conceptual model. *J Infect Dis* **210**, 338-343, doi:10.1093/infdis/jiu089 (2014).

162 Nunn, K. L. *et al.* Enhanced Trapping of HIV-1 by Human Cervicovaginal Mucus Is Associated with Lactobacillus crispatus-Dominant Microbiota. *mBio* **6**, e01084-01015, doi:10.1128/mBio.01084-15 (2015).
163 Wilson, C. *et al.* Quantitative and Qualitative Assessment Methods for Biofilm Growth: A Mini-review. *Res Rev J Eng Technol* **6** (2017).
164 Stepanovic, S. *et al.* Quantification of biofilm in microtiter plates: overview of testing conditions and practical recommendations for assessment of biofilm production by staphylococci. *APMIS* **115**, 891-899, doi:10.1111/j.1600-0463.2007.apm_630.x (2007).
165 Frank, K. L. & Patel, R. Poly-N-acetylglucosamine is not a major component of the extracellular matrix in biofilms formed by icaADBC-positive Staphylococcus lugdunensis isolates. *Infect Immun* **75**, 4728-4742, doi:10.1128/iai.00640-07 (2007).
166 Lock, J. Y., Carlson, T. L. & Carrier, R. L. Mucus models to evaluate the diffusion of drugs and particles. *Adv Drug Deliv Rev* **124**, 34-49, doi:10.1016/j.addr.2017.11.001 (2018).
167 Hjelm, B. E., Berta, A. N., Nickerson, C. A., Arntzen, C. J. & Herbst-Kralovetz, M. M. Development and Characterization of a Three-Dimensional Organotypic Human Vaginal Epithelial Cell Model1. *Biology of Reproduction* **82**, 617-627, doi:10.1095/biolreprod.109.080408 (2010).
168 Lawrence, J. R. *et al.* Scanning transmission X-ray, laser scanning, and transmission electron microscopy mapping of the exopolymeric matrix of microbial biofilms. *Appl Environ Microbiol* **69**, 5543-5554, doi:10.1128/aem.69.9.5543-5554.2003 (2003).
169 Woods, M. W. *et al.* Transcriptional response of vaginal epithelial cells to medroxyprogesterone acetate treatment results in decreased barrier integrity. *J Reprod Immunol* **143**, 103253, doi:10.1016/j.jri.2020.103253 (2021).
170 Machado, D., Castro, J., Palmeira-de-Oliveira, A., Martinez-de-Oliveira, J. & Cerca, N. Bacterial Vaginosis Biofilms: Challenges to Current Therapies and Emerging Solutions. *Front Microbiol* **6**, 1528, doi:10.3389/fmicb.2015.01528 (2015).
171 Braga, P. C., Dal Sasso, M., Culici, M. & Spallino, A. Inhibitory activity of thymol on native and mature Gardnerella vaginalis biofilms: in vitro study. *Arzneimittelforschung* **60**, 675-681, doi:10.1055/s-0031-1296346 (2010).